

## Durham E-Theses

---

### *Investigating Post-Translational Modification of the Net Protein Superfamily*

BUSH, SIMON,JOHN

#### How to cite:

---

BUSH, SIMON,JOHN (2016) *Investigating Post-Translational Modification of the Net Protein Superfamily*, Durham theses, Durham University. Available at Durham E-Theses Online:  
<http://etheses.dur.ac.uk/11718/>

#### Use policy

---

The full-text may be used and/or reproduced, and given to third parties in any format or medium, without prior permission or charge, for personal research or study, educational, or not-for-profit purposes provided that:

- a full bibliographic reference is made to the original source
- a [link](#) is made to the metadata record in Durham E-Theses
- the full-text is not changed in any way

The full-text must not be sold in any format or medium without the formal permission of the copyright holders.

Please consult the [full Durham E-Theses policy](#) for further details.

# Investigating Post- Translational Modification of the Net Protein Superfamily

Simon John Bush

Submitted in Accordance with the  
Requirements for the Degree of  
Master of Science

School of Biological and Biomedical  
Sciences

Durham University

December 2015



## Abstract

The Net protein superfamily represents a group of actin binding proteins contain a novel actin binding domain at their N termini. The aim of this project was to investigate post-translational modification of these proteins in order to explore how the interaction of these proteins with actin is regulated. A bioinformatics-based approach was used to predict sites for multiple types of modification, with a focus on phosphorylation, that were conserved between members of the superfamily. It became clear that there was some level of conservation of predicted post-translational modification sites at the C-terminus in multiple Net families. Net4B was identified as having a high probability of being phosphorylated at the C-terminus and predicted to have its N- and C-termini proximal to one another in its tertiary structure, and following this mutant forms of the protein were created to investigate how its actin binding activity would be affected if one site, S509, was phosphorylated or dephosphorylated. The mutants were transiently expressed in *Nicotiana benthamiana* and the appearance of the leaf cells assessed.

Whilst phosphomimicry of S509 resulted in no appreciable change in the appearance of the GFP-tagged protein, mutation to a residue imitating a non-phosphorylatable serine resulted in the formation of punctae, in some cases much like the 'beads-on-a-string' seen in other members of the Net superfamily. This finding may have implications for the regulation of actin binding in other Net proteins and for other proteins outside of the superfamily. Two models are presented in both of these contexts. This project may also provide groundwork for future experiments concerning phosphorylation and acylation, and may illuminate the mechanism by which Net proteins interact with actin and with the membranes with which they are respectively localised.

## Contents

### Chapter 1: Introduction

1.1	Introduction to Actin	1
1.2	Characteristics of the Net Superfamily	12
1.3	The importance of post-translational modification in plant development	18
1.4	Strategy of Investigation for this project	26

### Chapter 2: Materials and Methods

2.1	Plant Growth Conditions	27
2.2	Gel Electrophoresis	28
2.3	Western Blotting	32
2.4	Molecular Biology Methods	34
2.5	<i>In vitro</i> synthesis of proteins	39

### Chapter 3: Results

3.1	Prediction of phosphorylation sites in the Net proteins	41
3.2	Predicting the tertiary structure of Net proteins	46
3.3	Prediction of other post-translational modifications – Acylation and Sumoylation	53
3.4	Western Blotting analysis of the Net proteins	64
3.5	<i>In silico</i> experimentation	70
3.6	Site-directed mutagenesis	77

### Chapter 4: Discussion

4.1	Introduction	81
4.2	Phosphorylation of Net4B may facilitate the cleavage of another post-translational modification	86
4.3	Phosphorylation is a widespread post-translational modification of Net proteins	87
4.4	S-acylation may be a conserved post-translational regulatory mechanism in Net1, Net2 and Net4 protein families	88
4.5	Prenylation may be a conserved post-translational modification of the Net1 family	89
4.6	SUMO-interaction may be a conserved regulatory mechanism in the NAB domain	90
4.7	Concluding remarks	91

<b>Appendix 1</b>	92
-------------------	----

<b>Bibliography</b>	93
---------------------	----

## Acknowledgements

Throughout the course of this project I have been aided by a great number of people, all of whom deserve thanks for the help and encouragement provided. I would first like to thank my supervisor, Professor Patrick Hussey, for the design of this open-ended and exciting project and his support. Dr Tim Hawkins has been instrumental to the ongoing progress of the project and I am extremely grateful for the hours of his time he gave me to discuss hypotheses and his endless encouragement, particularly concerning the bioinformatics aspects. Thanks go to Joanne Robson and Dr Steve Chivasa for their advice and masterful demonstration of gel based proteomics techniques. I am thankful for my thesis committee, Dr Tony Fawcett and Dr Mark Knight, who gave words of inspiration when they were most needed, and provided equally needed doses of reality.

Thanks must also go to everyone in the Hussey Laboratory. I am thankful for the welcome that I received, the bolstering of my resolve when necessary, and the general atmosphere whether intellectual or frivolous. Dave, Pat, Greg, Peng, Rita and Martin – thanks so much for making the year so much more than just the project itself. And to Johan the ever-meticulous, the practical and workplace skills you have imbued me with are proving more valuable than ever. I really appreciate the day-to-day guidance you offered to me.

Outside the lab, the continued support of my parents has been instrumental to my growth as a scientist both prior to and during this project. Special thanks to my mum for proof-reading what to her must have seemed complete gobbledegook! And finally, thank you so much Stephanie for making home a space to relax in rather than an extension of the lab office! Cups of tea, hugs and strong doses of logic have made a challenging year that much easier.

*“The copyright of this thesis rests with the author. No quotation from it should be published without the prior written consent and information derived from it should be acknowledged.”*

## List of Abbreviations

2-DGE – 2-dimensional gel electrophoresis

ABP – Actin Binding Protein

ATP – Adenosine triphosphate

ADP – Adenosine diphosphate

BLAST – Basic local alignment search tool

ERM protein – Ezrin/Radixin/Moesin family protein

F-actin – Filamentous actin

FERM – Band four-point-one/ezrin/radixin/moesin, referencing a domain found in ERM proteins which facilitates localisation to membranes

G-actin – globular monomeric actin

GFP – Green fluorescent protein

GTP – Guanosine triphosphate

KASH - Klarsicht/Anc/Syne-1 homology protein

NAB domain – Net actin binding domain

Net protein – a protein from the Networked protein superfamily

HRP – Horseradish peroxidase

IEF – Isoelectric focussing

IRQ domain – domain identified in the C-terminal region of the Net4 proteins, containing the short peptide sequence Isoleucine-Arginine-Glutamine

LB – Lysogeny broth

PIP2 - Phosphatidylinositol 4,5-bisphosphate

ROP – Rho of plants

SIM – SUMO-interacting motif

SMC – Structural Maintenance of Chromosomes protein

SOC – Super optimal broth

SUMO – Small ubiquitin-like modifier

SUN - SAD1/UNC84 protein

SXA – Notation indicating the mutation of a serine (S) amino acid to an alanine (A) at numerical position X in the peptide sequence

SXD – Notation indicating the mutation of a serine (S) amino acid to an aspartic acid (D) at numerical position X in the peptide sequence

TAIR – The Arabidopsis Information Resource

VLN – Villin protein

VLN1 – Villin1

VLN3 – Villin3

VLN5 – Villin5

## List of Figures

1	Actin Treadmilling	4
2	Actin arrays in eukaryotes	7
3	Cytoskeletal arrays constructed during plant cell division	8
4	LINC complex-like arrangement at plant nuclei compared to animal nuclei	10
5	Characteristics of the Net superfamily	14
6	The general mechanism by which ERM proteins are activated	20
7	Non-covalent interaction of a SIM with the SUMO peptide	25
8	Conserved C-terminal regions of the Net families	42
9	BLASTp analysis	47
10	Diagram of the folding and dimerization of SMC	49
11	Tertiary structure prediction of Net3C	51
12	Tertiary structure prediction of Net4B	52
13	Tertiary Structure prediction of Net2A	53
14	Comparison of predicted S-acylation sites in the Net1 family	55
15	Comparison of predicted S-acylation sites in the Net2 family	57
16	Comparison of predicted S-acylation sites in the Net4 family	58
17	Prediction of farnesylation and geranylgeranylation in the Net1 family at high stringency	60
18	Aligned NET protein sequences with SIMs	63
19	Antibody testing by 1-dimensional electrophoresis	65
20	2-dimensional gel analysis of Net4B	68
21	Comparison of amino acids used for mutagenesis	72
22	<i>In silico</i> mutagenesis in S144 and S357	74
23	<i>In silico</i> mutagenesis of S509	76
24	Zeiss 880 confocal microscope images of Net4B mutants transiently expressed in <i>N. benthamiana</i>	79
25	Proposed model for ERM-protein-like regulation of NET4B	83
26	Proposed model for phosphorylation of S509	84
27	Proposed model for the recruitment of Net4B	86

## List of Tables

1	Results of one-to-one phosphorylation site comparison	43
2	Results of searching the representative gene locus numbers of the NET proteins in the PhosPhAt database	44
3	Results of the PhosPhAt-Scansite cross-reference	46
4	Protparam data concerning the GRAVY, pI and predicted molecular weight of the Net proteins	64
5	Summary of <i>in silico</i> mutagenesis experiments	75



## **Chapter 1: Introduction**

### **1.1 Introduction to actin**

Actin is one component of the fibrous network of proteins that constitute the cytoskeleton within cells; the cytoskeleton as a whole has a huge variety of functions relating to structure and transport within the cellular environment. It is crucial for processes such as cell division and morphology, organelle position and cell signalling (Fletcher & Mullins, 2010). Actin is a highly dynamic protein that occurs in two forms; G-actin, the globular monomeric form, and F-actin, the filamentous arrangement of G-actin into microfilaments which make up the actin based part of the cytoskeleton (Dominguez & Holmes, 2011). The relative abundance of these two forms, in combination with a variety of other proteins which bind to them, are the source of this dynamicity, as they can define the size, position and time period of existence of microfilaments (Lodish et al., 2007). The ability of microfilaments to polymerise and depolymerise dynamically and remain stable when necessary is the basis for their importance to a cellular environment.

#### **1.1.1 Actin Structure and Dynamics**

Microfilaments are formed from G-actin. G-actin has a molecular weight of 42kDa and contains four subdomains. It contains an adenosine binding cleft, which acts as a major regulator for its ability to form F-actin, with the adenosine triphosphate (ATP) bound form able to polymerise much more readily. It also contains four  $\text{Ca}^{2+}$  binding sites. It achieves this through changes to each of these four subdomains caused by the presence of the inorganic phosphate which disrupt certain hydrogen bonds and alpha helices (Otterbein et al., 2001), allowing the G-actin monomers to more closely associate with one another. The formation of an actin trimer acts as the basis for filament assembly, as other G-actin monomers nucleate around it. Microfilaments are polarised, which results from G-actin monomers themselves having inherent polarity, due to the position of this adenosine binding cleft. The two ends of the filament are termed the plus (barbed) and minus (pointed) ends; the minus end has the adenosine binding cleft exposed, whilst the plus end does not. Microfilaments have a variable diameter of 7-9 nm as a result of their torsional flexibility.

Microfilament polarity forms the basis of their dynamicity. ATP is hydrolysed upon G-actin incorporation into the filament, releasing an inorganic phosphate, returning G-actin to its unstable ADP-bound form. The minus end is comprised entirely of this form and depolymerises more readily. Depolymerisation state at both the minus and plus ends of the filament is defined *in vitro* by the local concentration of G-actin. The critical concentration, the concentration of ATP-bound G-actin required to stimulate polymerisation, is different for each end, being greater at the minus end ( $0.6\mu\text{M}$  compared to  $0.12\mu\text{M}$  at the plus end) due to its proclivity for depolymerisation. Below a concentration of  $0.12\mu\text{M}$  actin filaments are in steady state, with no net growth or shrinkage at either end. The different critical concentrations allow actin filaments to undergo the phenomenon of treadmilling when the critical concentration of G-actin is between the two critical concentrations (figure 1A), where polymerisation is occurring at the plus end and depolymerisation is occurring at the minus end, and there is no net growth or shrinkage of the actin filament. In addition, polymerisation or depolymerisation can occur at both ends simultaneously if the critical concentrations for each end are met or not, respectively (Lodish et al., 2007). These processes can be coordinated by actin binding proteins (ABPs), increasing the dynamicity of the actin cytoskeleton and allowing it to contribute to a wide range of cellular functions in plant cells.

### 1.1.2 Coordination of Actin Dynamics by ABPs

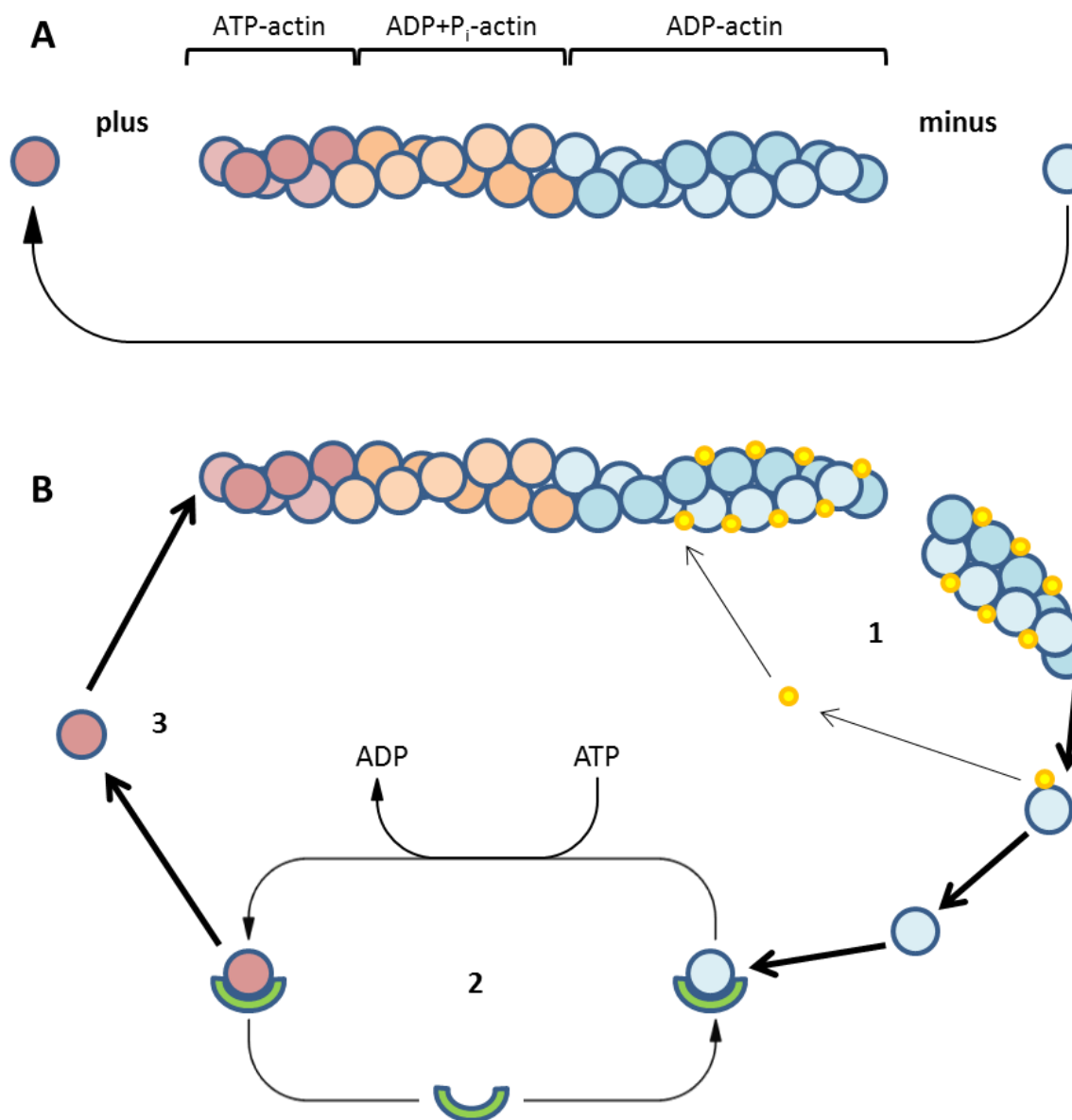
Many ABPs have the capability to improve the efficiency of actin filament polymerisation and depolymerisation by influencing critical concentrations of G-actin. This allows cellular responses to internal and external changes to occur much more rapidly relative to microfilament formation *in vitro*. Profilin and cofilin (also known as actin depolymerising factor, or ADF) are complementary proteins that function at the plus and minus ends of actin filaments respectively and function to increase their turnover.

Starting at the minus end, cofilin induces more rapid depolymerisation of ADP-bound G-actin by further destabilising the structure of the microfilament. It can bind to any of these G-actin monomers, rather than just the terminal

monomer, allowing the filament to break at multiple points towards its minus end. This in turn generates more minus ends from which actin readily depolymerises whilst also more rapidly reducing the length of the original microfilament (Lodish et al., 2007). This results in a 25-fold increase in depolymerisation at minus ends (Carlier et al., 1997). Specifically in plants, cofilin is regulated by multiple factors (Hussey et al., 2006), such as calcium by virtue of its negative regulation by calmodulin-like domain protein kinase, or binding to membranes via phosphatidylinositol 4,5-bisphosphate (PIP<sub>2</sub>). This 25-fold change in turn can be increased to a 125-fold increase in turnover by the effects of profilin (Didry et al., 1998). Profilin binds to ADP-bound G-actin released from the minus end by cofilin and catalyses the exchange of ADP for ATP by opening the adenosine binding cleft. Its binding to actin causes it to be unable to rebind to the minus end but still allows polymerisation at the plus end normally (Lodish et al., 2007) (figure 1B). High concentrations of profilin cause depolymerisation of the actin cytoskeleton by sequestering much of this G-actin. The result of this combination of proteins is a high concentration of G-actin that is not susceptible to spontaneous polymerisation, but can be used for rapid controlled polymerisation.

Actin polymerisation can be further regulated by proteins which cap filament ends, such as heterodimeric capping protein cytoskeleton (Huang et al., 2006) and gelsolin (Huang et al., 2004), which both cap the plus end of microfilaments in order to promote minus end elongation. In contrast, formins in plants bind to the plus end of microfilaments in order to promote their extension by inhibiting the binding of plus-end-capping proteins (Pruyne et al., 2002). Both cap proteins and formins have implications for transducing signalling pathways to a cytoskeletal response as well.

Figure 1: Actin Treadmilling; **A** Actin treadmilling *in vitro*. ADP-actin (blue) depolymerises from the minus end, exchanges ADP for ATP, and subsequently ATP-actin (red) can then be added to the plus end. Once incorporated into the filament, hydrolysis of ATP occurs, releasing an inorganic phosphate ( $P_i$ ) (orange). When this is lost from the filament altogether the actin is once again classified as ADP-actin. Treadmilling occurs when the concentration of G-actin is greater than the critical concentration needed for polymerisation at the plus end but less than the critical concentration required at the minus end. **B** The mechanism by which profilin and cofilin coordinate this process; **1** Cofilin (yellow) binds to actin filaments close to the minus end, causing individual monomers or large segments to ADP-actin to be severed, increasing the rate of depolymerisation. Cofilin is then recycled back to actin filament minus ends. **2** ADP-actin is sequestered by profilin (green), which catalyses the exchange of ADP for ATP, forming a population of profilin bound ATP-actin. **3** ATP-actin, when not sequestered by profilin, readily binds to the plus ends of actin filaments. Figure inspired by and adapted from figures from Lodish et al., 2007.

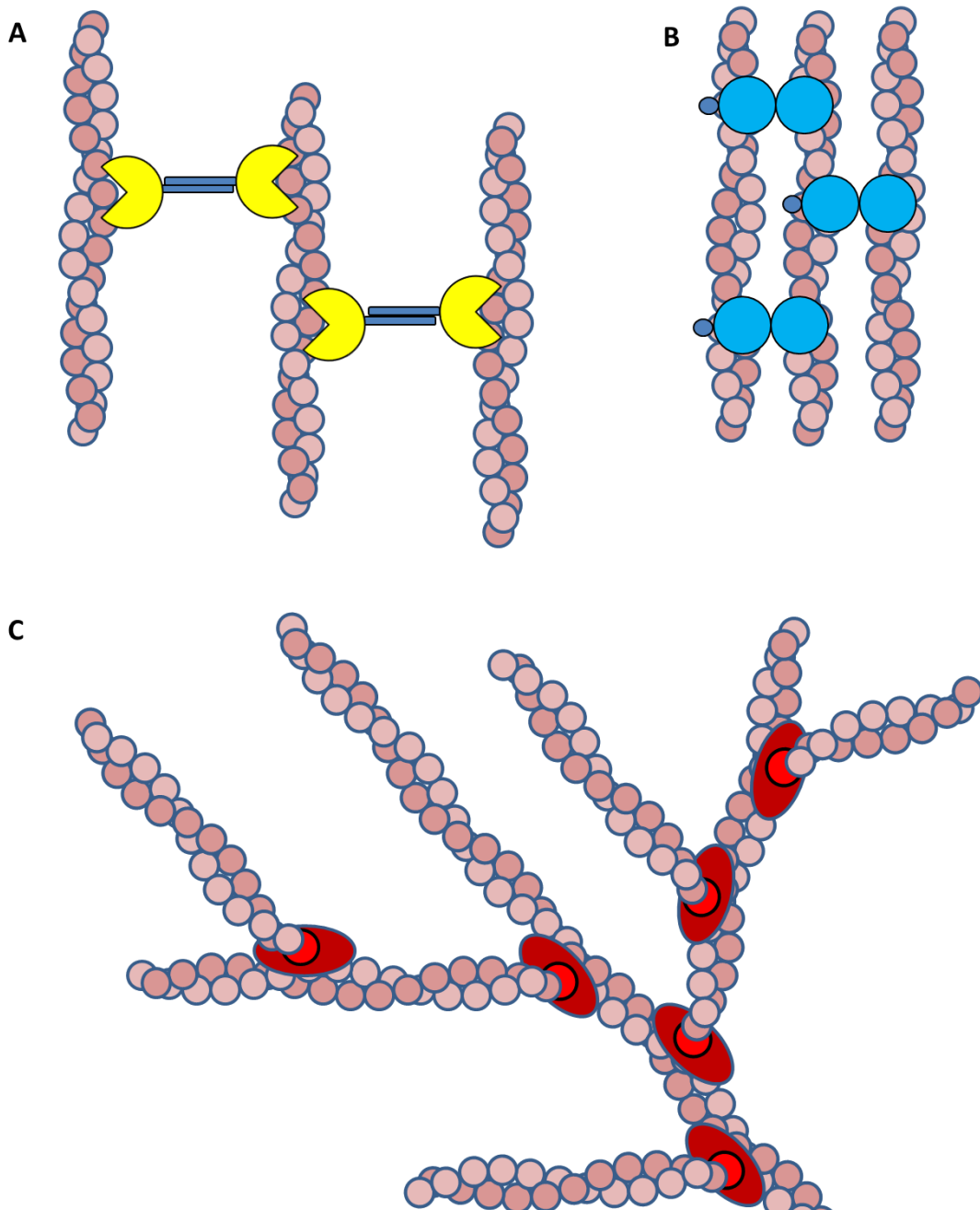


### 1.1.3 Actin arrays in Plants

Whilst some proteins organise the structure of individual filaments, other types of ABPs are responsible for organisation of these filaments into arrays which carry out particular functions in certain cell compartments. The most simple of these arrays is the actin bundle, whereby multiple microfilaments are aligned closely to one another, cross-linked by ABPs. Many villins in *Arabidopsis thaliana* have capping capabilities similar to that of gelsolin, but they also contain a head domain at their C-terminus which is responsible for this cross-linking. Loss of function mutation of VILLIN5 (VLN5) resulted in retardation in pollen tube growth (Zhang et al., 2010), and VLN2/3 truncations lacking the head domain result in twisting of a variety of plant organs due to non-uniform cell elongation (Honing et al., 2012). Some villins have lost their severing and capping capabilities, such as VILLIN1. This bundling protects microfilaments from cofilin mediated depolymerisation, allowing the maintenance of long cables (Huang et al., 2005), but there is evidence to suggest they do not maintain their activities in the presence of other villins. Human villin requires homodimerisation in order to achieve this bundling (George et al., 2007) (figure 2A), but VLN1 and VLN3 do not form dimers *in vitro*, and under certain  $\text{Ca}^{2+}$  concentrations the severing activity of VLN3 will occur in the presence of VLN1 (Khurana et al., 2010). Fimbrin can also enable actin bundling, but is unique amongst other actin-binding cross-linkers in that it contains two repeated actin binding domains. This causes bundles to form more tightly due to their proximity (figure 2B). The N and C termini also make contributions to the mechanical properties of actin networks, with truncations of either or both resulting in actin networks of reduced stiffness (Klein et al., 2004). CROLIN1, one of six CROLIN isoforms, is capable of actin bundling, and can also cross-link actin bundles to other structures, such as actin networks (Jia et al., 2013). Actin bundles have a diverse range of functions, from acting as tracks on which actin-binding transport proteins such as myosins can run (Lodish et al., 2007), which allows directional cell expansion (van der Honing, 2012) or organelle positioning (Avisar et al., 2009), or structurally, as their arrangement modulates the open status of stomata (Higaki et al., 2010). Transport along actin filaments is required for placement of cellulose synthase beneath developing cell walls (Wightman and Turner, 2008).

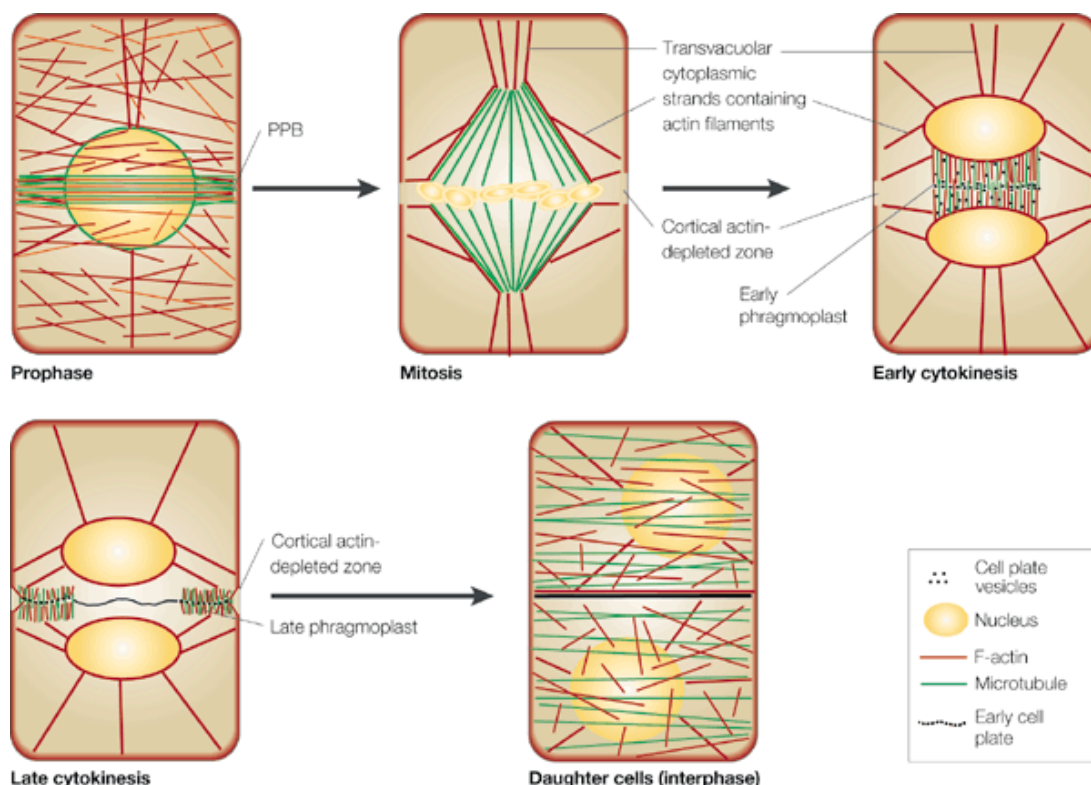
Actin networks similar require ABPs for their organisation. Fimbrin can also form orthogonal networks as well as actin bundles (Klein et al., 2004). In animals, filamin enables the formation of highly orthogonal actin networks at the leading edge of migrating cells (Feng and Walsh, 2004), and the Arp2/3 complex, which facilitates plus end elongation whilst capping the minus end at a point bound to an existing actin filament at a 70° angle (figure 2C), is essential for life (Deeks and Hussey, 2005). In plants however, relatively innocuous phenotypes are observed following the mutation of different protein constituents of the complex (Hussey et al., 2006). The Arp2/3 complex, which is regulated at membranes by the SCAR/WAVE complex, is required for correct trichome structure and cell growth but its role in actin nucleation is less important to plant organisms on the whole. The presence of formins offers some explanation of this; in animals, they act as capping proteins at microfilament plus ends, but in *Arabidopsis* multiple formin homologs promote extension from the barbed end (Hussey et al., 2006). Formins are split into two groups, with group 1 containing transmembrane domains and group 2 only possessing FH1 and FH2 domains necessary for actin binding (Deeks et al., 2002). Group 1e formins interact with profilin and are localised to the plasma membrane, and overexpression of dominant negative AtFH8 causes reduction in root hair length (Deeks et al., 2005). Overexpression of AtFH1 caused retardation or arrest in pollen tube elongation, plasma membrane deformation and pollen tube tip bulging, but transformants at lower levels of expression exhibited increased initial growth rate. AtFH1 caused the formation of supernumerary actin filaments at the leading membrane, preventing elongation (Cheung and Wu, 2004). Formins can be localised to membranes by interactors such as FIPs (Deeks et al., 2002).

Figure 2: Actin arrays in eukaryotes; **A** Animal villins homodimerise with their actin binding domains (yellow) facing away from one another to generate thick actin bundles. **B** The two adjacent actin binding domains (light blue) of fimbrin allow for close alignment of actin filaments, resulting in thinner actin bundles. **C** The Arp2/3 complex (red) binds laterally to existing actin filaments, creating a point of nucleation at a  $70^\circ$  angle. Polymerisation of actin from this point of nucleation forms actin arrays. Figure generated from adaptations of figures from George et al., 2007 (**A**) and Lodish et al., 2007 (**B, C**).



Disruption of actin arrays by altering the expression of or mutating ABPs is a common feature of cell deformations in plants. Actin arrays are also a key component of cell division, during which plant cells exhibit a number of defined cytoskeletal arrays (figure 3). Actin is important for the organisation of the preprophase band which defines the plane of cytokinesis; actin depolymerisation drugs cause asymmetrical division in normally symmetrically-dividing tobacco BY-2 cells (Sano et al., 2005). The roles of actin and microtubules are also intertwined during late stage cytokinesis, during cell plate formation. In myosin VIII null mutants cells fail to orientate the cell plate perpendicular to the direction of cell expansion (Wu and Bezanilla, 2014). It is thought to allow the collection of peripheral microtubules into the forming cell plate. Formin 2A also localises to the phragmoplast (Gisbergen et al., 2012) and nucleates actin close to the newly formed plasma membrane allowing myosin VIII to perform this role.

Figure 3: Cytoskeletal arrays constructed during plant cell division. Both the preprophase band (PPB) and phragmoplast rely heavily on the actin component (Smith, 2001).

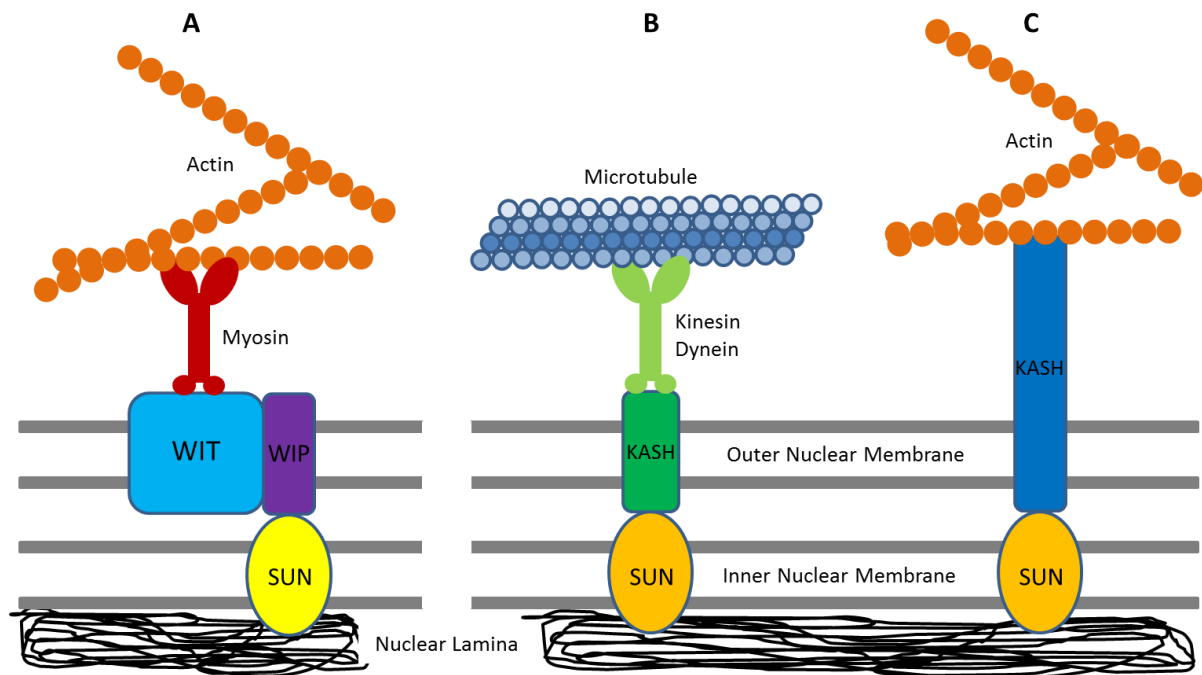


Nature Reviews | Molecular Cell Biology

Actin also has a role in the organisation of internal membranes; the actin cytoskeleton is associated with both the nuclear and vacuolar membranes. At the

nucleus, SAD1/UNC84 (SUN) and Klarsicht/Anc/Syne-1 homology (KASH) proteins are present in plant genomes, including some plant specific homologs (Evans et al., 2014). These proteins form the LINC complex, which can link the outer nuclear membrane to the actin cytoskeleton. In plants, Myosin XI-i-WIT complex linkages facilitate actin-based nuclear migration and act as a determinant for nuclear shape (Tamura et al., 2013) (figure 4). WIT acts like a KASH protein in the sense that it is found at the outer nuclear membrane and interacts with SUN proteins via an interaction with WIP (Zhou et al., 2012)(figure E). *Myosin XI-i* null mutants had more spherical, intricately invaginated nuclei (Tamura et al., 2013). Spectrin-like proteins have also been observed in onion nuclei which connect the actin cytoskeleton to the nuclear matrix (Pérez-Munive and de la Espina, 2011). Actin co-localises with the vacuolar membrane and is responsible for its movement and shape; the actin-depolymerisation drug bistheonellide A causes the formation of small spherical vacuoles and the disruption of transvacuolar cytoplasmic strands. Acto-myosin is required for the formation of grooves in the vacuolar membrane from which transvacuolar strands form. These strands in turn may have a role in nuclear migration during cell division (Higaki et al., 2006).

Figure 4: LINC complex-like arrangement at plant nuclei compared to animal nuclei; **A** in plants, nuclear migration and shape are thought to be defined by the linkage between actin and a complex for proteins including myosin and a SUN protein. **B** microtubular attachment to the LINC complex in animals fulfils via kinesin/dynein the migration and shape definition role performed in plants by the actin-based attachment. **C** Certain KASH proteins have actin binding domains which allow the LINC complex to interact directly with the actin cytoskeleton. This kind of structure has a role in nuclear anchorage as well as shape definition. In all cases, SUN proteins are linked to the nuclear lamina (Starr et al., 2010) (Tamura et al., 2013). Image inspired by a similar figure in Tamura et al., 2013.



#### 1.1.4 The Role of Actin in Signalling

It is clear that actin is regulated by a great number of ABPs in ways that are crucial for cell and organelle morphology and function, and that actin is dynamic. These characteristics allow actin to be an excellent effector of signalling messages. Actin responds via its associated proteins to a number of messengers to allow both intra- and intercellular signalling.

Calcium ions have a two-way relationship with actin. On one hand,  $\text{Ca}^{2+}$  signalling can have dramatic effects on the actin cytoskeleton through calcium regulated ABPs.  $\text{Ca}^{2+}$  can stimulate the spontaneous polymerisation of G-actin *in vitro* (Yokota et al., 2005). The gelsolin-like protein PrABP80 has been shown to mediate the depolymerisation of actin in pollen induced by large influxes of  $\text{Ca}^{2+}$ ,

resulting in the inhibition of fertilisation (Huang et al., 2004). LILIM1 is another ABP from lily (*Lilium longiflorum*) pollen which is regulated by  $\text{Ca}^{2+}$ , which modulates the transport of vacuolar vesicles and golgi apparatuses to the pollen tube apex by promoting microfilament bundling. Villins are sensitive to  $\text{Ca}^{2+}$ , with the presence of the ion able to promote the microfilament severing activity of VLN3 over the bundling activity of the calcium insensitive VLN1 (Khurana et al., 2010). On the other hand, however, actin may have a role in regulating intracellular calcium levels; influx of  $\text{Ca}^{2+}$  into growing pollen tubes follows oscillatory tube growth, with the depolymerisation of actin abolishing oscillatory growth and causing a decline in the tip focused  $\text{Ca}^{2+}$  gradient (Cardenas et al., 2008). F-actin dependent  $\text{Ca}^{2+}$  channels have also been identified in pollen tube protoplasts (Wang et al., 2004). In this way actin may act as a kind of precursor signal to  $\text{Ca}^{2+}$  dependent signalling pathways in pollen, or the two are part of a feedback loop.

Actin may also have a role in the control of plasmodesmata, channels between adjacent cells through the cell wall, which form as a result of incomplete cytokinesis, and are required for intercellular signalling in plants (Sager and Lee, 2014). They are important for trafficking of molecules below their size exclusion limit; the pore size of plasmodesmata can be altered. Plasmodesmata connect cells through a shared section of ER called the desmotubule and these channels are comprised of multiple components including actin, the Arp2/3 complex and myosin (Maule, 2008). The *Cucumber mosaic virus* movement protein has been shown to sever actin filaments at plasmodesmata in tobacco, resulting in an increased plasmodesmal size exclusion limit (Chen et al., 2010) (Su et al., 2010). Stabilisation of actin filaments via phalloidins reduced the rate of transport (Su et al., 2010). Myosins are thought to have a greater role in defining transport through plasmodesmata, as myosin inhibitors will prevent or slow the transport of 1-3kDa FITC-labelled dextran, whereas Latrunculin B, a well-known actin polymerisation inhibitor, did not reduce the rate of transport (Radford & White, 2011). There is a great deal of contradictory evidence on this matter, however (Maule, 2008), possibly due to the methods used. How actin is anchored in and around plasmodesmata is unknown, but would presumably require some kind of ABP that can interface with the plasma membrane, ER or both. Finding such proteins may clarify the role of actin in plasmodesmatal regulation.

Rho of plants (ROPs) GTPases have more widespread signalling functions in plants, regulating cell expansion, endocytosis and pollen tube and root hair growth, amongst others (Hussey et al., 2006). ROPs have been shown to act prior to root hair elongation (Molendijk et al., 2001) and are thought to initiate actin polymerisation; experiments to inhibit ROPs reduce the amount of fine F-actin and experiments to promote them increase F-actin network density (Hussey et al., 2006). RICs (ROP interacting CRIB motif proteins) interact with GTP-bound ROPs and add an additional level of control, for instance the balance of Ric3 and Ric4 in the pollen tube defines actin polymerisation, the former able to increase cytoplasmic calcium concentration when overexpressed (Gu et al., 2005).

Given the role of actin arrays at membranes, signalling to coordinate actin at cell membranes takes multiple forms. The SCAR/WAVE complex, which activates the Arp2/3 complex, is localised to the plasma membrane, when it is itself activated by Rac, by a large basic region of the wave regulatory complex (Davidson and Insall, 2011). Heterodimeric Capping Protein (CP) binds to membrane-bound phosphatidic acid and PIP2. CP mutants that were insensitive to the level of phosphatidic acid exhibit abnormal cell and organ growth early in development. It is thought that these phospholipids sequester CP making it unavailable for capping of actin filaments, as these mutants appeared similar to wild-type plants that had been treated with phosphatidic acid (Li et al., 2012). Formins are also sensitive to phospholipids, for example in the case of Formin 2A being localised to the developing cell plate, where phosphoinositide-3, 5-bisphosphate is required (van Gisbergen et al., 2012). Phosphatidylinositol-4-phosphate and PIP2 can also sequester cofilin/ADF isoforms in order to inhibit its activity at membranes where polymerisation needs to occur (Hussey et al., 2002). Membranes are therefore clearly important for actin mediated signalling.

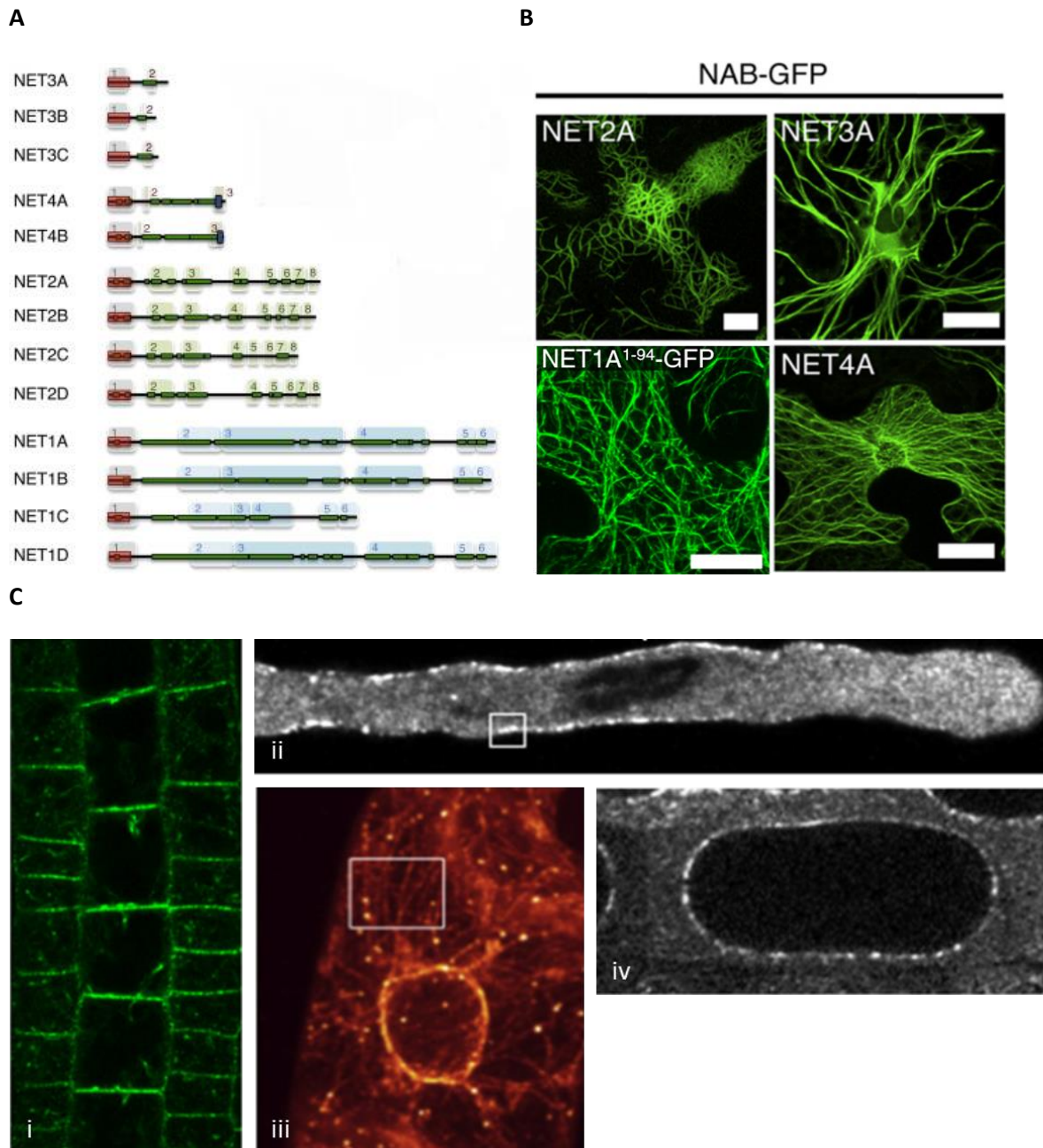
## **1.2 Characteristics of the Net Superfamily**

The identification of the Networked (Net) protein superfamily as a group of ABPs occurred following a high throughput screen of *Arabidopsis thaliana* proteins transiently expressed via a *Tobacco mosaic virus* GFP vector in *Nicotiana benthamiana* leaves, during which the N-terminal 288 residues of an unknown

protein labelled a filamentous network. This fragment was then shown to colocalise with actin. The first 94 amino acids of this fragment were found to be required for this colocalisation. The protein from which this fragment is derived was subsequently named Net1A (Deeks et al., 2012). This region was found to have homology with a region previously unknown function of KIP1, a kinase interacting protein from *Petunia integrifolia* (Skirpan et al., 2001). It was from this region, which became known as the Net Actin Binding (NAB) domain, that 12 other members of the superfamily came to be known through investigation of the *A. thaliana* genome. This domain is unlike any other previously documented actin binding motifs, and is unique to the plant kingdom (Deeks et al., 2012).

The superfamily is composed of four families based on their homology to one another, but all possess two common characteristics; Net proteins are membrane localised and bind to actin via the NAB domain (figure 5) (Deeks et al., 2012). Site-directed mutageneses of homologous residues in Net1A/2A in order to disrupt predicted structural arrangements have been found to alter the actin binding capabilities of these proteins (Cartwright, 2011). Many proteins required for actin-membrane interactions in animals are absent in plants (Hussey et al., 2002), and as such the discovery of the Net superfamily will increase our understanding in this area of plant biology. All members also exhibit extensive regions of coiled-coil. Net1A for instance is highly coiled at its N terminus, but also has regions in its central and C terminal regions (Calcutt, 2009). These alpha helices define the Net families, as there is recognisable homology between family members (figure J). The implications of conservation outside the NAB domain are being increasingly investigated.

Figure 5: Characteristics of the Net superfamily; **A** the 13 Net proteins, divided by their respective families. **B** the NAB domain, found at the N-terminus, binds to actin filaments when transiently expressed in *N. benthamiana*. **C** Net proteins are localised to membranes. A member from each Net family is shown here; (i) Net1A in *A. thaliana* root meristem, (ii) Net2A in *A. thaliana* pollen, (iii) Net3A in stable BY-2 culture and (iv) Net4A in *A. thaliana* root epidermal cells. Images adapted from Deeks et al., 2012, with the permission of the author.



### 1.2.1 The Net1 Family

The Net1 family is comprised of the largest members of the Net superfamily. There are four members of this family (Deeks et al., 2012). Work on Net1A and Net1B (Calcutt, 2009) allowed determination of the plasma membrane binding character of the Net1 family, which is also present in Net1C and Net1D (Ingle, 2011). Transient expression of GFP-labelled sections of Net1A showed that the N-terminus was localised to the actin cytoskeleton, the middle to the endoplasmic reticulum (ER) and the C terminus to the nucleus. Transient expression of the full Net1A protein with tagged GFP gave a 'beads on a string' appearance, where actin filaments are decorated by aggregates. Expression of GFP-Net1A *in situ* revealed that it was localised to the plasmodesmata at the transverse edges of vascular root cells. GUS staining demonstrated that Net1A was expressed in the root vasculature and also in lateral root buds (Deeks et al., 2012). The exact role of Net1A at plasmodesmata has not been elucidated, but null mutants for both Net1A and Net1B exhibit root stele cell elongation, which results in a long root phenotype (Ingle, 2011). Given an apparent lack of hormone influence, a structural role coordinating the diameter of plasmodesmata, which is regulated by actin/myosin, is a likely function for Net1A/1B. Net 1D is found at longitudinal cell boundaries (Ingle, 2011).

### 1.2.2 The Net2 Family

The Net2 family is composed of four members, Net2A through D (Deeks et al., 2012). This family contains the second largest proteins, and these proteins are most similar to KIP1 in terms of size and their overall structure, having been identified to possess the same PRK1 interacting domain as KIP1 in their central region. Protein receptor-like kinases (PRKs) are membrane bound regulators of anisotropic growth in pollen tubes and are associated with ROP signalling (Dixon, 2013) (Kaothien et al., 2005). The Net2 proteins are all found in pollen, and bioinformatics analysis suggests that Net2D may also be expressed in other tissues. They are thought to be functionally redundant as single mutants did not generate significant phenotypes and all are upregulated in extended pollen tubes. Net2A has been more extensively studied by Dr. Martin Dixon (Durham

University) and has been shown to form punctae at the pollen tube membrane away from the pollen tube tip. It is present early in pollen tube development, being expressed at the bi- and tri-cellular stage. Knockdown of Net2A causes aberrant positioning of the male germ unit, leading to the belief that it has a role in microspore development. It is hypothesised that these punctae are associated with lipid rafts that allow the deposition of callose or callose synthase into the cell wall. These lipid rafts would contain PRKs. Net2A has also been used to investigate regulation of the actin binding qualities of the NAB domain. Y58 and Y59 were investigated as possible tyrosine phosphorylation sites, but it was found that substitution of these residues to either phosphomimic or non-phosphorylatable residues reduced or abolished actin binding (Dixon, 2013).

### 1.2.3 The Net3 Family

The Net3 family is composed of the three smallest members of the Net superfamily, which are only ~30kDa in size (Deeks et al., 2012). Stable transformation of Net3A-GFP into BY-2 cells showed that it localised to endoplasmic filaments and more predominantly to the nuclear membrane (Deeks et al., 2012). Net3C has also been shown to localise to the ER and to the plasma membrane (PM) in a complex with VAP27 and is thought to coordinate the actin cytoskeleton to ER-PM contacts (Wang et al., 2014). Net3B is the oddball of the Net superfamily as a whole as it fails to bind actin, and has a poorly conserved NAB domain when compared to other Nets (Cartwright, 2011), but the double mutant *Net3C RNAi/net3b* has been shown to be gamete lethal (Wang et al., 2014). This means that both Net3B and 3C are essential. Mutagenesis of K211 in Net3C caused actin-ER associated punctae to become more mobile. The mutation of C-terminal F209 and F210 to alanine residues caused enhanced F-actin binding, but disrupted the ER network and the mobility of VAP27-labelled ER-PM contact sites was increased. Both imply that an interaction is occurring between the C-terminus of Net3C and phospholipids at the ER-PM contact site in order to anchor the actin cytoskeleton there (Wang et al., 2014).

#### 1.2.4 The Net4 family

The Net4 family is composed of two members, both of about 60kDa in molecular weight (Deeks et al., 2012). They are most like the Net ancestor which evolved around the same time as vascular plants (Hawkins et al., 2014). Net4A and Net4B are both associated with the tonoplast in roots but have differing affinities for actin binding, with Net4B having lower affinity. Yeast-2-hybrid analyses have shown that the Net4 proteins can form homo- or hetero-oligomers. This family has the potential to organise actin arrays at the vacuole (Hawkins and Mentlak, unpublished), which may in turn facilitate the development of the central vacuole seen in mature root cells. Net4B is also expressed in guard cells, which depend heavily on actin array and vacuolar morphology for their dynamic function (Higaki et al., 2006) (Gao et al., 2008). The Net4 family, along with Net3A and Net3C, contain a conserved C-terminal IRQ domain, which has been shown in Net4B to facilitate interactions with Rab3 GTPases (Mentlak, unpublished), which are involved in vacuolar trafficking and their fusion (Zhang et al., 2014).

#### 1.2.5 The importance of the Net Superfamily

The Net superfamily represents a diverse group of ABPs, with a previously functionally unidentified actin binding domain, which bind to a diverse range of membranes in plant cells. ABPs, as previously discussed (section 1.1) have wide ranging effects on cell morphology and development in organisms of all kinds. The way in which actin is linked to cellular membranes is not known in plants. Specifically, Net proteins have the potential to elucidate actin-membrane interactions at multiple membranes in plant cells, which may form the basis for the viability of plant tissues. They are evolutionarily important given their evolution alongside vascular plants (Hawkins et al., 2014), and thus may give evidence as to the structural and signalling support required for vertical growth in plants. From an industrial perspective, they may allow for the investigations into new avenues of pesticide development or genetically modified crops that are resistant to multiple kinds of stress, given that actin cytoskeleton remodelling often occurs during stress. Overall, therefore, the implications for elucidating the functionality of these proteins are great. One key aspect in understanding their

function is identifying the mechanisms by which they are regulated; of which one facet is post-translational modification, which is the focus of this project.

### **1.3 The importance of post-translational modification in plant development**

Post-translational modification is the process by which accessory groups are covalently linked to translated proteins in order to confer additional or altered functionality. It may involve the addition of non-peptides, such as carbohydrates and lipids. Three major types of post-translational modification will be investigated in the context of the Net Superfamily in this project; acylation, sumoylation and phosphorylation, the latter of which will be the major focus. It is therefore important to discuss the roles of these modifications in plant development and in the function of certain ABPs.

#### 1.3.1 Phosphorylation

In proteins, phosphorylation is the addition of a phosphate ( $\text{PO}_4^-$ ) group to a serine, threonine, or more rarely a tyrosine residue, although there is tentative evidence to suggest that tyrosine phosphorylation of plant proteins may be more abundant than previously expected (Sugiyama et al., 2008) (de la Fuente van Bentem and Hirt, 2009). Indeed, the general state of tyrosine phosphorylation has been found to influence plant petiole bending (Kameyama et al., 2000). Phosphorylation events control the activity of many of the ABPs that have already been discussed. The intertwined relationship between calcium signalling and actin in pollen tubes is connected by calcium-regulated kinases. In maize ZmADF3 is phosphorylated at S6 by calmodulin-like domain protein kinases (Allwood et al., 2001), which likely abolishes its cofilin activity (Smertenko et al., 1998). Other ADFs have also been found to be regulated by phosphorylation (Allwood et al., 2002) (Augustine et al., 2008).

Phosphoregulation of actin-related processes has been studied extensively. The WAVE regulatory complex (WRC), part of the aforementioned SCAR complex, is phosphorylated multiple times on serine, threonine and tyrosine residues by a number of kinases crucial to development. This includes tyrosine phosphorylation of residues conserved in WAVE2 and WAVE3 between

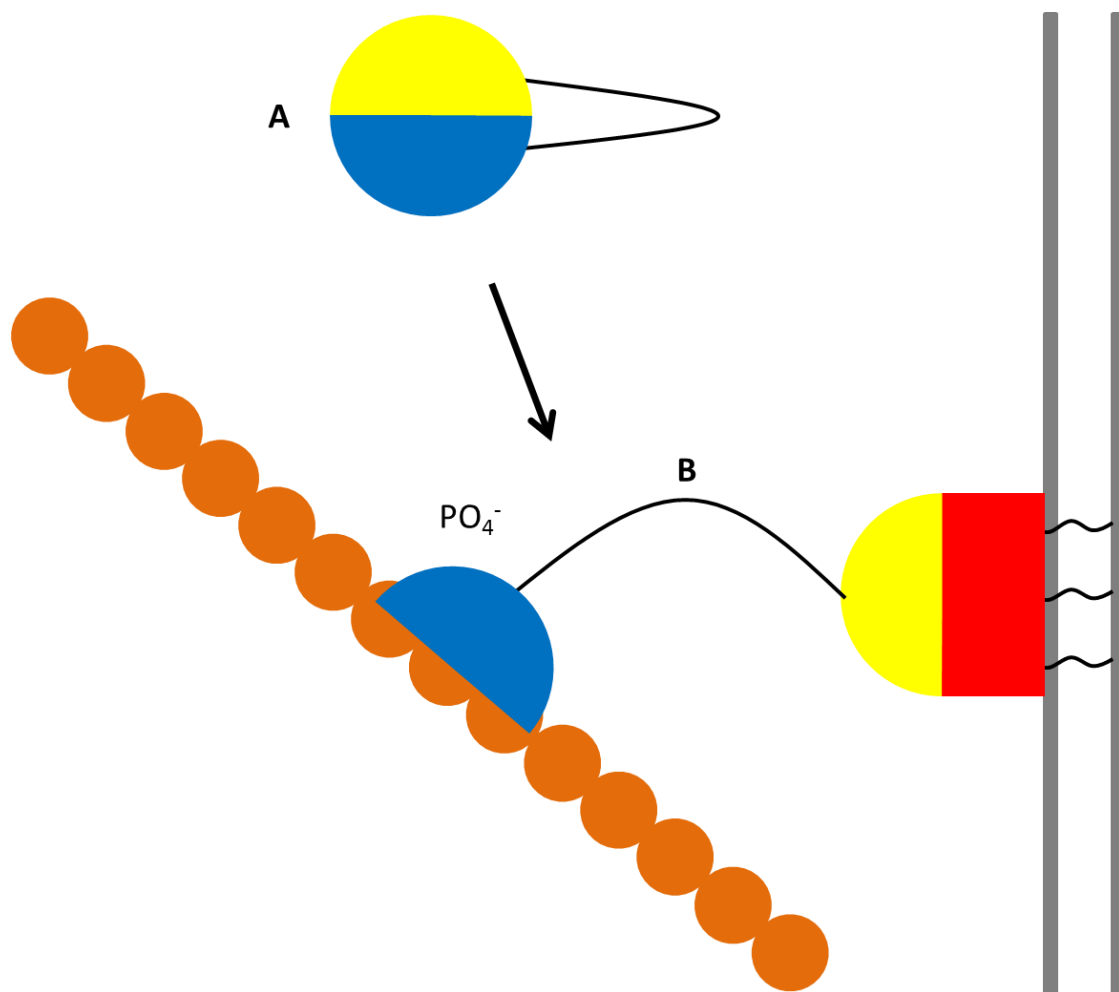
animals and plants (Mendoza, 2013). ROPs are also regulated by phosphorylation, with phosphorylation of the S74 site of ROP6 in *Medicago* preventing its interaction with its RopGEF (ROP guanosine exchange factor) upstream interactor. The mutation S74E of ROP4 in *A. thaliana* had the same effect, suggesting a conserved model for ROP activation in plants, where the phosphorylation of this residue affects the binding of RopGEFs to the nearby plant-conserved S76. Phosphorylation of S74 may have implications for the activation of kinases downstream in the signalling pathway. Given its attenuation of the effect constitutively active ROP6 (Fodor-Dunai et al., 2011), phosphorylation of ROP6 could have implications for signalling which prevents actin accumulation at the pollen tube tip. Phosphorylation of LePRK2 in *Solanum lycopersicum*, from the same superfamily of kinases as PRK1, the interactor of KIP1 (Skirpan et al., 2001), is required for pollen tube elongation (Salem et al., 2011). Similarly the phosphorylation of T161 of cyclin-dependent kinase A, is required for cell division, by allowing the activation of a downstream kinase (Harashima et al., 2007). It is clear therefore that phosphorylation is a key component of multiple signalling pathways in plants, including those relevant to ABPs and actin arrays.

#### 1.3.1.1 Moesin, Ezrin and domain masking

Certain members of the FERM-domain family of proteins in animals are membrane-bound ABPs. Moesin (Pearson et al., 2000) and Ezrin (Fievet et al., 2004) have both been shown to require phosphorylation events to occur at their respective C-termini to facilitate unfolding, and interact with PIP2 at membranes via their FERM domain (Maniti et al., 2012). The C-terminus acts as an actin binding domain to connect the two (Pearson et al., 2000) (Fievet et al., 2004). In the folded state, the interaction of these two domains inhibits their respective binding functions (figure 6). This model was used as a starting point for investigation of whether phosphorylation sites outside the NAB domain could influence the actin binding of Net proteins, given their highly coiled-coiled nature and defined terminal actin binding domain. These two proteins are similar in size to the Net4 proteins, the first members of the Net superfamily to evolve (Hawkins

et al., 2014), so it was perceived that this model could have implications for the Net4 proteins specifically or the superfamily as a whole.

Figure 6: The general mechanism by which ERM (ezrin/radixin/moesin) proteins are activated; **A** when inactive, the N- (yellow) and C-termini (blue) of ERM proteins interact with one another, inhibiting the function of their actin binding and membrane interacting domains. **B** phosphorylation of a C-terminal threonine residue (indicated by  $\text{PO}_4^-$ ) creates a hydrophilic pocket which causes the termini to move apart, allowing the functionality of the actin (orange) binding C-terminus (blue) and allowing the N-terminal FERM domain (yellow) to interact with a membrane bound adaptor protein (red). Image inspired by a similar figure in Pearson et al., 2001.



### 1.3.2 Acylation

Acylation is the covalent attachment of fatty acid groups of various sizes to specific residues and motifs of proteins. It is largely thought to facilitate either protein-protein or protein-membrane interactions by the formation of hydrophobic regions, which kinetically allows the interaction (Zhang & Casey, 1998) (Resh

1999). There are multiple types of acylation which can confer specific or altered functionalities, some of which are discussed in this thesis; S-acylation, prenylation, glycosylphosphatidylinositol (GPI) anchorage and N-myristoylation. Pathways involving the addition of these groups are important for morphological and developmental reasons in plants. Given the membrane bound nature of all Nets, and the oligomerisation of others, this group of modifications have the potential to be extremely important for their regulation and localisation.

### 1.3.2.1 S-acylation

S-acylation, or palmitoylation, represents a dynamic post-translational modification. It is the addition of a fatty acid, most often a palmitate or stearate group, which often results in permanent attachment to a membrane. This is often in tandem with another acylation event (Shahinian & Silvius, 1995). Despite this, S-acylation is also a dynamic modification and is the only type of acylation that is reversible, allowing for precise regulation of proteins at membranes (Hemsley and Grierson, 2008). As such this type of modification has wide implications for regulated protein-membrane interactions in plants.

ROPs, as previously discussed, have their roles intertwined with membrane interactions. GTP-bound active ROP6 is membrane bound and S-acylated, but the inactive GDP-bound form is not, suggesting that its S-acylation is integral to its active role at the plasma membrane. There is the potential, like phosphorylation of S74 (section 1.3.1), that S-acylation is a general activator for ROPs (Sorek et al., 2007). One could speculate that one of these post-translational modifications influences the other. The presence of hydrophobic amino acid residues adjacent to S-acylated cysteine residues in other ROPs is thought to facilitate the strengthening of membrane binding by protecting against cleavage by S-acyl protein thioesterases (Hemsley & Grierson, 2008). S-acylation itself can be critical for actin-requiring developmental processes in plants. Recently it was found that polar growth of root hairs in *A. thaliana* is affected by 2-bromopalmitate (2-BP), a specific inhibitor of S-acylation, the addition of which caused mislocalisation of PIP2, increased vacuolarisation and impairing actin dynamicity, the latter of which involved the formation of highly crosslinked networks of short, highly-bundled microfilaments. This suggests that

S-acylation may have significant control over the function of ABPs, given treatment with 2-BP does not mimic the effects of the actin-depolymerising drug latrunculin B (Zhang et al., 2015).

### 1.3.2.2 Prenylation

Prenylation, in contrast to S-acylation, is a non-reversible post-translational modification that adds either a farnesyl or geranylgeranyl fatty acid group to specific C-terminal motifs. The most common of these motifs is the CaaX (Cysteine-aliphatic-aliphatic-various) C-terminal motif, to which both types of prenylation groups can be added depending on the transferase enzyme involved (Gao et al., 2009). Prenylation is thought to act as a guide, giving proteins a tendency to associate with membranes due to the hydrophobicity of the added group, which then facilitates stronger membrane interactions following a S-acylation event (Helmsley & Grierson, 2008). Two other known motifs exist, specifically for the geranylgeranylation of Rab proteins, which normally C-terminate in a CC or CXC motif, and are prenylated by geranylgeranyltransferase II at one or both of the cysteines present (Khosravi-Far et al., 1992).

Prenylation of CaaX motif proteins by farnesyltransferase and geranylgeranyltransferase I, collectively CaaX prenyltransferases, is not essential in plants, but is crucial for a number of developmental processes. Mutations to farnesyltransferase I have been shown to affect cell adhesion, polar growth and cell differentiation (summarised by Thole et al., 2014). CaaX prenyltransferases have a shared alpha subunit, mutation of which also causes dramatic developmental faults (Running et al., 2004). Mutations in geranylgeranyltransferase II cause a loss of apical dominance and response defects in *Arabidopsis* (Corbin et al., 2013) (Hala et al., 2010). The loss of prenyltransferases often confers abscisic acid related defects and sensitivity (Johnson et al., 2005) (Corbin et al., 2013). All of these defects are thought to be conserved between plants and caused by mislocalisation of prenylated proteins (Thole et al., 2014). These defects are recoverable by the overexpression of other prenyltransferases, suggesting that there may be functional overlap (Johnson et al., 2005).

### 1.3.2.3 GPI anchorage

GPI anchorage is the addition of a large glycolipid to the C-terminus of a protein (Izekawa, 2002), and acts as an alternative to transmembrane domains for attaching proteins to the cell surface (Lalanne et al., 2004). In *Arabidopsis* function-abolishing mutations to SETH1 and SETH2, components for the GPI anchor biosynthetic pathway partially inhibit pollen germination and cause a reduction in pollen tube length. Overabundant deposition of callose was observed both at the tube tip and transverse to the pollen tube axis, and is the probable cause of these defects (Lalanne et al., 2004). Mutations of PNT proteins, homologs of mammalian GPI biosynthesis proteins, were embryonic lethal and also resulted in a failure to deposit cell wall material, which in turn points to a key role for GPI anchorage in plant development as a whole (Gillmor et al., 2005). Overexpression of GPI-anchored plasmodesmal neck proteins also resulted in the deposition of callose at plasmodesmata, which reduced cell-to-cell transport (Simpson et al., 2009). Cell wall composition and plasmodesmata are heavily dependent on actin-related processes (see sections 1.1.3 and 1.1.4).

### 1.3.2.4 N-myristoylation

N-myristoylation is the addition of a 14-carbon myristate group to a specific N-terminal consensus sequence, MGXXXS/T, where the methionine is cleaved to leave an exposed N-terminal glycine. N-myristoyltransferase (NMT) enzymes transfer the myristate group, and are dependent on the presence of the serine/threonine at position 6 and on lysine/arginine residues at position 7-8 (Resh, 1999). This process is important for the development of the shoot apical meristem in *A. thaliana*. Low level expression of NMT1 causes a dwarf phenotype with abnormal flower buds, followed by premature silique opening, resulting in immature seed production and sterility (Pierre et al., 2007). Knockout of NMT1 disrupts embryo viability due to disorganisation of the shoot apical meristem. Knockout of NMT2 causes a delay in flowering (Pierre et al., 2007). The N-myristoylation of the caspase cleavage product of the ABP gelsolin in humans appears to inhibit apoptosis due to the association of a small amount of gelsolin associated with mitochondrial membranes (Sakurai and Utsumi, 2006).

Connections between actin and N-myristoylation in plants remain to be determined.

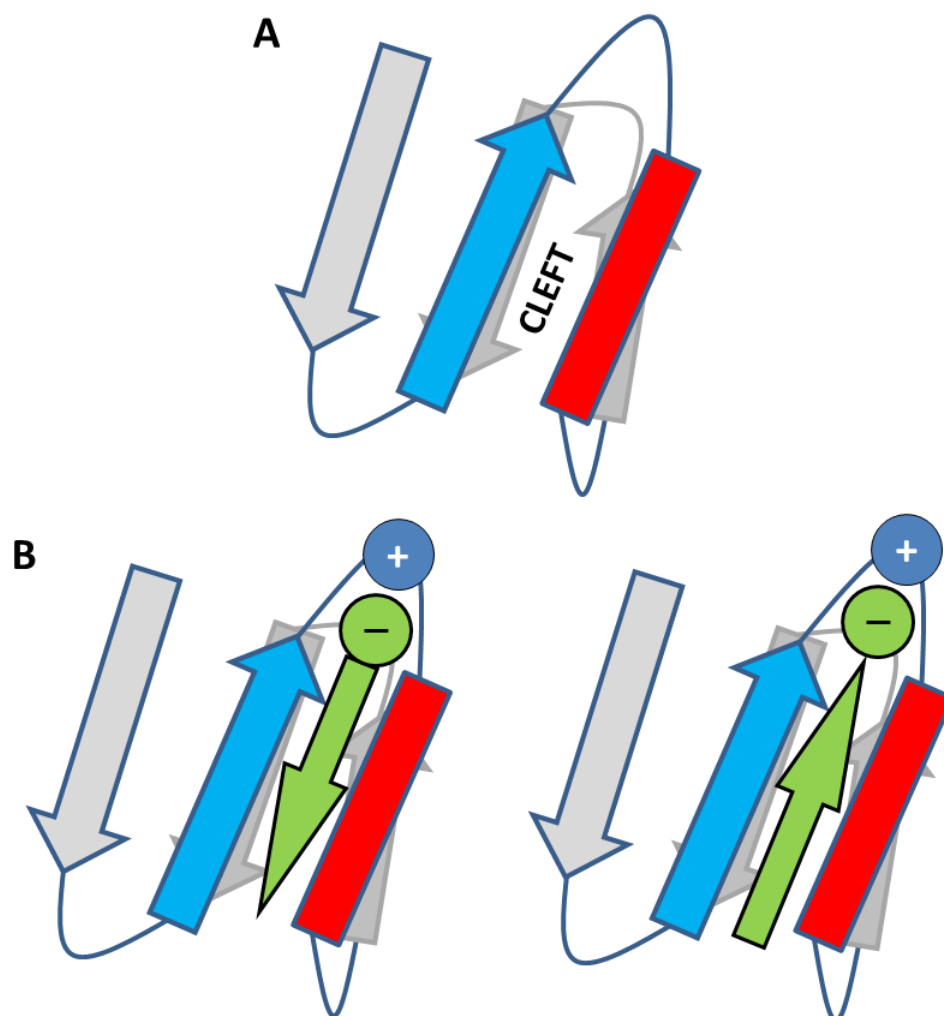
### 1.3.3 SUMOylation and SUMO-interacting motifs

Sumoylation is the reversible covalent attachment of a small ~92-103 amino acid peptide called SUMO (small ubiquitin-like modifier) to proteins that occurs via a three step process, requiring E1 activating, E2 conjugating and E3 ligase enzyme to act in a sequential fashion (Miura et al., 2007), to the consensus sequence  $\psi$ KXE/D ( $\psi$  is a hydrophobic residue). It differs from ubiquitination in the sense that it is not always used for protein turnover and can regulate protein function through determining its location or interactions, and can be considered dynamic and widespread (Meulmeester and Melchior, 2008). Covalent sumoylation is thought to be essential in plants, as well as animals and yeast (Meulemeester & Melchior, 2008), as the knockout of the *A. thaliana* SUMO activating or conjugating enzymes or double mutations of the SUMO isoforms SUMO1 and SUMO2 results in developmental arrest at the early embryo stage. It is thought that there are a significant number of essential sumoylated proteins at the nucleus (Saracco et al., 2007). The mutation of the *A. thaliana* E3 ligase SIZ1 causes hypersensitivity phenotypes in response to phosphate deficiency (Miura et al., 2005). It also has roles in other stress tolerances (Miura et al., 2007) (Yoo et al., 2006) (Catala et al., 2007).

SUMO-interacting motifs (SIMs, also known as SUMO-binding motifs) are an alternative mechanism of SUMO-based regulation. As opposed to covalent sumoylation, SIM-containing proteins interact with sumoylated proteins. The SIM consensus sequence is currently poorly defined; they are generally thought to contain a core of 4-5 hydrophobic residues (leucine, isoleucine and valine) flanked by acidic residues (aspartic or glutamic acid) on one side (Song et al., 2005), which determine the orientation and specificity of the interaction (Hecker et al., 2006) (Kerscher, 2007) (figure 7). In plants, SIM mediated interactions have been shown to allow plant growth regulation independent of gibberellins by the sequestration of GID1, a gibberellic acid receptor, by a sumoylated population of DELLAs (Conti et al., 2014). SIM containing proteins also regulate chromatin

activity and floral transitions (Elrouby et al., 2013). On the whole sumoylation and SIM protein activity appears to be largely associated with the nucleus.

Figure 7: Non-covalent interaction of a SIM with the SUMO peptide is dependent on a small group of hydrophobic residues, and the orientation of this interaction depends on an adjacent group of hydrophilic residues when they are present; **A** SIMs interact with the  $\beta$  grasp fold of SUMO, with the hydrophobic residues slotting into the cleft between the  $\beta 2$  strand (blue) and the  $\alpha 1$  helix (red). **B** SUMO is oriented to the SIM (green) in such a way that the group of hydrophilic residues adjacent to the SIM (-) are associated with the amino acid sequence between the  $\beta 2$  strand and  $\alpha 1$  helix (+). As such these residues cause the interaction to take place in one of two orientations, which are indicated by the arrow-point on the SIMs. Image inspired by a figure from Kerscher, 2007.



A connection between sumoylation and actin is less apparent in plants but inroads have been made. Predominantly nuclear actin is sumoylated, which prevents it being exported from the nucleus and from forming filaments in the nucleoplasm (Hofmann et al., 2009). It may also regulate the formation of actin

structures not seen in the cytoplasm (Jockusch et al., 2006). Sumoylation is also important in Rho-dependent actin control in animal cell migration. Rac, a Rho GTPase, is thought to be sumoylated in order to maintain its activity, with mutations of C-terminal sumoylation sequences causing defects in lamellipodia-membrane ruffling (Castillo-Lluva et al., 2010). Rho GDP-dissociation inhibitors (RhoGDIs) regulate Rho GTPase activity by preventing their binding to membranes, which reduces actin polymerisation. Sumoylation of RhoGDIs is thought to be responsible for this, as inhibiting sumoylation reduces RhoGDI levels and allows actin polymerisation via Arp2/3 complex recruitment to the cytoplasm (Yu et al., 2012). Multiple members of the Arp2/3 complex have also been identified as sumoylated (Alonso et al., 2015). It remains to be determined whether these sumoylation events translate to plant systems, however.

#### **1.4 Strategy of investigation for this project**

The three types of post-translational modification discussed in section 1.3 are to be investigated with a bioinformatics approach to determine their potential for occurring on Net proteins, with phosphorylation being the main initial target. Homologous sites between Net superfamily members are to be determined. A general picture of post-translational modification for Net proteins will be determined using 2-dimensional gel analysis. Upon visualisation of a western blot indicative of phosphorylation, phosphorylation will be investigated experimentally using a number of techniques (see section 3.4.2). Phosphorylation sites predicted to be relevant to the actin binding capabilities of any phosphorylated proteins would then be investigated by site-directed mutagenesis. The outcomes of these processes are detailed in section 3.

## **Chapter 2: Materials and Methods**

### **2.1 Plant Growth Conditions**

#### **2.1.1 *Arabidopsis thaliana* seed collection**

Seeds were collected using an ARACON container system to protect against contamination by other nearby plants. Plants taken from an initial nursery (see 2.1.3) were replanted individually in intercept- or later calypso-treated soil in wells of a seed tray and placed in a growth room (21°C, 16 hour day). Once a rosette was formed the ARACON base was placed over it and the ARACON tube added to allow the plants to grow vertically as it developed. Once siliques were fully formed and parts of the plants were visibly senescent, the tray was taken to a drying room. Seeds were sieved from other plant material, placed into parafilm-sealed petri dishes and left to dry out. After 2 weeks, the seeds were transferred to 1.5ml Eppendorf tubes for storage.

#### **2.1.2 *Arabidopsis thaliana* for seedling total protein extraction**

Whole plants used for protein extraction were grown in sterile conditions. *Arabidopsis thaliana* ecotype Col-0 seeds were sterilised in 10% bleach, diluted in dH<sub>2</sub>O. Seed Eppendorf tubes were inverted five times in 5 minutes to ensure all seeds were exposed to the bleach. The seeds were then washed in dH<sub>2</sub>O for a further five inversions, twice. Washed seeds were distributed onto horizontal and vertical Petri dishes containing ½ MS medium, which had been made in a sterile flow hood and left open to prevent condensation. Vertical plates were favoured as they generated more accessible root tissue. Seed numbers varied from 15 to 50 per plate, and were spaced at regular 1 centimetre intervals. Petri dishes were sealed using Parafilm (Sigma Aldrich), and placed in a 4°C fridge for 3 days to synchronise germination. Petri dishes stored in a Sanyo growth cabinet for approximately 12 days at 21°C with a 16 hour day. Plants were deemed to be ready for protein extraction once 4-6 true leaves had grown and were taken immediately for grinding (see 2.2.1).

### 2.1.3 *Arabidopsis thaliana* for flower protein extraction

Plants grown for flower collection were grown initially in non-sterile conditions. A pinch of Col-0 seeds was sprinkled onto an intercept-, and later calypso-, treated soil, to create a nursery. Plants were then grown in a Sanyo growth cabinet for approximately 12 days at 21°C with a 16 hour day. Once 4-6 true leaves had grown multiple plants were spaced at an interval of 1 inch in a seed tray filled with soil treated with intercept or calypso. Only plants that could be transferred with their complete root tissue intact were transferred. Plants were then allowed to proceed to the flowering stage in a growth room. Flowers were harvested at a time when white petals were visible and siliques were still green, and there were more than 20 flowers per plant. Flowers were harvested using a pair of tweezers to remove flowers from just below their base. Collected flowers were then immediately taken for grinding (see 2.2.1).

## **2.2 Gel Electrophoresis**

### 2.2.1 Protein extraction

Plant material (see 2.1.2 and 2.1.3) was transferred immediately to a liquid-nitrogen-cooled mortar and ground into a fine powder with a liquid-nitrogen-cooled pestle. A spatula cooled in liquid nitrogen was then used to transfer the grindings to liquid nitrogen cooled 1.5ml Eppendorf tubes, which were filled approximately to half-volume. These tubes could then be stored immediately at -80°C or taken straight away for solubilisation. Plant grindings were solubilised in 1-1.5ml TE buffer (10mM pH 8.0 Tris/HCl and 1mM pH 8.0 EDTA in dH<sub>2</sub>O) depending on the volume of grindings. The solution was rocked for 15 minutes at a low rpm and then spun down for 5 minutes at maximum speed (13200 rpm) in a microcentrifuge to remove insoluble material. The green supernatant was then transferred to a 15ml Falcon tube and 4 volumes of 100% acetone were added. Falcon tubes were then stored at -20°C for 30-45 minutes to allow protein precipitation. The resulting precipitate was then separated from the supernatant by repeated 10 minute maximum speed microcentrifuge spins of 1.5ml volumes of the acetone solution. The supernatant was discarded and 1ml 80% acetone added to the precipitate, which was broken up by a short vortex. This acetone solution was then placed at -80°C for 30 minutes, spun down at maximum speed

for 10 minutes and the supernatant discarded. This was repeated if any pigment was left in the precipitate after this step. The precipitate was then left to air dry for up to 5 minutes to allow any residual acetone to evaporate. Lysis buffer (8M Urea, 2M Thiourea, 4% CHAPS in dH<sub>2</sub>O, never brought above 37°C) was then added to the protein precipitate, at a volume depending on the size of the precipitate, and shaken at a low rpm for 1 hour. The solution was then spun down for 5 minutes at maximum speed and the supernatant extracted and put into fresh, sterile Eppendorf tubes.

### 2.2.2 Bradford Assay

Bradford assay was used to determine protein concentration. Bovine serum albumin (BSA) standards were made and samples prepared in 1ml cuvettes according to the following table;

Standards	0	1	2	5	10	15	20	Samples	X
1mg/ml BSA (μl)	0	1	2	5	10	15	20	Sample (in Lysis Buffer)	2
0.1M HCl (μl)	10	10	10	10	10	10	10		10
Lysis Buffer (μl)	2	2	2	2	2	2	2		0
H <sub>2</sub> O (μl)	88	87	86	83	78	73	68		88

900μl 20% Bradford solution (BioRad) was added to each cuvette and left for 10-15 minutes. Readings were recorded at 595nm on a spectrophotometer (Eppendorf AG), and were then analysed in Microsoft Excel. Average readings were taken for each sample and calculations performed to determine a relevant mass or volume from the determined protein concentration, depending on the future use of the sample. Samples were then stored at -20°C until use or taken forward immediately for further experimentation.

### 2.2.3 Alkaline Phosphatase Treatment

Calf intestinal phosphatase (CIP) was used to dephosphorylate protein samples. Following Bradford assay, protein samples were precipitated by acetone

precipitation in the same manner as in 2.2.1. The protein was then re-suspended in CIP buffer (100mM NaCl, 50mM Tris-HCl, 10mM MgCl<sub>2</sub>, 1mM DTT, pH 7.9 at 25°C) at a ratio of 10µl per 1µg protein and a protease inhibitor cocktail (leupeptin, pepistatin A, TAME and PMSF) added. One unit of CIP was then added per µg of protein, and the sample incubated at room temperature for up to one hour. The sample was then acetone precipitated again and returned to the lysis buffer.

### 2.2.4 Running Gel Preparation

Running gels for both 1- and 2-dimensional electrophoresis were both made from the following recipes, depending on the size of protein being investigated;

Ingredient	Gel Percentage				
	5%	7.5%	10%	12%	15%
<b>30% Acrylamide</b>	1.66 ml	2.5 ml	3.33 ml	4.0 ml	5.0 ml
<b>0.8% SDS</b>	1.25 ml	1.25 ml	1.25 ml	1.25 ml	1.25 ml
<b>3M Tris pH 8.8</b>	1.25 ml	1.25 ml	1.25 ml	1.25 ml	1.25 ml
<b>Milli-Q ultrapure water</b>	5.77 ml	4.93 ml	4.1 ml	3.43 ml	2.43 ml
<b>10% Ammonium Persulphate</b>	50 µl	50 µl	50 µl	50 µl	50 µl
<b>TEMED</b>	20 µl	20 µl	20 µl	20 µl	20 µl

The 30% acrylamide was pre-made (Protogel, National Diagnostics) and the 10% ammonium sulphate either made up on the day or drawn from a stock kept at 4°C for no more than 2 weeks. The small amount of 100% ethanol was used to make a straight edge at the top of the gel, and was washed out using dH<sub>2</sub>O and sterile paper towels prior to use.

### 2.2.5 1-Dimensional Gel Electrophoresis

A stacking gel was also made on top of the running gel from the following recipe;

Ingredient	Gel Percentage
	5%
<b>30% Acrylamide</b>	0.8 ml
<b>0.8% SDS</b>	0.625 ml
<b>1M Tris pH 6.8</b>	0.625 ml
<b>Milli-Q ultrapure water</b>	2.905 ml
<b>10% Ammonium Persulphate</b>	25 $\mu$ l
<b>TEMED</b>	20 $\mu$ l

Wells were made using the appropriate comb for 1mm thickness gels. Gels were then used immediately or stored in damp tissue and cling-film at 4°C for up to 24 hours.

Protein samples consisted of a 4:1 ratio of protein extract to sample buffer (Ingredients). Protein samples were boiled at 95°C for 5 minutes before use. Gels were run in the Protean II electrophoresis kit (BioRad), which was filled completely with SDS running buffer (14.4g/L glycine, 3g/L Tris, 1g/L SDS in dH<sub>2</sub>O). Samples were added to a volume of 10-20 $\mu$ l depending on the sample concentration. The molecular weight ladder used was (dual colour). Electrophoresis was run at 80-150V and the wave-front was allowed to reach the bottom of the gel.

### 2.2.6 2-Dimensional gel electrophoresis

First dimension was performed using 7cm, pH 3-10 or 4-7 immobilised pH gradient (IPG) strips (Immobiline DryStrip, GE Healthcare). Strips were loaded with 80-160 $\mu$ g protein samples made up in 110 $\mu$ l lysis buffer, 10 $\mu$ l bromophenol blue diluted in lysis buffer, 2.5 $\mu$ l 50% dithiothreitol (DTT) and 2.5 $\mu$ l 3-10 ampholytes. Samples were pipetted into a level re-swelling tray and the IPG strips placed gel-side down on top of them, covered by 2-3ml DryStrip cover fluid (PlusOne), and left overnight at room temperature. The IPG strips were then rinsed using dH<sub>2</sub>O and underwent electrophoretic separation gel side up at 21°C using the Multiphor II (Pharmacia Biotech), under voltage gradients as specified by the GE Healthcare Immobiline DryStrip handbook. Strips were then equilibrated at room temperature in 5ml equilibration buffer (50mM Tris/HCl pH

8.8, 6M Urea, 30% Glycerol, 10% SDS), with DTT (10mg/ml), and then iodoacetamide (48 mg/ml), for 15 minutes each, on a shaker moving at 30 rpm. The strips were rinsed with dH<sub>2</sub>O and placed horizontally in dH<sub>2</sub>O across the top of a premade running gel (see 2.2.3). A molecular weight ladder was made from a small piece of filter paper soaking 2.5 $\mu$ l (dual colour) and placed at the high pH end of the strip. Water was then blotted out and replaced by approximately 750 $\mu$ l agarose sealer (stock made from 100ml SDS running buffer (see 2.2.3), 0.5g agarose, and a few grains bromophenol blue). Gels were run at 60V for 10 minutes and then at 120V until the wave-front had reached the bottom of the gel.

### 2.2.7 Coomassie Staining

Gels were placed in dH<sub>2</sub>O, followed by Instant Blue (Expedeon), and left to stain for 1-12 hours under light shaking. Gels were then left in dH<sub>2</sub>O until imaged.

### 2.2.8 Nitrocellulose membrane phosphostaining

Membranes were stained using the Pro-Q Diamond Phosphoprotein Blot Stain Kit (ThermoFisher Scientific) according to the manufacturer's instructions. Briefly, proteins were fixed onto the nitrocellulose membrane by immersion in Fix Solution (7% acetic acid, 10% methanol) for 10 minutes, washed in dH<sub>2</sub>O for 3x5 minutes, stained with the diluted phosphostain and destained using the appropriate destain solution. The membrane was then washed again for 3x5 minutes. The membrane was then allowed to air dry or was taken wet to be imaged on the Typhoon 9400 (Amersham Biosciences).

## **2.3 Western Blotting**

### 2.3.1 Protein Transfer

Protein transfer was performed using the Protean II Transfer Kit (BioRad). All components were immersed in transfer buffer (20% ethanol, 2.4g/L Tris, 11.34g/L Glycine). Transfer cassettes were arranged from the anode as follows; sponge, 2x filter paper, nitrocellulose membrane, SDS-PAGE gel, 2x filter paper, sponge. Nitrocellulose membranes with pore sizes of 0.45 $\mu$ m and 0.2 $\mu$ m were used. Transfer was run at 70V and 4°C for 1 hour or 20V and room temperature overnight. Transfer efficiency was tested using 0.25% Ponceau S solution, which

was washed off using TBS-T (1% 1M Tris/HCl pH 8.0, 0.15M NaCl, 0.1% Tween 20) prior to antibody probing.

### 2.3.2 Antibodies

The following primary antibodies were sourced internally, from other members of the Hussey group, or externally as shown.

Name	Raised in	Raised against	Source
Net1A	Mouse	Net1A	Calcutt, 2009
Net1B	Mouse	Net1B	Calcutt, 2009
Net1C	Rabbit	Net1C	Ingle, 2011
Net1D	Rat	Net1D	Ingle, 2011
Net3C	Mouse	Net3C	Wang et al., 2014
Net4B	Rabbit	Net4B	Mentlak, unpublished
Mouse Anti-actin, monoclonal (C4 clone)	Mouse	Actin	ICN Biochemicals

The following secondary antibodies were sourced externally as shown.

Name	Raised in	Raised against	Source
Goat anti-rabbit immunoglobulins HRP	Goat	Rabbit	DAKO
ECL sheep anti-mouse IgG horseradish peroxidase linked	Sheep	Mouse	GE Healthcare
Anti-rat IgG Horseradish Peroxidase Linked whole antibody	Goat	Rat	Amersham

### 2.3.3 Antibody probing

Nitrocellulose membranes were blocked in 5% milk/TBS-T in order to reduce non-specific antibody binding by shaking for one hour at room temperature or 4°C overnight. Antibodies were diluted in this blocking solution at a range of dilutions, depending on the antibody used. Antibody incubations were performed in a

square petri dish lined with two damp pieces of filter paper with a square of parafilm on top, were 1-1.5 hours long and at room temperature, for both primary and secondary antibodies. Nitrocellulose strips, from 1D gels, were placed protein side up on the parafilm and the relevant antibody pipetted on top, and full membranes, from 2D gels, were placed gel side down on top of 3ml diluted antibody solution, which was already pipetted onto the parafilm. Washes in TBS-T following antibody incubations were 3x5 minutes long. Nitrocellulose strips were washed in individual 15ml Falcon tubes.

#### 2.3.4 Blot Imaging

Western blots were imaged using Immobilon Western Chemiluminescent HRP (HorseRadish Peroxidase) substrate (Millipore) because all secondary antibodies were HRP-conjugated. It was applied to the nitrocellulose as described for antibody incubation (see 2.3.2), and left for 5 minutes. The nitrocellulose was then exposed to chemiluminescent film for periods of time ranging from 10 seconds to 10 minutes. Images were generated by (dark room machine).

### 2.4 Molecular Biology Methods

#### 2.4.1 Transfection of chemically competent cells by heat shock

##### 2.4.1.1 *Escherichia coli*

Aliquots of cells (50-100 $\mu$ l) were thawed on ice, to which approximately 100ng of the relevant DNA was added. The mixture was left on ice for 1 hour. The mixture was then placed in a heat block at 42°C for 40 seconds, and then back on ice for 2-5 minutes. A 500 $\mu$ l volume of SOC medium (2% tryptone, 0.5% yeast extract, 10 mM NaCl, 2.5 mM KCl, 10 mM MgCl<sub>2</sub>, 10 mM MgSO<sub>4</sub>, and 20 mM glucose) was added to the cells and the mixture placed on a shaker at 37°C for 1 hour at 180 rpm. Cells were then spread over plates containing LB medium (10g/L Tryptone, 5g/L Yeast Extract 10g/L NaCl, 15g/L Agar, adjusted pH to 7.0 with NaOH) with the relevant antibiotic(s) for selection, and incubated overnight at 37°C. Colonies were then taken and incubated in liquid LB medium with the same antibiotic(s) overnight at 37°C.

##### 2.4.1.2 *Agrobacterium tumefaciens* GV3101 Strain

Aliquots of cells (~100 $\mu$ l) were thawed on ice, to which approximately 100ng of the relevant plasmid was added and the two mixed. The mixture was then frozen in liquid nitrogen for 5 minutes, and then immediately removed to a heat block set at 37°C for 5 minutes. Immediately after this 500 $\mu$ l SOC medium was added. The mixture was then shaken at 200rpm for 3 hours at 30°C. After this the mixture was spun down at <3000rpm for three minutes. Cells were then spread onto plates containing YEB medium (5g/L Meat Extract, 1g/L Yeast Extract, 5g/L peptone, 5g/L sucrose, 0.5g/L MgSO<sub>4</sub>•7H<sub>2</sub>O, 8g/L Agar, adjusted to pH 7.2 with NaOH) with rifampicin, gentamicin and kanamycin, and incubated at 30°C for 2 days. Single colonies were then taken and grown in liquid YEB (no agar) overnight at 30°C.

#### 2.4.2 Transformation of electrically competent cells

Electrically competent cells were used for transformations following the use of Gateway Cloning as they were thought to perform better with this technology.

##### 2.4.2.1 *Escherichia coli*

Aliquots of cells (50-100 $\mu$ l) were thawed on ice, to which approximately 100ng of the relevant DNA was added. The mixture was then transferred to an ice cold electrocuvette, which was then transferred immediately to the Micropulser (BioRad). A 500 $\mu$ l volume of SOC medium was added to the cells immediately and the mixture placed on an orbital shaker at 37°C for 1 hour at 180 rpm. Cells were then spread over plates, incubated, and transferred to liquid medium as in the manner of section 2.4.1.1.

##### 2.4.2.2 *Agrobacterium tumefaciens*

Aliquots of cells (50-100 $\mu$ l) were thawed on ice, to which approximately 100ng of the relevant DNA was added. The mixture was then transferred to an ice cold electrocuvette, which was then transferred immediately to the Micropulser (BioRad). A 500 $\mu$ l volume of SOC medium (ingredients) was added to the cells immediately and the mixture placed on an orbital shaker at 30°C for 3 hours at 200 rpm. Cells were then spread over plates, incubated, and transferred to liquid medium as in the manner of section 2.4.1.2.

### 2.4.3 Plasmid DNA Purification

Plasmid DNA was purified using the Wizard Plus SV Minipreps DNA Purification system (Promega) according to the manufacturer's instructions. Briefly, cells in 6-8ml of the relevant liquid media were spun down at 4000rpm in a centrifuge for 20 minutes, allowing the removal of the cells from the media. A volume of 250 $\mu$ l Cell Re-suspension Solution was added allowing re-suspension of the cells. To this was added 10 $\mu$ l Alkaline Protease Solution and 250 $\mu$ l Cell Lysis Solution, and the mixture left for 5 minutes at room temperature after being inverted 6 times. 350 $\mu$ l Neutralisation Solution was added and the mixture underwent 6 further inversions, and was then centrifuged at maximum speed for 10 minutes. The supernatant was then extracted without the pellet and transferred to a Wizard SV minicolumn. It was centrifuged for a further minute and the supernatant discarded. 750 $\mu$ l Column Wash Solution (CWS) was then added to the column, which was then centrifuged at maximum speed for 1 minute. The supernatant was discarded and a further 250 $\mu$ l CWS added to the column, which was centrifuged at maximum speed for a further 2 minutes. The column was then transferred to a sterilised Eppendorf tube and 100 $\mu$ l sterilised ultrapure water added, and centrifuged at maximum speed for 1 minute. The flow-through supernatant was then put into a fresh sterilised Eppendorf tube used immediately or stored at -20°C. DNA concentration was quantified using the ND-1000 Spectrophotometer (Nanodrop).

### 2.4.4 Agarose Gel Electrophoresis

Gels were made by dissolving 1% (agarose) in 1x TAE buffer (ingredients) by microwave heating and adding 5 $\mu$ l ethidium bromide solution (0.3mg/ml) per 200ml of 1x TAE. The gels were set by pouring this mixture into trays containing combs and leaving for 30 minutes. Electrophoresis was carried out by placing the gel into an electrophoresis tank containing 1x TAE buffer. DNA was loaded into a well at a 5:3 ratio with DNA loading buffer (source) and the gel run at 150V for up to 40 minutes. 5 $\mu$ l of 2-Log DNA ladder was used as DNA molecular weight marker. Gels were visualised under UV using the Syngene InGenius gel documentation system.

### 2.4.5 Site Directed Mutagenesis

Site-directed mutagenesis was performed using the QuikChange II XL Kit (Aligent) according to the manufacturer's instructions. Primers were designed in accordance with the protocol using the PrimerX (<http://www.bioinformatics.org/primerx/>) primer design software. Reactions were made from the following constituents; 5 $\mu$ l 10x Reaction Buffer, 50ng Net4B in pDONR207 dsDNA template, 125ng forward primer, 125ng reverse primer, 1 $\mu$ l dNTP mix, 3 $\mu$ l QuikSolution, made to 50 $\mu$ l with nuclease free water. PfuUltra HF DNA Polymerase (2.5U/ $\mu$ l) was then added at a volume of 1 $\mu$ l. The reaction was then performed at the following cycling parameters

Phase	Number of Cycles	Temperature[ $^{\circ}$ C]	Time
1	1	95	1 min
2	18	95	50 sec
		60	50 sec
		68	1 min/kb plasmid length
3	1	68	7 min

The reactions were then cooled to 4 $^{\circ}$ C until ready for *Dpn* 1 treatment. The *Dpn* 1 restriction enzyme (10U/ $\mu$ l) was added at a volume of 1 $\mu$ l and mixed thoroughly. The reactions were then spun down in a microcentrifuge for 1 minute and incubated for 1 hour at 37 $^{\circ}$ C to digest any non-mutated dsDNA. Mutated vectors were then taken forward for transformation (see sections 2.4.1 and 2.4.2).

#### 2.4.6 LR Reaction

Mutated genes were conjugated to GFP tags by LR reaction into the relevant destination vector. The LR reaction was performed according to the Life Technologies Gateway Cloning Protocols. Briefly, 100-150ng of entry clone (Net4B in pDONR207) was added to 150ng of destination vector per reaction. Reactions were made up to 4 $\mu$ l with TE buffer (10mM Tris HCl, 1mM EDTA, pH 8.0). The LR Clonase II enzyme was then added at a volume of 1 $\mu$ l per reaction and mixed by careful pipetting. Reactions were then incubated at 25 $^{\circ}$ C for 1 hour. Following this, 1 $\mu$ l of Proteinase K solution was added to terminate the reaction. Reactions were then vortexed briefly and incubated at 37 $^{\circ}$ C for 10 minutes, before immediately being transferred to a transformation reaction (see sections 2.4.1 and 2.4.2).

#### 2.4.7 Colony PCR

Colony PCR was used to determine the efficacy of the LR reaction of the Net4B gene from pDONR207 to PMDC83. Single colonies drawn from plates containing transformed *E. coli* were streaked out onto new plates with rifampicin, gentamycin and kanamycin split into a grid system. Streaks were allowed to grow overnight, after which 20% of the streak was taken and the cells lysed in 30µl dH<sub>2</sub>O. PCR reactions were then made (15µl lysed cells, 5µl 10x NH<sub>4</sub>, 2µl 50mM MgCl<sub>2</sub>, 5µl 2mM dNTPs, 1.5µl each Net4B internal primer, 0.25µl BioTaq HF Polymerase, made to 50µl with nuclease free water) and a PCR performed at the following conditions;

The LR reaction was deemed successful upon detection of the correct size of fragment following completion of the PCR.

#### 2.4.8 Transient expression of Net4B mutant constructs in *N. benthamiana* leaves

*A. tumefaciens* strain GV3101 was used for infiltration. Plants used were 4-5 weeks old. Infiltration was performed following the protocol made by Chris Hawes of the Plant Endomembrane Research Group at Oxford Brookes University. Overnight cultures (5ml) of cells in LB with rifampicin, gentamycin and kanamycin were spun down for 5 minutes at 4000rpm using the (Big centrifuge). The supernatant was then removed using a Pasteur pipette, using a different pipette for each culture. Cells were re-suspended in 1ml infiltration medium (250mg D-glucose, 500µl 500mM MES, 500µl 20mM Na<sub>3</sub>PO<sub>4</sub>•12H<sub>2</sub>O, 25µl 200mM Acetosyringone) and then spun down again under the same conditions. The supernatant was removed and the cells re-suspended in a further 1ml infiltration medium. A 10x dilution of the resuspension solution was made in a 1ml cuvette using 100µl resuspension plus 900µl infiltration solution. The (spectrophotometer) was used to measure the relative optical density (OD) of the solutions at 600nm. Agroinfiltration solutions were then made containing GV3101 cells with both P19 and the Net4B genes, both at an OD of 0.1, made up to 1ml with infiltration medium. Infiltration was performed using 1ml needle-less syringe, which was used to inject the underside of leaves which had been kicked using a scalpel blade. Infiltrated plants were left for 2 days for protein expression to occur, after

which small 3x3mm sections of the leaf were removed, mounted on slides in either distilled water or (the other thing) and imaged.

#### 2.4.9 Imaging using the Zeiss 880 Laser Scanning Confocal Microscope

The slides described in 2.4.6 were viewed using a x63 oil immersion lens. Since all constructs were GFP tagged, imaging was performed at an excitation wavelength of 488nm, and emission wavelengths of 505-530nm detected.

### **2.5 *In vitro* synthesis of proteins**

#### 2.5.1 Total RNA extraction

Total RNA was extracted using the Spectrum Plant Total RNA kit (Sigma Aldrich) according to the manufacturer's instructions. Briefly, 100mg of ground frozen plant tissue (see 2.2.1) was lysed in 500 $\mu$ l Lysis Solution/2-mercaptoethanol (100:1) and incubated at 56°C for 5 minutes. Cell debris was then removed by centrifugation, and the lysate supernatant was then filtered, also by centrifugation. 500 $\mu$ l binding solution was then added to the lysate supernatant as detailed by Protocol A, and the RNA collected in a binding tube by centrifugation. Three wash steps were then performed by centrifugation using Wash Solution 1 initially, and then Wash Solution 2 for the latter steps, followed by a drying step performed by centrifugation. RNA was eluted from the binding column in a single elution step. RNA concentration was quantified using ND-1000 Spectrophotometer (Nanodrop). RNA was stored at -20°C or used immediately.

#### 2.5.2 mRNA enrichment

Enrichment of mRNA from total RNA was performed using the Dynabeads mRNA DIRECT™ Kit (Life Technologies), according to the manufacturer's instructions. Briefly, Dynabeads were extracted from their storage solution and re-suspended in lysate containing ~100 $\mu$ g total RNA. The mixture was then incubated at room temperature for 3-5 minutes on a rotating mixer. A magnet was then applied to the outside of the tube for 2 minutes to pull down the Dynabeads. The supernatant was then removed and the beads washed with 600 $\mu$ l Washing Buffer A 2 times, followed by a third wash in 300 $\mu$ l Washing Buffer B. The Dynabeads were pulled out of solution using the magnet between each step. The mRNA was

then eluted from the beads using Elution Buffer (10mM Tris/HCl pH 7.5) and incubated at 70°C for 2 minutes. The Dynabeads were pulled down and the supernatant removed to an RNase free Eppendorf tube and placed on ice.

### 2.5.3 *In vitro* translation

*In vitro* translation was performed using the Rabbit Reticulocyte Lysate System, Nuclease Treated (Promega) according to the manufacturer's instructions. Radioactive elements were not included as to enable the results to be used for a western blot. Total RNA was added at a final concentration of 200µg/ml to a 50µl reaction volume containing the rabbit reticulocyte and RNasin Plus RNase inhibitor, made up with sterile ultrapure water. A control containing no RNA was also run in tandem. The 50µl reaction was then incubated at 30°C for 90 minutes, after which 5µl was taken for 1D SDS-PAGE/western blot analysis, the total volume was taken for processing for 2D SDS-PAGE/western blot analysis (see 2.2) or stored at -20°C.

## **Chapter 3: Results**

### **3.1 Prediction of phosphorylation sites in the Net proteins**

Phosphorylation, the addition of a phosphate group to serine, threonine or tyrosine amino acids within a protein, was chosen as the primary post-translational modification to be investigated for two reasons; its role in the unfolding and activation of certain ERM proteins and the homology of NET proteins to Kinase-Interacting-Protein 1 (KIP1). A kinase is an enzyme which acts to phosphorylate proteins. Multiple pieces of phosphorylation prediction software exist, each with advantages and disadvantages, and for this reason two of these programmes were used together in order to elucidate both the sites with the highest potential for phosphorylation and what type of kinases were responsible for that phosphorylation. The two pieces of software used were Scansite (Obenauer et al., 2003) and PhosPhAt (Heazlewood et al., 2008) (Durek et al., 2010) (Zulawski et al., 2013), the latter of which works in conjunction with The *Arabidopsis* Information Resource (TAIR). This allows the prediction of *Arabidopsis*-specific sites.

Net proteins vary in size but Net1 and Net2 proteins in particular are large. For this reason the sequence alignment tool ClustalW2 (Larkin et al., 2007) was used to narrow down sequences of amino acids that displayed good conservation. This was performed for both comparison of members of the same family and members from different families. Comparing proteins from the same family yielded multiple areas of extensive conservation in three families - Net1, Net2 and Net4 (figure 8). The Net3 family members only displayed conservation in their N-terminal regions. Comparisons of proteins from different families revealed very little conservation outside of the N-terminus also. The NAB domain, a defining feature of the NET family, is present at the N-terminus of all Net proteins, so conservation in this region was unsurprising. There was also evidence of conservation C-terminal to the NAB domain in multiple families, as previously described (Deeks et al., 2012) (Hawkins et al., 2014); Net families possess similar arrangements of predicted coiled-coil regions.

Having identified the C-terminus as a strong candidate for the location a common phosphorylation event in closely related Net proteins, Scansite was then used to determine potential phosphorylation sites based on whether the



compared to determine which specific sites were conserved. Scansite also gives a scoring system, with lower scores denoting more common phosphorylation sites.

The major disadvantage of Scansite with this work is that it does not show phosphorylation sites specific to plant proteins. For this reason PhosPhAt was used alongside it, as it could identify those phosphorylation sites which could occur specifically in the target organism, *Arabidopsis thaliana*. The N-terminus was also mapped and also yielded a number of conserved predicted phosphorylation sites, mostly within the NAB domain. This method allowed the identification of possible interactors which may be investigated further in future

Table 1: Results of one-to-one phosphorylation site comparison. Pairs of phosphorylation sites likely to be conserved between species were determined by cross-referencing Scansite and PhosPhAt, which identify predicted phosphorylation sites. Predicted sites in conserved regions were identified as described (figure 8).

Pair of Proteins	Respective residues
1A/1B	S1580/S1563
1A/1B	T1637/T1620
1A/1B	S1652/S1635
1C/1D	S570/S679
1C/1D	S890/S1500
1C/1D	S924/S1531
1C/1D	S927/S1534
2A/2B	Y223/Y215
2A/2B	T270/T262
2C/2D	T588/T653
3B/3C	S111/S100
3B/3C	S118/S107
4A/4B	S175/S144
4A/4B	S393/S357

work whilst also allowing the elimination of phosphorylation sites that would not be present in an *A. thaliana* protein. Relative to their lengths, the Net3 family were found to have very few phosphorylation sites compared to the other NET proteins. PhosPhAt also gives a scoring system for phosphorylation sites similar to Scansite, but the scores generated vary wildly for those predicted phosphorylation sites they have in common. For this reason the scoring system was not used as a defining factor in the selection of phosphorylation sites.

Table 2: Results of searching the representative gene locus numbers of the NET proteins in the PhosPhAt database. The returned results represent peptide sequences within individual NET proteins which have been modified by a phosphorylation or other event. Phosphorylated residues are labelled (pS/T/Y). Carbamidomethylated cysteine residues are labelled (\*C). Phosphorylated recognition sequences with multiple serine residues as phosphorylation candidates are labelled (s). The results have experimentally identified in the manner described in the attached reference. The database is not formatted correctly in its current state so some identified phosphorylation sites do not have a reference attached to them.

Protein	Phosphorylated residue within recognition sequence	Residue Position	Tissue	Reference
1A	VE(pT)LEEILK	1115	Seedlings	Engelsberger WE, et al. (2012)
1B	F(pS)NADLVIVKRQLK	1585	Cell culture	Benschop J, et .al. (2007)
1C	GQLEEGEEAIEKLF(pT)VNR	1010	Seedling	Engelsberger WE, et al. (2012) Sugiyama N, et al. (2008)
1C	SVF(*C)G(*C)VQQPE(pS)P	1110	Cell culture	Nakagami H, et al. (2010)
1C	DIVLDQT(pS)DGSSYEIVSK	886	Cell culture	Engelsberger WE, et al. (2012)
1C	(pT)IGDKLTAETENLQLK	643	Seedling	Engelsberger WE, et al. (2012)
1C	LD(pS)DLQKLENLQITVEDLK	957	Cell culture	Nühse T, et al. (2004)
1C	VLERLD(pS)DLQK	957	Cell culture	Engelsberger WE, et al. (2012)
1D	GKENE(pY)ETIK	1597	Seedlings	none
1D	DENQH(pS)AIENLVLIEFLR	993	Cell culture	none
1D	LN(pS)DLQK	1564	Cell culture	Nühse T, et al. (2007) Wang P, et al. (2013)
1D	LN(pS)DLQKLSNLHVAVEDLK	1564	Rosette	Reiland S, et al. (2011)
2A	NV(pS)SAQAKR	470	Cell culture	none
2A	(pS)VSTKTKK	783	Seedlings	none
2A	SV(pS)TEKTKK	785	Seedlings	none
2A	FADVDD(pS)PR	668	Pollen	Mayank P, et al. (2012)
2C	SDIITTQE(s)(s)DELFLQK	537/538	Pollen	Mayank P, et al. (2012)
2C	(s)A(s)EVVFAEK	487/489	Pollen	Mayank P, et al. (2012)
2D	LIDFALS(pS)KNK	896	Seedlings	Wang X, et al. (2013)
2D	LIDFALS(pS)K	896	Cell culture	Sugiyama N, et al. (2008) Nakagami H, et al. (2010) Zhang H, et al. (2013) Wang P, et al. (2013) Xue L, et al. (2013)
2D	LIDFALS(pS)KNK	896	Roots	Meyer LJ, et al. (2012)
2D	LIDFAL(pS)GSK	894	Cell culture	Sugiyama N, et al. (2008) Nakagami H, et al. (2010) Zhang H, et al. (2013) Wang P, et al. (2013) Xue L, et al. (2013)
2D	NK(pS)DLDLQHSDSR	900	Pollen	Mayank P, et al. (2012)
2D	SDLDLQHSD(pS)R	909	Seedlings	Wang X, et al. (2013)
2D	SDLDLQH(pS)DSR	907	Seedlings	Wang X, et al. (2013)
4B	MA(s)(s)TAQSKK	3/4	Seedlings	none
4B	VVAGHK(pS)K	509	Cell culture	none

By performing one to one comparisons of different proteins it was possible to drastically narrow down the sites which were most likely to be important (table 1), assuming that Net families were regulated by conserved phosphorylation events. Sites were selected based on an increased number of criteria; whether they would be phosphorylated by the same kinase, or type of kinase, according to Scansite, the similarity of the sequence around the phosphorylation site between the proteins of interest, and whether the site was predicted by PhosPhAt. A good example of the efficacy of this process is the S357 site in Net4B, which is part of an as yet un-investigated domain of the Net4 family. When looking at Scansite, there are two sites, S372 and S393 that appear in this domain in Net4A, and both sites would be predicted to be phosphorylated by a basophilic kinase, protein kinase C zeta. It becomes much more apparent that S393 is a conserved site, as its recognition sequence is extremely similar to that of S357 in Net4B, and both sites are recognised in the PhosPhAt database, whereas S372 is not. In this case, a new domain in the Net4 proteins may have been discovered using this analysis, as this region is conserved. One particularly surprising result from this analysis was that the Net2 family did not appear to have any predicted conserved C-terminal phosphorylation sites despite almost all of the conserved regions of the Net2 from the alignment study being present at the C-terminus.

The data which PhosPhAt uses to predict phosphorylation sites is drawn from over thirty different studies, which have performed high-throughput experiments on a range of *A. thaliana* tissues under different conditions of stress to identify phosphorylated peptides. Searching the TAIR accession number codes of a number of the NET proteins yields a number of results within this database, showing that 8 of the 13 NET proteins have one or more phosphorylation sites (table 2). All of these sites are produced by the PhosPhAt predictor software and some of them are also produced by Scansite. No NET3 family members are identified as phosphorylated in the PhosPhAt database. Conservation of these known sites was investigated and yielded limited results; one conserved site was found between Net1C and Net1D. These sites were also cross-referenced with Scansite in order to determine if similar phosphorylation sites are predicted, based on the aforementioned alignments, which yielded further results that may express conservation of phosphorylation sites (Table 3). The results imply that there are conserved phosphorylation sites across the Net1 and Net2 families. No

phosphorylation sites have been experimentally identified within the NAB domain according to the PhosPhAt database.

Table 3: Results of the PhosPhAt-Scansite cross-reference. Experimentally determined phosphorylation sites found in the PhosPhAt database (table 2) were cross-referenced with sites predicted by Scansite, and their surrounding peptide sequences compared. Sites were recorded as potentially conserved if the sequence and position of the sequence within the protein were similar.

Protein	Phosphorylation Site	Peptide fragment	Conserved with
1A	T1115	VE(pT)LEEILK	1B
1C	T643	(pT)IGDKLTDAETENLQLK	1B
1D	Y1597	GKENE(pY)ETIK	1C
2D	S907	SDLDLQH(pS)DSR	2C

This initial investigation added weight to the idea that the Net superfamily underwent phosphorylation events. The presence of C-terminal predicted sites in the Net1s and Net4s also implied that the ERM protein unfolding mechanism may be a possible model for these proteins' activation. Prediction of the tertiary structures of Net proteins was therefore performed to further investigate the ERM protein-like model in terms of the Net superfamily. It remained important however to continue to investigate the other Net proteins as well to try to elucidate their regulatory mechanisms through bioinformatics analysis as to better infer from the outcome of 2-dimensional electrophoresis, so the Net2 and Net3 proteins were investigated in this manner as well.

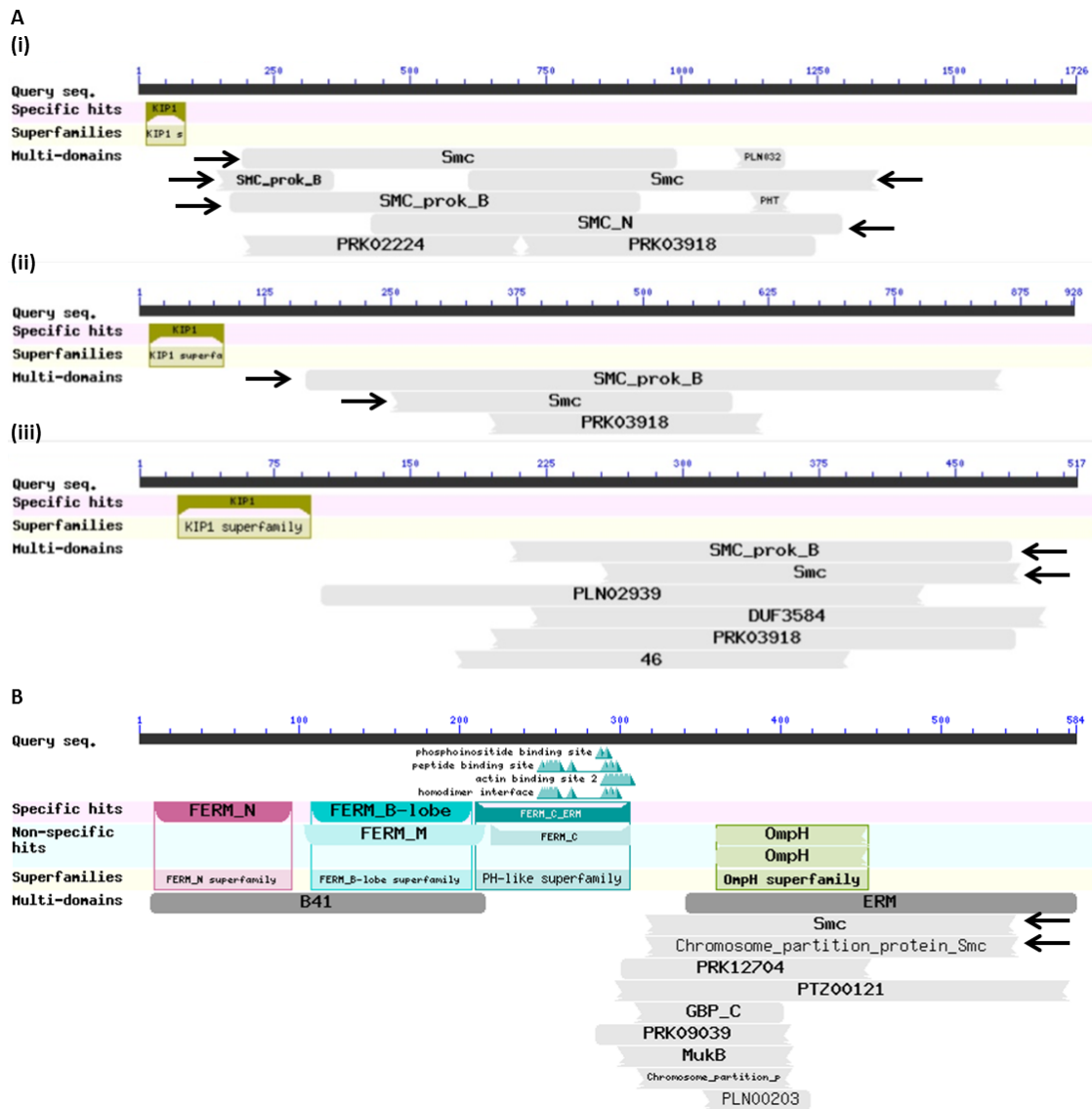
## 3.2 Predicting the tertiary structure of Net Proteins

### 3.2.1 BLASTp analysis

NET proteins have been defined since their discovery, in part, by their N-terminal actin binding (NAB) domain. Other than this there are no common domains between subfamilies or within subfamilies, and this is confirmed by entering the amino acid sequences of NET proteins into the protein alignment tool BLASTp (Camacho et al., 2009). Entering any NET1, NET2 or NET4 protein into BLASTp produces a result which indicates that the general character of the central region of the protein is similar to a protein called Structural Maintenance of Chromosomes (SMC) (figure 9A). Entering Moesin M, an ERM protein known to have an unfolding mechanism involved in its activation, in terms of binding to

actin and the plasma membrane (Pearson et al., 2001), also gives a result showing this ‘multi-domain’, the term used by the tool to show a general similarity

Figure 9: BLASTp analysis; **A** Results from BLASTp showing both the KIP1-homologous NAB domain and the SMC multidomain of Net1A (i) Net2A (ii) and Net4B (iii). SMC-like areas are referenced with black arrows **B** Result from BLASTp showing the domains present in Moesin M (*D. melanogaster*).



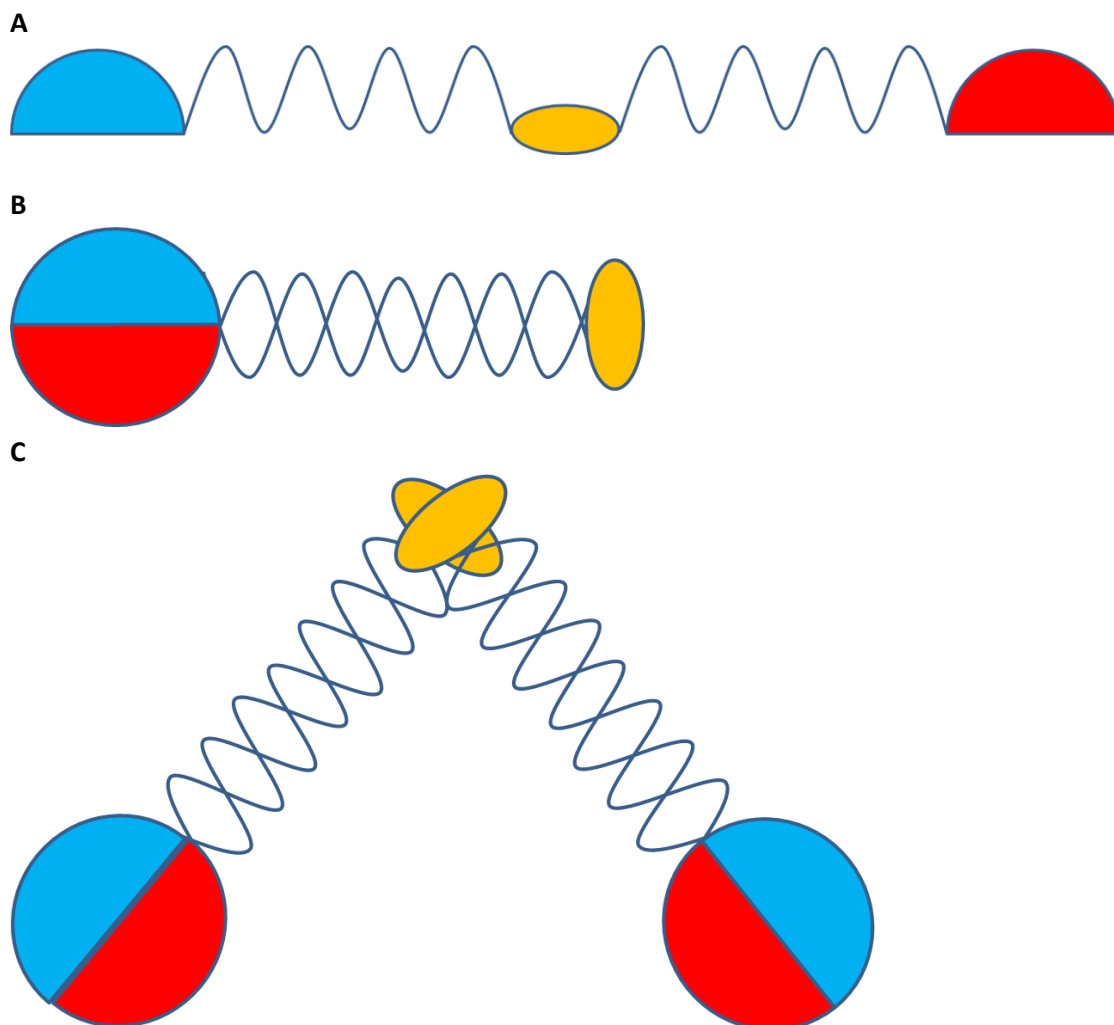
in amino acid character (figure 9B). The probability that this result is not due to random similarity between the sequences, the E value, is  $6.49e^{-12}$ . The E values for each of the NET proteins are in a similar range of  $e^{-10}$  to  $e^{-17}$ , with the low values demonstrating the unlikelihood that this SMC character is random. None of the NET3 family members display this SMC multi-domain.

The SMC-like character shown by the NET proteins with BLASTp is due to their extensive coiled-coil regions. The protomer molecules that make up the

SMC protein dimer are formed primarily from two long, anti-parallel coiled coils. The SMC-like areas closely follow the coiled-coil regions of NET1 and NET4 proteins, but the NET2 proteins have several very short, relatively sparse coiled-coils (Deeks et al., 2012).

The significance of this SMC multi-domain is that SMC is a hinged protein dimer composed of two identical 'head' domains, which are composed of the joined N- and C-termini of each monomer. This is facilitated by a hinge domain in the centre of the protein separated by the two anti-parallel coiled coils. The hinge domains of each protomer anneal to one another in order to form a V shape (figure 10). The head domains bind to chromosomes and hence the position of these chromosomes depends on the angle made by the central region. It has been shown that KIP1 is self-interacting (Skirpan et al., 2001), and that the Net4 proteins interact with each other and themselves (Hawkins and Mentlak, unpublished). Net3C has also been shown to form a homodimer or –multimer (Wang et al., 2014). The position of the two head domains relative to one another is dependent on ATP binding and hydrolysis. BLASTp does not generate a result showing the specific SMC hinge domain for the NET proteins, but these results still indicate that some of the Net proteins may be folded over in a similar way. A novel hinge structure may be present.

Figure 10: Diagram of the folding and dimerization of SMC; **A** the N- and C-termini are marked in blue and red respectively, and the hinge domain in yellow, and are connected by alpha helices (dark blue), **B** the N and C termini fold together around the hinge, **C** the dimers are attached at their hinge domains.



### 3.2.2 Tertiary structure modelling using PHYRE2

To further test the viability of Net proteins having a tertiary structure similar to that of SMC proteins, their amino acid sequences were entered into the PHYRE2 tertiary structure prediction software (Kelley et al., 2015), which uses a database of over 50,000 known tertiary structures. It compares the alignment, the confidence (the percentage probability that the presented structure is

homologous to your input amino acid sequence) and the percentage identity between the protein model and the input amino acid sequence. It also has two modes, normal and intensive, for modelling. The SMC tertiary structure model appears upon the input of the Net1A and Net4B sequences in normal modelling mode, with over 95% confidence and over 15% identity. This means that these proteins are likely to adopt a folding arrangement similar to that of SMC. Many of the other models presented were also folded. Tropomyosin however, a linear protein dominated by alpha-helical regions, was also presented, but this was to be expected given the extensive alpha-helical regions of the Net proteins (Deeks et al., 2012). Nonetheless, the general message from this analysis was that the Net proteins had the potential to be folded, and it had been shown independently of BLASTp that many of them may adopt an SMC-like tertiary structure.

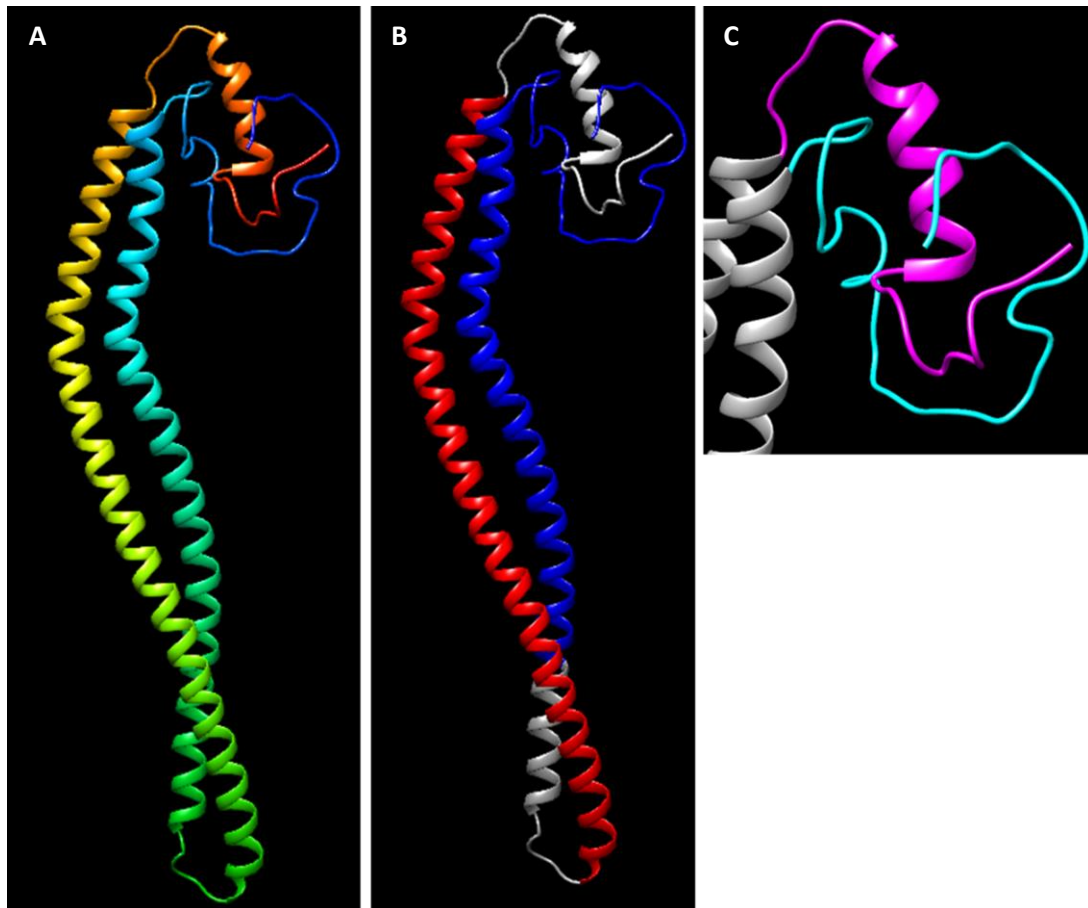
Performing a search in intensive modelling mode uses the same software but aims to create a unique model for the inputted amino acid sequence based on a number of models, and if there is no sequence available, the tertiary structure is determined *ab initio* by another piece of software named Ploig. This modelling process is limited to sequences <1000 amino acids, so the Net1 proteins were excluded from this analysis. The aim of this process was to determine if folded models were favoured in novel tertiary structure prediction for the Net proteins.

#### 3.2.2.1 Structural analysis of Net3C

Net3C produces a tertiary structure which is folded in half, aligning two alpha-helical regions of similar length, with the absolute N- and C-termini intertwined with one another (figure 11). The N-terminal alpha helix includes the majority of the NAB domain. 83% of the amino acids were modelled with over 90% confidence, these amino acids being in the middle of the protein. The N- and C-termini are also shown to interact, but this prediction has a low confidence score. It can be seen, however, that the initial short alpha helix at the N terminus has some measure of interaction with an area of high confidence after the most C-terminal alpha helix. This result is surprising because NET3C was predicted to have no SMC-like character (see section 3.2.1). It is more likely that these alpha

helices are predicted to align because of their similar length and proximity in such a small protein.

Figure 11: Tertiary structure prediction of Net3C; **A** Rainbow labelled Net3C, N-terminus in blue, C-terminus in red **B** Arrangement of the NAB domain (blue) with the large alpha helix in the C-terminal half of the protein (red) **C** Low confidence model of the interaction between the absolute N-terminus (cyan) with the absolute C-terminus (pink).

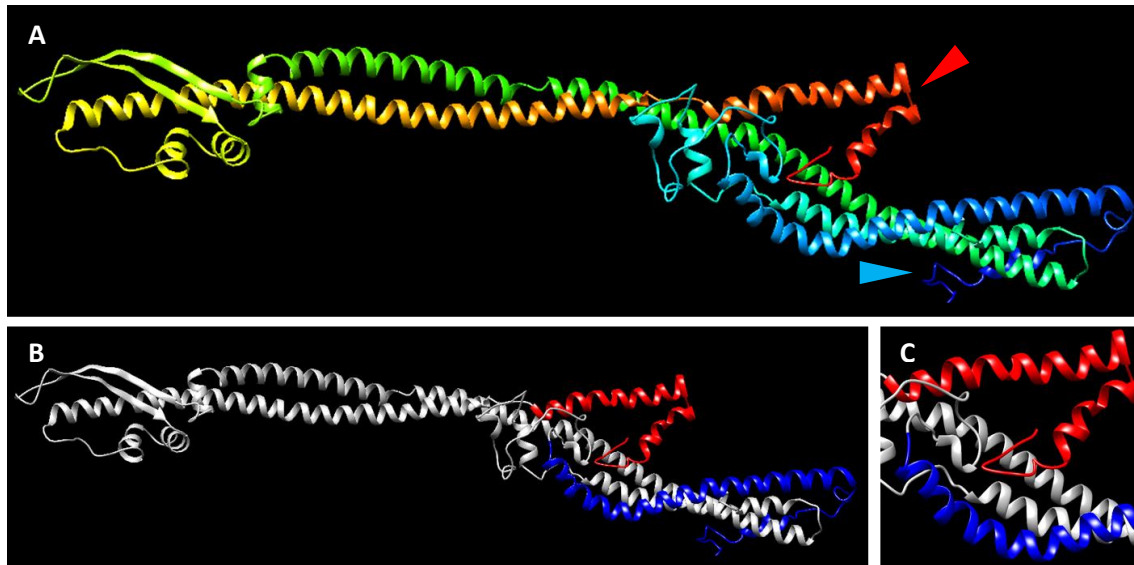


### 3.2.2.2 Structural analysis of Net4B

In Net4B 83% of amino acids were modelled with over 90% confidence, with the C-terminus sitting in a cleft made by three alpha helices (figure 12). The most N-terminal of these alpha helices is comprised of most of the NAB domain of NET4B. Both of these areas were predicted with >90% confidence. NET4B also appears to have a more developed turn-like structure, although the displayed beta-sheet secondary structure does not reflect the predicted secondary structure of Net4B. The C-terminus of the protein is predicted to lie close to the NAB domain. In particular, the absolute C-terminus and the 65-94 amino acid region of the NAB domain are closely adjacent. This model adds weight to the hypothesis

that the C-terminus inhibits the binding of actin to the NAB domain for the Net4 proteins.

Figure 12: Tertiary structure prediction of Net4B; **A** Rainbow coloured predicted structure demonstrates that Net4B is folded along its length, the turn region present towards the middle of the amino acid sequence (yellow). The N and C termini are indicated by blue and red arrowheads, respectively **B** the NAB domain (blue) and C-terminus (red) lie adjacent to one another and **C** the point of closest association occurs between the absolute C-terminus and the latter third of the NAB domain.

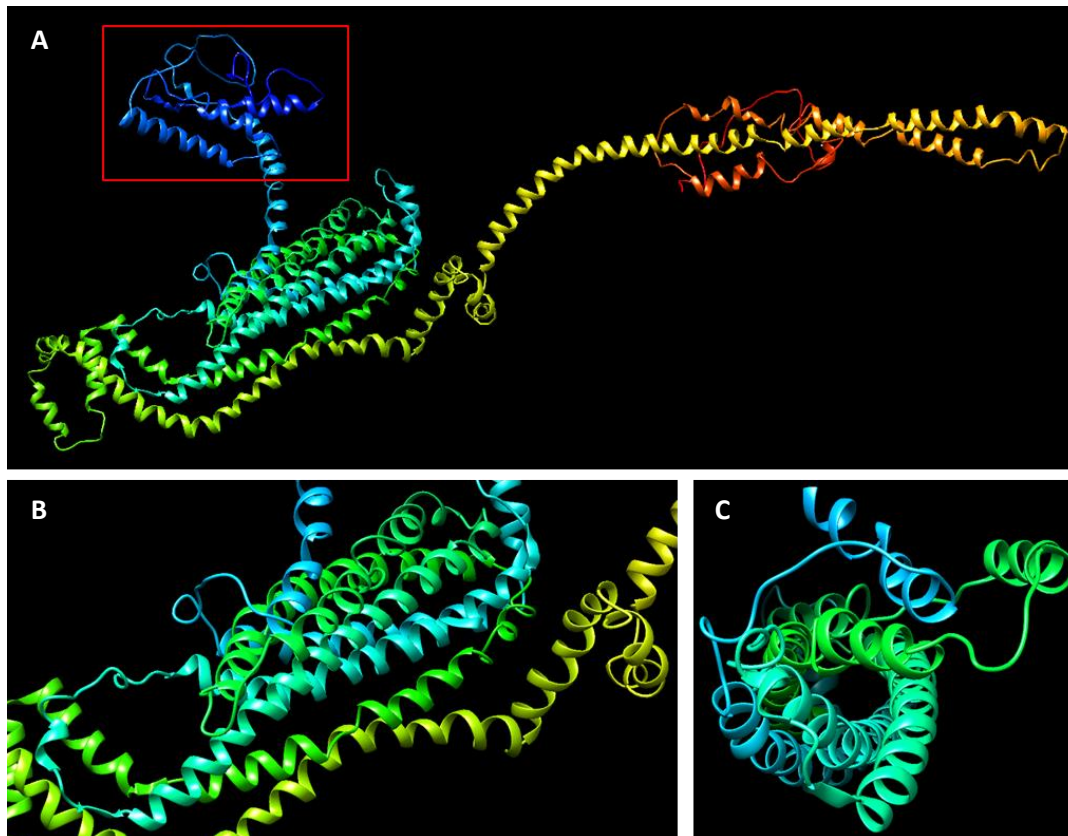


### 3.2.2.3 Structural analysis of Net4B

Only 74% of the amino acids of NET2A were modelled with over 90% confidence. The C-terminus, as suggested by the BLASTp analysis of NET2A, does not have a character similar to other proteins and the prediction was made with low confidence (figure 13). The N and C termini are not close to one another, and the NAB domain is away from all other regions of the protein. The NAB domain itself is modelled with over 90% confidence. This does not support the ERM protein model hypothesis. Interestingly, here is an array of antiparallel alpha helices from amino acids 163 to 461. These alpha helices are arranged into a channel-like structure, also with a high confidence value. An interesting note in relation to this is that Net2A aligns much more closely to membranes than other Net proteins (Dixon, 2013). A transmembrane domain would be contradictory to the predicted hydrophobicity of this protein, however (see section 3.3.7). In general, this

evidence detracts from the ERM-protein-like model being applicable to the Net2 family.

Figure 13: Tertiary Structure prediction of Net2A; **A** Rainbow coloured predicted structure does not show any region of the protein interacting with the NAB domain (red box). When the highly folded 163-461 region **B** is excised from the rest of the protein and rotated through 90°, a channel **C** can be seen running through the angled helices.



### 3.3 Prediction of other post-translational modifications – Acylation and Sumoylation

#### 3.3.1 Acylation

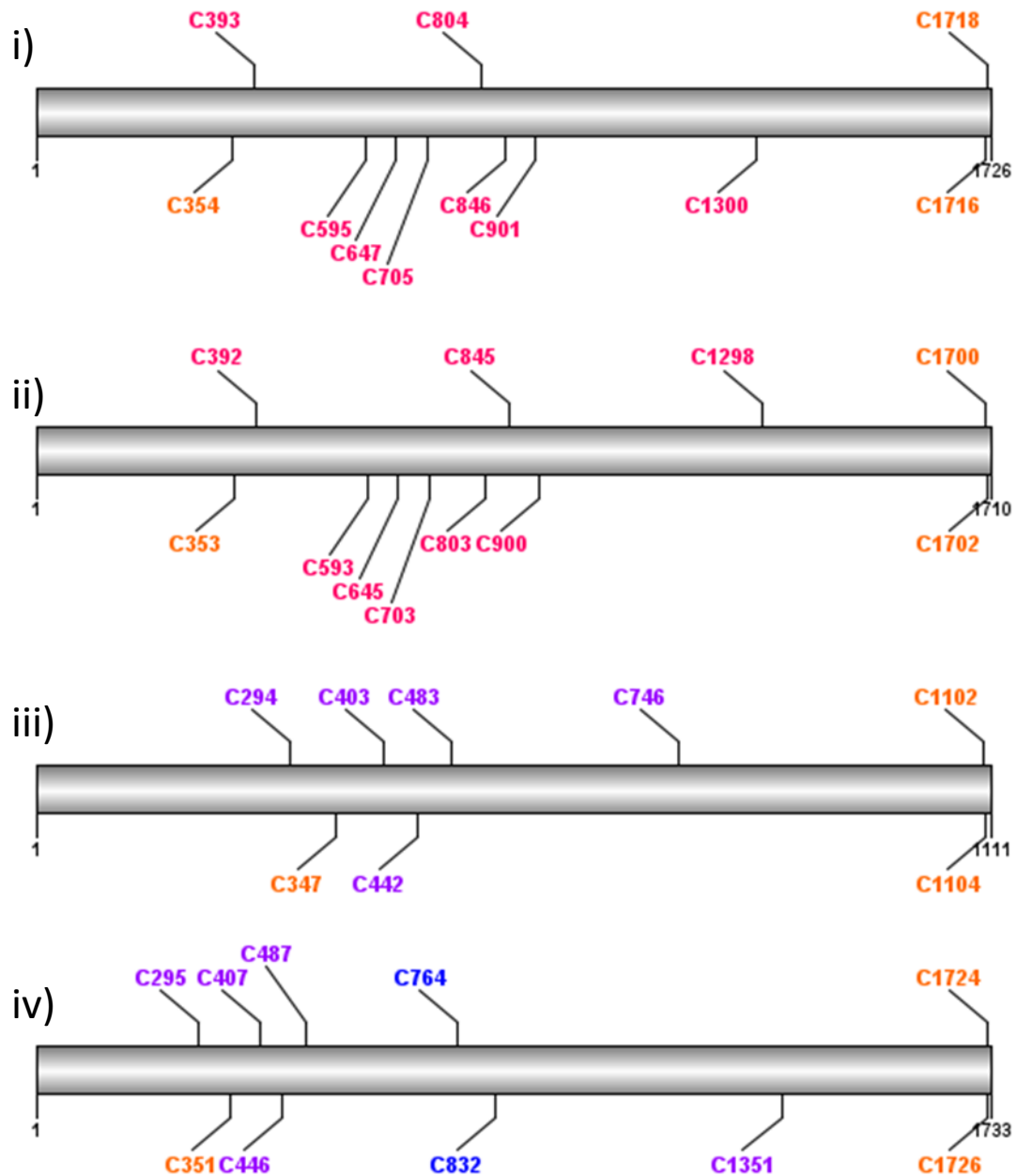
A common characteristic of NET proteins is that they are found at a variety of membranes within plant cells. This has been shown by fluorescently tagging of these proteins *in situ* (Hussey et al., 2006). Cell membranes are comprised of phospholipids, which are amphipathic molecules arranged into a bilayer, with hydrophilic phosphate groups exposed to the cell internal environment, for example to the cytosol. The inside of the membrane is hydrophobic and is composed of fatty acids and other molecules, such as cholesterol, that affect membrane viscosity. The addition of fatty acid chains, or acylation, allows

proteins to become associated with membranes as these chains enter this hydrophobic environment by increasing the hydrophobicity of proteins that they are attached to. It therefore seemed prudent to investigate the potential for the addition of these chains to Net proteins. The addition of fatty acids can be split into multiple categories depending on the type of chain and the location that the chain is added. S-acylation, prenylation, myristoylation and GPI anchor attachment have been investigated in this bioinformatics work. There are multiple pieces of prediction software available for predicting acylation site locations for these types of modifications.

### 3.3.2 S-acylation

S-acylation, also known as palmitoylation, is the covalent attachment of a fatty acid chain primarily to cysteine residues, and rarely to serine and threonine residues. Notably it is a reversible process and can therefore be hypothesised to regulate the positioning of NET proteins at their respective membranes. The software used for prediction was CSS-PALM 4.0 (Ren et al., 2008), which uses a clustering and scoring system to select residues that could be S-acylated based on their cluster, the category of site to which they belong. If the given score is higher than the cut-off value then it is determined to be a positive S-acylation site. CSS-PALM was used on the lowest stringency setting because the aim of the investigation was to look for S-acylation sites exhibiting conservation and belonging to the same cluster, as opposed to looking for specific sites on each protein with the highest scores. Using high stringency settings would often result in a failure to display sites that were very similar in sequence on different proteins. This may be due to the limited size of the database of experimentally determined S-acylation sites used. There were also no instances of serine or threonine S-acylation, potentially for this reason. The use of higher settings may be useful in narrowing down targets for site-directed mutagenesis experiments, but work done for this project did not progress to that stage for S-acylation.

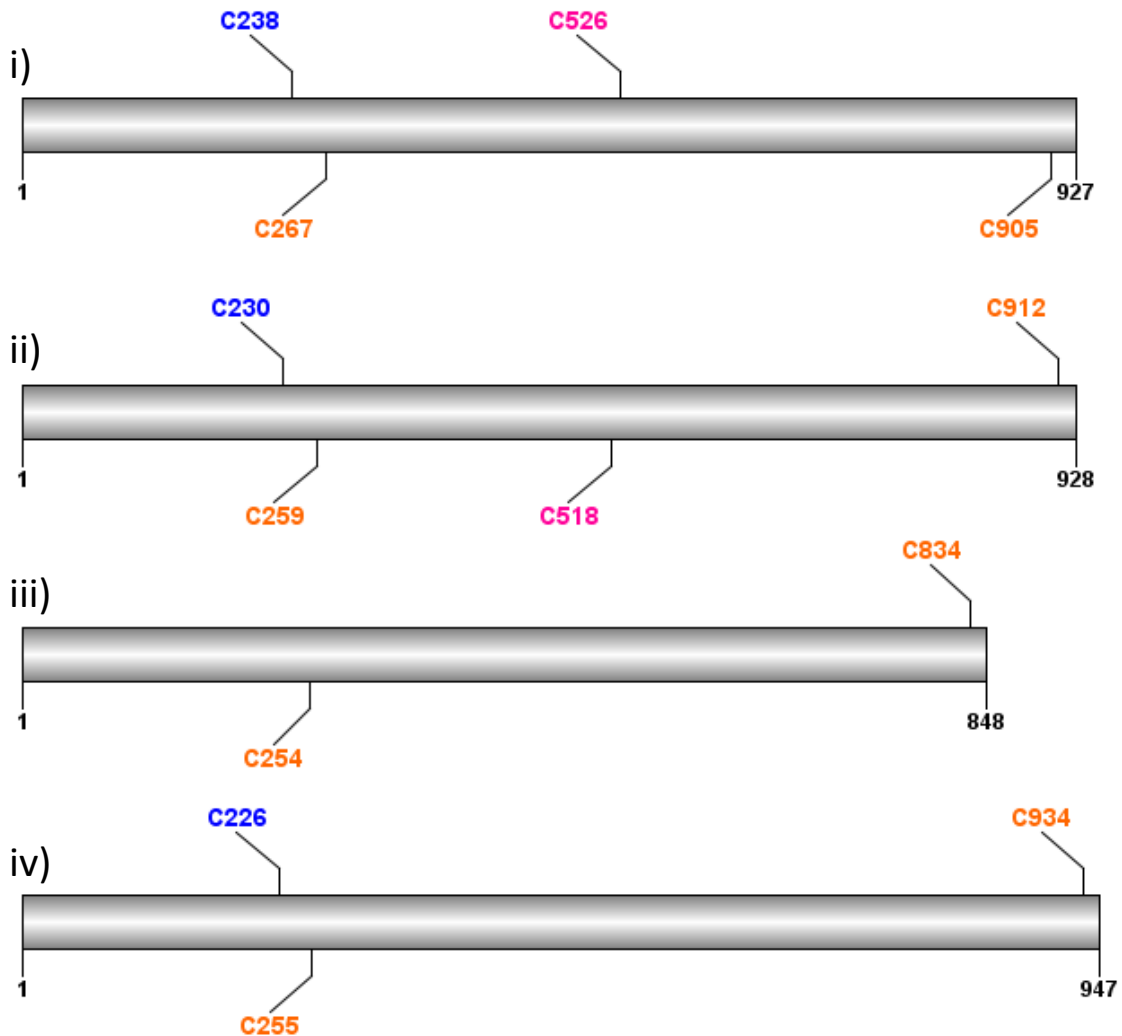
Figure 14: Comparison of predicted S-acylation sites in the Net1 family; Net1A (i) Net1B (ii) Net1C (iii) and Net1D (iv). The colour of the sites denotes their conservation; pink denotes conservation between 1A and 1B, purple between 1C and 1D, and orange between all four members of the family. The blue sites on Net1D represent two sites which may be conserved with Net1A and Net1B.



The Net1 family contained by far the most predicted S-acylation sites, having up to 25 sites predicted per protein. Upon visualisation of these sites, it was immediately apparent that there were sites that had similar positions, most notably a pair of predicted sites at the C-terminus, one residue apart from one another (figure 14). Looking at the peptide sequence around the S-acylation sites it was possible to identify other sites which may be common between all four members of the Net1 family. Other sites that were common between the most closely related pairs, Net1A/1B and Net1C/1D, could also be determined in this way. Overall, conserved predicted sites were observed along much of the length of the proteins, but there were no conserved sites, and only one site predicted (C93 of Net1A), within the NAB domain. The presence of the conserved C-terminal sites may have more significance (see section 3.3.2).

The Net2 family contained far fewer sites relative to their length. Again, however, it was possible to elucidate the presence of multiple predicted conserved sites (figure 15). There was less emphasis on the pairwise conservation as seen in the Net1 family, with Net2C only having sites conserved with all of the other members, rather than Net2D in particular. Once again a site conserved between all members was identified at the C terminus. The Net3 family, despite having a good number of sites relative to their short lengths, offered no predicted conserved S-acylation sites. This may be due to their very short length, combined with a distinct absence of predicted S-acylation sites within their main region of homology, the NAB domain. This does

Figure 15: Comparison of predicted S-acylation sites in the Net2 family; Net2A (i) Net2B (ii) Net2C (iii) and Net2D (iv). The colour of the sites denotes their conservation; pink denotes conservation between 2A and 2B and orange between all four members of the family. Blue represents a conserved site between all members except Net2C.

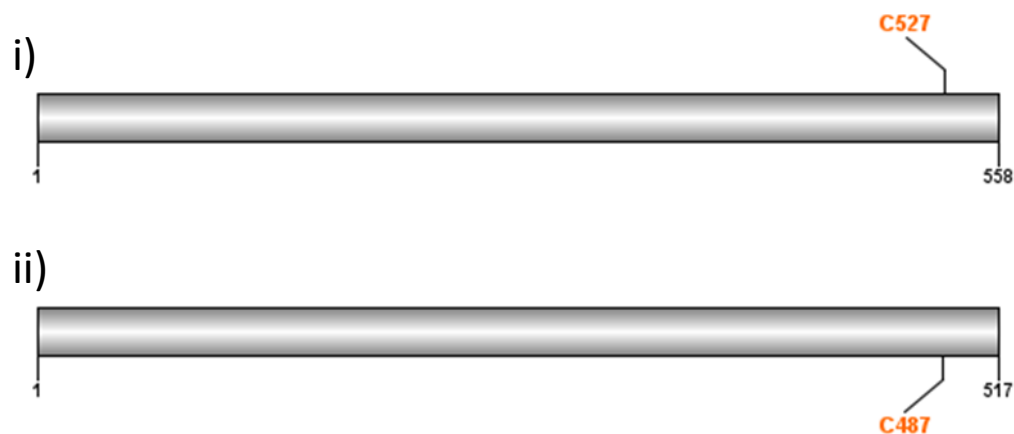


not mean that the Net3 proteins are not S-acylated, but rather any S-acylation event is likely to be member specific. The Net4 family had very few predicted S-acylation sites, with a total of five across both members. Despite this, the family did present a single predicted conserved site – C527 of Net4A and C487 of Net4B (figure 16). This correlates with existing experimental data that has shown Net4B as acylated in this region (Hussey and Helmsley, personal correspondence).

Overall, this means that three of the four Net families have at least one conserved C-terminal S-acylation site predicted. The Net1 and Net2 families also

demonstrate more widespread conservation, with these families giving a second conserved site immediately C-terminal to the NAB domain. These two areas should therefore be targeted for site-directed mutagenesis or diagnostic studies to determine their actual S-acylation status. The Net1 family also appear to have a great number of partially conserved sites, which may also prove good targets when looking for member-specific S-acylation events. These predictions mean that a key S-acylation-mediated interaction with membranes is certainly a possibility for three of the Net families. The presence of C-terminal sites provides some tentative evidence that some of these proteins may operate in an ERM-protein-like fashion.

Figure 16: Comparison of predicted S-acylation sites in the Net4 family; Net4A (i) Net4B (ii). These two sites are conserved between the proteins.



### 3.3.3 Prenylation

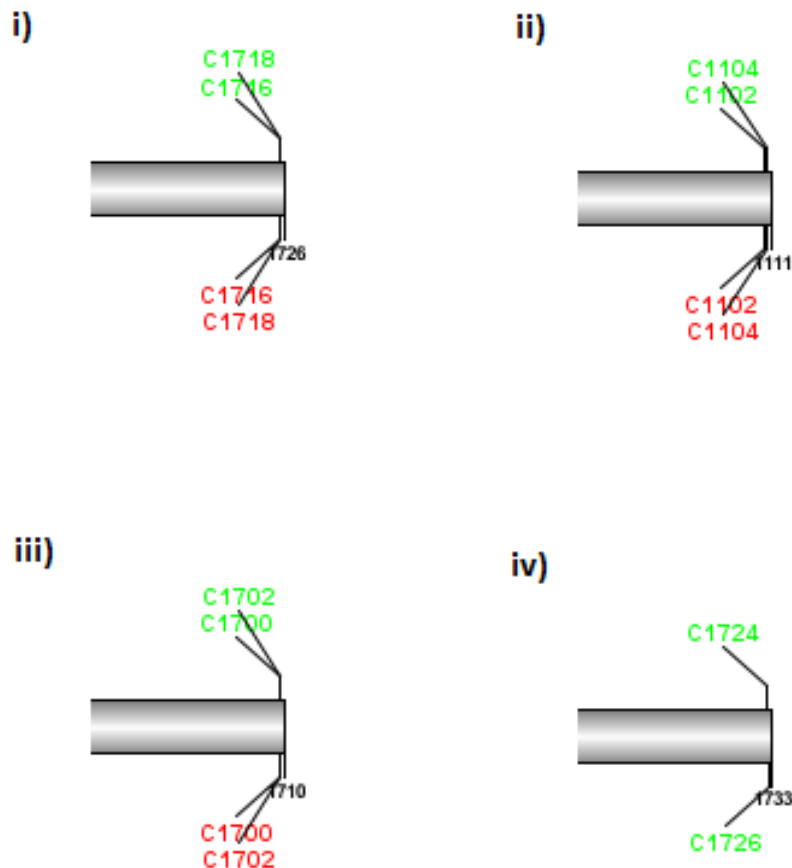
Prenylation is the addition of one of two types of lipid modifications, farnesyl and geranylgeranyl groups to cysteine residues. These modifications have a similar role in membrane anchorage as S-acylation. It differs from S-acylation in two ways; modifications only occur at the C-terminus and are irreversible. The functional overlap between S-acylation and prenylation is discussed in more detail in section 1.3.2.2. GPS-Lipid (Ren et al., 2008) (Xie et al., 2014) allows for the prediction of both types of prenylation alongside S-acylation for comparative scoring, in a similar format to that of CSS-PALM.

Interestingly, there are no predicted sites for prenylation in any of the NET2 or NET4 proteins. Those sites identified in the S-acylation prediction

exercise for these sites will therefore be S-acylated if the prediction is correct. Of the NET3 subfamily, only Net3C is predicted to have a prenylation site (Figure 17), a farnesylation site at C219. This site is also predicted to be S-acylated, but at a lower stringency level. Net3C is known to exhibit fixed punctae at the interface between the plasma membrane and endoplasmic reticulum in a complex with VAP27 (Wang et al., 2014). A point mutation of a lysine residue at position 211 in a so-called basic C-terminal motif to an alanine caused these punctae to become more mobile, suggesting that some kind of direct interaction of Net3C with phospholipids was occurring, but did not abolish the punctae. A combination of a farnesyl group and the basic motif, given their predicted proximity, may therefore be required for association to the plasma membrane. This farnesylation would be described as 'non-consensus' however, as the normal Net3C sequence does not contain a CaaX motif at its C terminus, with C219 placed six residues from the absolute C terminus rather than the normal three. An S-acylation event may therefore be more probable.

The Net1 proteins are all predicted to be prenylated at the same pair of C-terminal cysteine residues discussed in the S-acylation prediction. Net1A, 1B and 1C exhibit both types of prenylation. NET1D, however, only exhibits a farnesylation prediction. The geranylgeranylation predicted for the former three Net1s is based on the recognition sequence for Rab protein Geranylgeranyltransferase II, CXC (Khosravi-Far et al., 1992). Given that Net1D contains the same CGC motif of the other Net1s, the reason for its exclusion is unclear. Nonetheless, this recognition sequence only applies to Rab proteins. The farnesylation predictions are described as 'non-consensus', as they do not have the CaaX sequence at their C-terminus. It therefore seems more likely that the Net1 proteins are S-acylated.

Figure 17: Prediction of farnesylation (green) and geranylgeranylation (red) in the Net1 family at high stringency using CSS-PALM 4.0; i) Net1A ii) Net1B iii) Net1C iv) Net1D.



### 3.3.4 Myristoylation

Myristoylation is the addition of 14-carbon myristate groups to N-terminal glycine to a recognition sequence MGXXS/T. Only NET3B is recognised as being myristoylated out of the whole NET family at high stringency, with NET1D and NET1B becoming predicted at lower stringency levels. This is due to the presence of glycine residues close to the N-terminus, but only NET3B has a glycine adjacent to methionine, an important factor (Resh, 1999). It is unlikely that these sites are responsible for membrane association for two reasons; these sites are extremely close to the NAB domain and close alignment to the membrane may inhibit actin binding, and that a single myristate group is not hydrophobic enough to allow for strong membrane association (Resh, 1999), and there are no predicted S-acylation sites proximal to the predicted N-myristoylation

site. This avenue is unlikely to elucidate information about the regulation of the NET protein family through post-translational modification.

### 3.3.5 GPI anchorage

Glycophosphatidylinositol (GPI) anchorage of proteins involves the covalent attachment of this glycolipid to the C terminus of a protein. The protein is then anchored to the membrane via two fatty acid linkages (Ikezawa, 2002). GPI anchorage would be a possible explanation for larger mass differences observed during 2-dimensional gel electrophoresis. The online program big-Pi plant (Eisenhaber et al., 2003) was used as a plant-specific predictor of GPI-anchor motifs within the Net proteins. No Net proteins were found to have predicted GPI-anchorage sites.

### 3.3.6 Sumoylation

Sumoylation is the addition of a small protein, Small Ubiquitin-like Modifier, to proteins with the recognition sequence  $\Psi$ -Lysine-x-Aspartic Acid/Glutamic acid, with  $\Psi$  representing a hydrophobic residue (Miura et al., 2007). This post-translational modification is involved in the regulation of trafficking of the proteins it modifies, making it a candidate for regulating the position of NET proteins at their respective membranes. Proteins may also interact with SUMO non-covalently, through SUMO interaction motifs (SIMs). The program GPS-SUMO (Ren et al., 2009) (Zhao et al., 2014) is designed for the prediction of the presence of both sumoylation sites and SIMs in input proteins. The results generated are subjected to a score system which determines the probability that a given site has an interaction with SUMO. This tool is useful for narrowing down potential sites but the algorithms used are limited by the relatively small dataset of experimentally identified sumoylation sites, particularly in the case of SIMs, which have no established motif (Kerscher, 2007). Nonetheless, GPS-SUMO presents potential sumoylation sites and SIMs for a number of NET proteins at the higher stringency settings.

Comparison of proteins from the same subfamily and between subfamilies was used in this approach to select sumoylation sites and SIMs most likely to be significant in the regulation of NET proteins. Sumoylation sites were predicted for all input proteins, but there were no sites present in a recognisable conserved

position. This is true both within and between subfamilies. Comparisons were particularly difficult using the 'all' setting because GPS-SUMO would present the vast majority of lysine residues as potential sumoylation sites. As soon as the 'low' setting was selected instead, any semblance of conservation was lost and the number of predicted sites drastically reduced, and often there was no difference in the sites detected when moving to increasingly stringent settings.

Conserved SIMs can be predicted within the NAB domain of all of the tested NET proteins at the 'all' stringency threshold. Upon visualisation of these results (figure 18) it becomes apparent that there are two predicted SIMs present near to the N-terminus in all of the NET proteins. The sequences are not necessarily similar to one another but they are all 5 amino acids long and are present in the 40-60 and 60-80 amino acid regions of all proteins. An alignment using the program ClustalW2 (Larkin et al., 2007) demonstrates their conservation in terms of amino acid quality. Of significance is the proximity of a group of glutamic/aspartic acid residues between the two sites, which make up a conserved EDXDS motif in many of the Nets from different families. Hydrophilic, negatively charged residues such as these are important for the orientation of a SIM-containing protein when it binds to SUMO (Kerscher, 2007). The importance of these findings is that the SIMs are conserved even when there are alterations to the sequence of the NAB domain between different Net proteins. The true significance of these findings is subject to further refinement of the SIM general sequence, however. Further SIMs are predicted outside of the NAB domain for all of the Net proteins, but there is a surprising lack of conservation; no conserved SIMs were identified in the Net3 and Net4 families, a single SIM identified in the Net2 family at around residue position 700 and a single was SIM in the Net1 family very close to the C-terminus. These two sites could only be detected as conserved at the 'all' stringency setting. These sites would be of lower priority to those in the NAB domain for further investigation.

Figure 18: Aligned NET protein sequences with SIMs highlighted to show conservation at the N-terminus. Amino acids are coloured to indicate their charge or hydrophobicity of the side chain; red indicates positive charge, purple indicates negative charge, blue indicates hydrophobicity and green indicates uncharged.

	50	60	70	80	90
<i>Net1A/1-1726</i>	SKVKAM	I K L I E	- - - EDADSFARRAEMYYKKRPEL	M K L V E	E F Y R A Y R A L A E R Y
<i>Net2A/1-927</i>	EKVEYT	L K I I D	- - - EDGDTFAKRAEMYYRKRPEI	V N F V E	E A F R S Y R A L A E R Y
<i>Net3C/1-225</i>	AKTKAM	L K L L D	- - - GNADSF AQRAETYYKKRPEL	I S F V E	D F Y R A H R S L A V N F
<i>Net4B/1-517</i>	DRVNHML	L K L I E	- - - EDADSF AKKAQMYFQKRPEL	I Q L V E	E F Y R M Y R A L A E R Y
<i>Net1D/1-1733</i>	SKVKQM	I K V I E	- - - EDADSFARRAEMYYKKRPEL	M K L V E	E F Y R A Y R A L A E R Y
<i>Net4A/1-558</i>	RSVKRM	V K L I E	- - - EDADSF AKKAEMYYQSRPEL	I A L V D	E F H R M Y R A L A E R Y
<i>Net3B/1-215</i>	SKTKEM	L S V I D	E V E D E G D S L M K R A K I N Y E N K P K L	I E L L E	E L Y R S H R S L A Q K H
<i>Net1B/1-1710</i>	SKVKTM	I K L I E	- - - ADADSFARRADMYFKKRPEL	M K L V E	E L Y R A Y R A L A E R Y
<i>Net1C/1-1111</i>	SNVKQM	I K V L E	- - - EDADSFARRAEMYYRKRPEL	M K L V E	E F Y R A Y R A L A E R Y
<i>Net2B/1-928</i>	EKVKYT	L K I I D	- - - GDGDSFAKRAEMYYRKRPEI	V N F V E	E A F R S Y R A L A E R Y
<i>Net2C/1-848</i>	EKVEYAL	L K L L E	- - - DEGDSFAKRAEMYYKKRPEL	I S F V E	E S F K A Y R A L A E R Y
<i>Net2D/1-947</i>	EKVQYV	L K L L D	- - - EDGDSFAKRAEMYYKKRPEL	I S F V E	E S Y R A Y R A L A E R Y

### 3.3.7 Isoelectric point prediction

In order to perform 2D gel analysis of the Net proteins an estimated isoelectric point (pI) was determined using ProtParam (Gasteiger et al., 2005). This would allow confirmation that the antibodies were detecting the correct protein, alongside their predicted molecular weights. ProtParam also generates a measure of hydrophobicity, the Grand Average of Hydrophobicity (GRAVY). All of the Net proteins were found to have a negative GRAVY value, meaning that they are predicted to be hydrophilic (table 4). This means that they are unlikely to be transmembrane or compartmentalised in such a way that they are not exposed to the cytoplasm. This information correlates with the hypothesis that membrane interaction arises from a modification, rather than an inherent membrane interacting motif within the proteins themselves. It does not exclude, however, the possibility that they may interact with other membrane bound proteins and do not require an acylation event.

Table 4: ProtParam data concerning the GRAVY, pI and predicted molecular weight of the Net proteins.

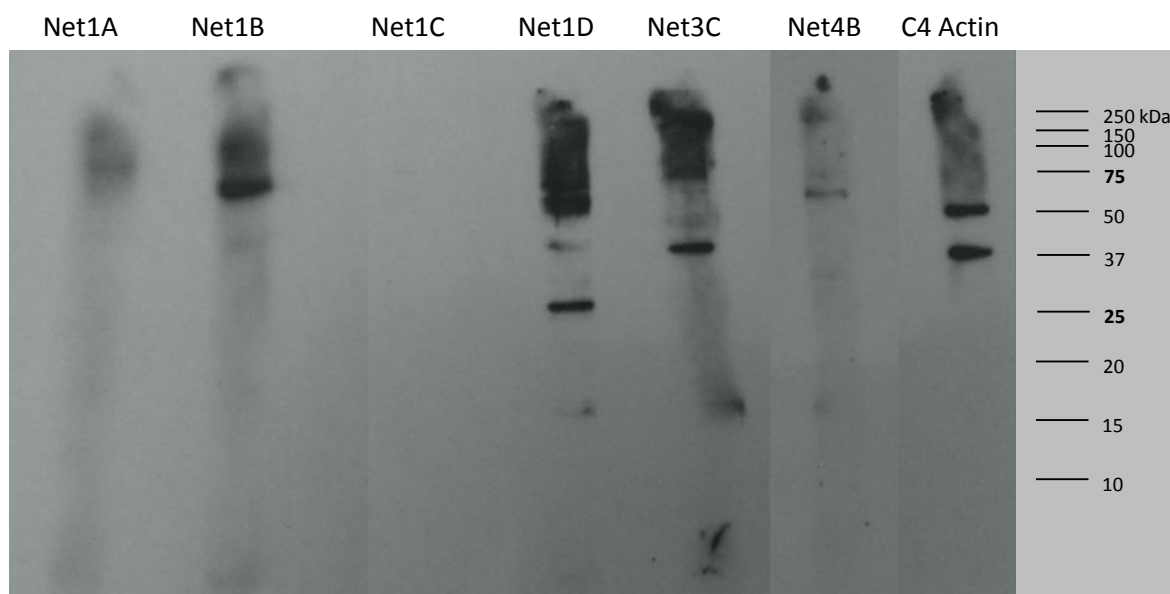
Protein	Grand Average of Hydropathicity	Theoretical pI	Predicted molecular weight [kDa]
1A	-0.746	5.27	198.6
1B	-0.763	5.22	197.0
1C	-0.767	5.72	127.7
1D	-0.703	5.01	198.5
2A	-0.875	5.31	105.7
2B	-0.806	5.32	106.8
2C	-0.810	5.05	96.9
2D	-0.863	5.00	108.2
3A	-0.991	4.96	31.5
3B	-0.532	4.87	25.4
3C	-0.859	5.69	26.5
4A	-0.846	5.14	64.2
4B	-1.055	5.36	60.2

### 3.4 Western Blotting analysis of the Net proteins

#### 3.4.1 Testing of Existing Antibodies

Since their discovery in 2006, antibodies have been raised to many of the Net proteins (Calcutt 2009) (Ingle 2011) (Wang et al., 2014) (Mentlak, unpublished). These antibodies had been used successfully for 1-dimensional gel analysis and immunolabelling. These antibodies have never been used for 2-dimensional (2-DGE) gel analysis previously, and it was important to demonstrate that these antibodies would still function in this new context given the alternate preparation of protein samples. Performing initial 1-dimensional gel analysis of these antibodies had the additional advantage of indicating any change in running molecular weight that may occur due to the alternative way proteins are denatured; SDS alters the charge of proteins, so would interfere with the isoelectric focusing (IEF) step, so proteins are denatured initially using a combination of the chaotropes urea and thiourea alongside a detergent, CHAPS, which allows the dissolving of lipids and the maintenance of protein solubility during IEF. This work was aimed at eliminating confusion upon progression to full 2D-gel analysis of the Net proteins.

Figure 19: Net protein antibody testing by 1-dimensional electrophoresis (see section 2.3.2 for details). C4 Actin was used as a positive control. Protein samples were solubilised in the standard rehydration buffer. This image is generated from the same western blot at a range of exposure times, depending on how strong the signal was during chemiluminescent detection.



Initial results were promising as to the functionality of the antibodies in this context (figure 19). Bands were identified for four of the Net proteins; Net1B, Net1D, Net3C and Net4B. No band was identified for Net1C and Net1A gave a weak, diffuse band that appeared close to its predicted molecular weight. Further western blotting was then performed to try to confirm the functionality of Net1A, and the pollen-specific Net3B and Net2A. Results for these proteins were not forthcoming. Furthermore, the bands identified for Net1B and Net1D were not close to the molecular weight predicted by bioinformatics analysis (table 6). Net4B and Net3C were therefore taken as the primary targets for proteomic analysis in this project. Net4B, in this context, runs at a molecular weight of between 50 and 60kDa, slightly below its predicted molecular weight, and Net3C runs at about 37kDa, which is its predicted molecular weight.

### 3.4.2 Identification of post-translational modification presence in Net4B by two-dimensional gel electrophoresis

Two-dimensional gel analysis allows the separation of proteins based on two factors; their isoelectric point (pI), which is based on their charge, and their molecular weight. This allows the separation of proteins which have very similar molecular weights but different pI, which would not be visible as different proteins on a 1-dimensional gel. Probing a western blot with a particular antibody allows the identification of protein modifications, where proteins have undergone a change in molecular weight or pI as a result of a covalent attachment, as all spots identified in this instance will be the same protein. It was by this method that the Net proteins would be investigated generally to experimentally determine the presence of post-translational modifications predicted by the bioinformatics analysis. In particular the presence of a horizontal run of dots was sought, as this is indicative of multiple phosphorylation events according to ProtParam (Gasteiger et al., 2005). Acylation events would cause variable effects on both pI and molecular weight. The covalent attachment of the SUMO peptide would increase the molecular weight of a protein by ~12kDa per SUMO peptide.

Performing the full 2D gel protocol had further implications for the locations of these proteins, as the proteins separated by IEF would undergo an equilibration step to coat proteins in SDS in preparation for running the second dimension. It was therefore possible that a further difference in running molecular weight could be observed depending on how well SDS infiltrated into the IPG strips.

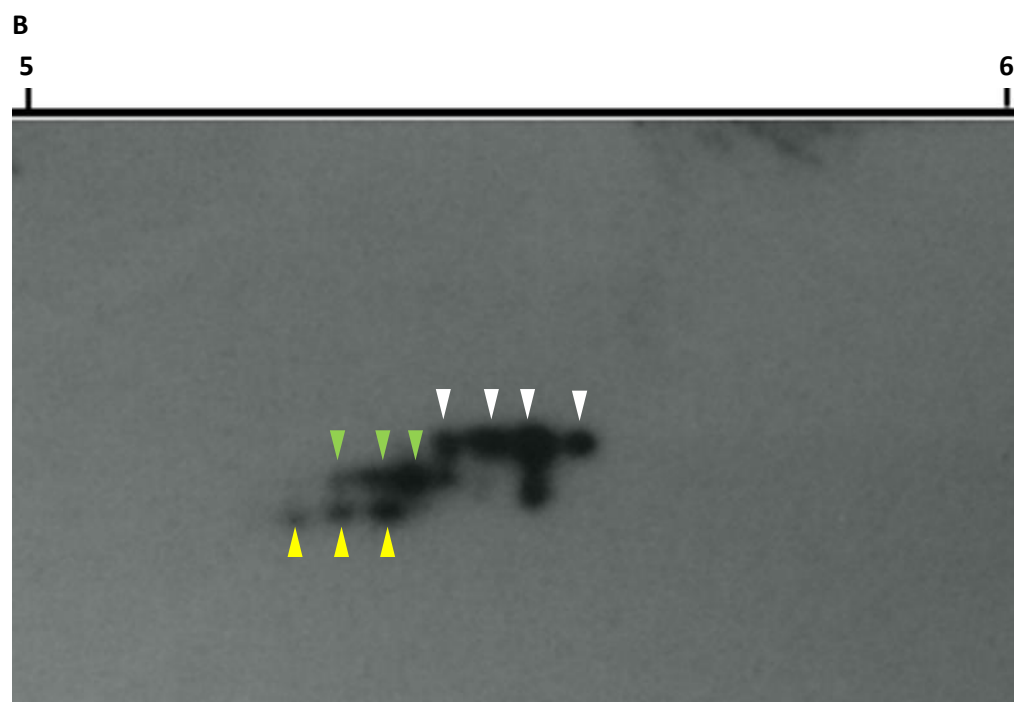
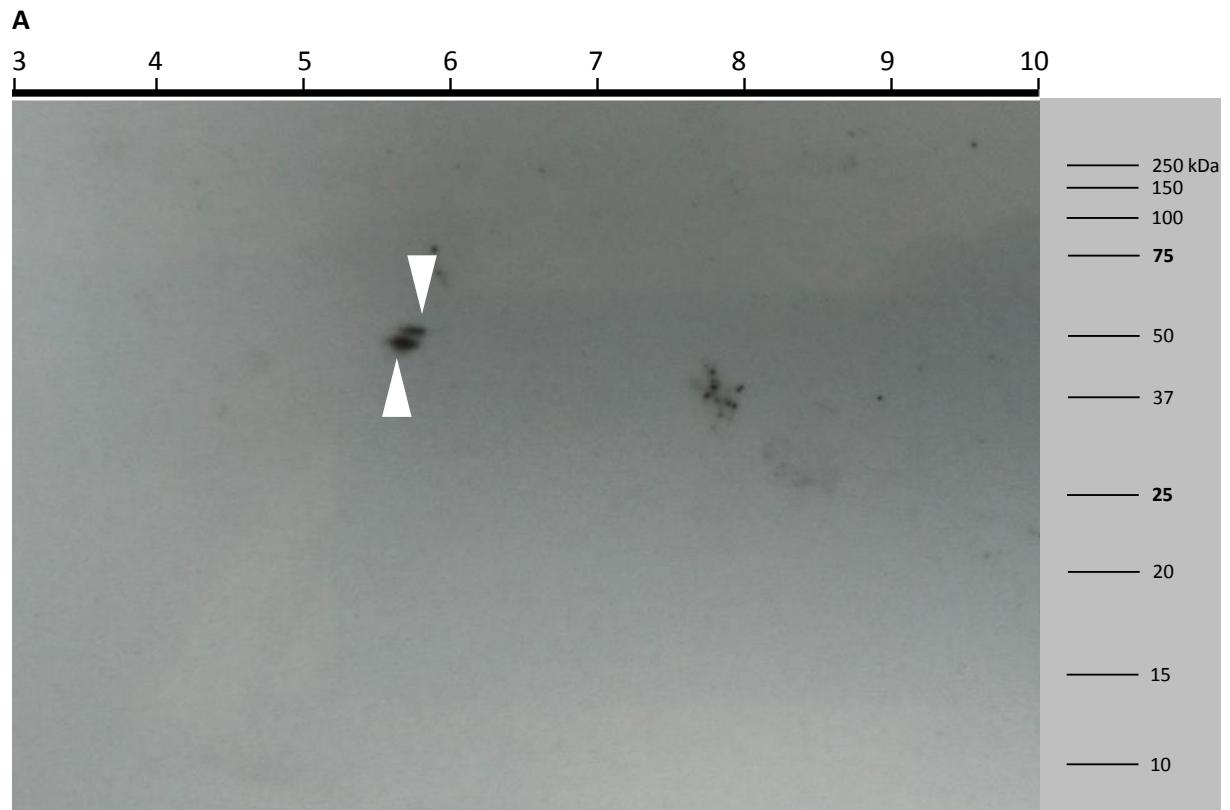
Net4B was selected as the primary target for this investigation as it represented the protein which had the highest probability of matching the ERM protein model, due to its predicted folded structure. The initial investigation was performed using a 3-10 IPG strip in order to cover any potential large changes in pI, as a 4-7 IPG strip had the potential to exclude large changes in pI, given the predicted pI of Net4B is 5.36. This experiment showed that there were two spots that were both recognised by the Net4B antibody; one with a pI of ~5.3 and another of ~5.5, both with a molecular weight of ~50kDa (figure 20a). Given the introduction of SDS onto the protein sample occurs in gel and therefore relies on its infiltration into the IPG strip, it is conceivable that proteins may still contain

some disulphide bonds or even retain some secondary structure arising from uneven or incomplete coating with SDS. This would make them run faster as they would have a shorter molecular length when compared to a fully denatured protein. This would not account, however, for the change in pI. Furthermore, closer inspection of these spots showed that they were slightly elongated. The spot with lower molecular weight also appeared larger and to cover a greater pI range. To eliminate the possibility that this was arising from poor IEF, the experiment was repeated on a 4-7 IPG strip, which would increase the resolution of the final gel in the region of interest, a pI of 5-6, since it was now possible to exclude the possibility that Net4B had any post-translational modification configurations which caused it to have a pI <4 or >7.

The result of the 4-7 IPG strip western blot was remarkably complex (figure 20b). These two spots could now be seen to be comprised of ~12 individual spots, which are split unevenly between them making the lower spot appear more intense. More importantly, this experiment gave evidence of the characteristic run of spots – the ‘shotgun’ pattern – which is indicative of multiple phosphorylation events. The post-translational modification prediction software ProMost (Halligan et al., 2004) predicts phosphorylation events on serine or threonine residues to cause a shift in pI of 0.03 towards the acidic end in the 5-6 pI range, and measurements between spots within these shotgun patterns gave similar values, ranging from 0.03-0.04. There were at least three instances of this within the twelve dot pattern. There was also evidence of a small decrease in molecular weight associated with the phosphorylation events, given the diagonal shift of the pattern in both the 4-7 and the 3-10 western blots. There are two possible explanations for this; an independent post-translational modification with a 1-2kDa molecular weight or a certain number of phosphorylation (or other charged modification) events enable the addition/removal of another covalent modification to/from Net4B. It was therefore important to determine which of these spots represented phosphorylation and which represented other modifications.

Elucidating the presence and number of phosphorylation events was attempted in two ways. Initially, protein samples were treated using alkaline phosphatase, which would remove phosphate groups and potentially remove spots from the 2-DGE pattern. Comparison of the number of spots to a western

Figure 20: 2-dimensional gel analysis of Net4B. **A** Western blot of a gel using a 3-10 pI range IPG strip; two distinct spots (white arrowheads) are clearly visible at an appropriate pI and molecular weight. The spots appear elongated laterally. **B** Zoomed-in western blot of a gel using a 4-7 pI range IPG strip; it is now possible to observe distinct spots within the elongated regions. There are at least 12 distinct spots, with three instances of the phosphorylation 'shotgun' effect (white, green and yellow arrowheads; different colours indicate different shotgun effects).



blot of an untreated protein sample run in tandem would then give the number of phosphorylation events that occur on Net4B. A disadvantage of this process is that comparison of individual spots cannot be made due to gel-to-gel variation which occurs for multiple reasons; differences in IEF, differences in second dimension gel, slight differences in voltage during second dimension run and variable equilibration step quality. Running a phosphatase treated sample alongside an untreated sample, both of which would be labelled with distinct fluorescent markers in the same gel would be an improvement to this experiment. A secondary approach was to use the Pro-Q Diamond Phosphoprotein Blot Stain Kit (Life Technologies), which allows the staining of nitrocellulose membranes with a fluorescent compound that detects phosphoproteins, and then probing the same membrane with the Net4B antibody, allowing direct comparison between the two generated images. Overlaying the two resulting images would show overlapping spots. These spots would represent a phosphorylated form of Net4B. This approach was not successful because it was not possible to eliminate background signalling from the phosphostain. A potential solution to this would be to use PVDF membrane as nitrocellulose became difficult to handle during the staining process.

The changes in molecular weight were not investigated experimentally, as the main target of the project was phosphorylation, but their apparent association with changes in pI are cause enough for discussion. The predicted pI of Net4B is 5.36-38 based on data from a range of pI prediction programs – ProtParam (Gasteiger et al., 2005), ProMost (Halligan et al., 2004) and Scansite (Obenauer et al., 2003) – with this value decreasing per phosphorylation event. In both the 3-10 and 4-7 IPG strip western blots spots are observed between a pI 5.4 and 5.6.

To eliminate the possibility that some of the spots in the array had arisen due to alternate splicing of the Net4B gene, an *in vitro* translation experiment was performed using rabbit reticulocyte lysate (Promega). The aim of this was to show that all but one of the spots was eliminated if post-translational modification of Net4B could not occur. Rabbit reticulocyte lysate was used as opposed to wheat germ extract in order to reduce the chance that other modifications could be made to Net4B. This experiment also failed to produce a result due to the low signal to noise ratio of the resulting Western Blot. The Net4B antibody would need likely to detect Net4B at least 10x greater dilution to eliminate the

background associated with the lysate. Extracting mRNA, as opposed to total RNA, for the translation reaction to increase translational efficiency had no appreciable effect on this. In theory this would have greatly increased the amount of the plant protein in the sample relative to animal protein in the lysate, improving the signal to noise ratio. For future similar experiments this mRNA extraction should be performed for this reason.

2-DGE analysis was attempted on multiple Net proteins under different conditions based on their molecular weight, in order to determine the best candidate for site-directed mutagenesis. These varied conditions included a change in the composition of the rehydration buffer (7M Urea, 2M Thiourea, 1.2% CHAPS, 0.4% ASB14, 0.25% ampholytes, (Khoudoli et al., 2004) and introducing 10% SDS into the transfer buffer. A limitation of 2-DGE protocol is that larger proteins have a low uptake into the IPG strip during the rehydration step, which may account for difficulties in generating results for both the Net1 and Net2 proteins, as all members of these families have molecular weights above 100kDa. Nonetheless, Net4Bs result was highly indicative of a highly phosphorylated protein and given the time constraints associated with the project, Net4B alone was taken forward for further bioinformatics analysis and site-directed mutagenesis. The sum of the evidence prior to this work had already made Net4B a major focus for the project, so it was highly advantageous to investigate it further in preference to other Net proteins.

### **3.5 *In silico* experimentation**

#### **3.5.1 Selection of Net4B and predicted phosphorylation sites**

The 2-DGE experimentation showed that Net4B had at least 12 different configurations of modification, but elucidating the nature of these modifications had limited success, so a new approach was needed in order to narrow down the predicted phosphorylation sites that lay within areas of homology in the Net4 family. Having already predicted that Net4B had a structure where it was folded along almost its entire length, with the NAB domain and the C-terminus in close proximity to one another, it was prudent to test whether a phosphorylation event could change their positions relative to one another. The alignment study had shown that there were three regions along the length of Net4B that were

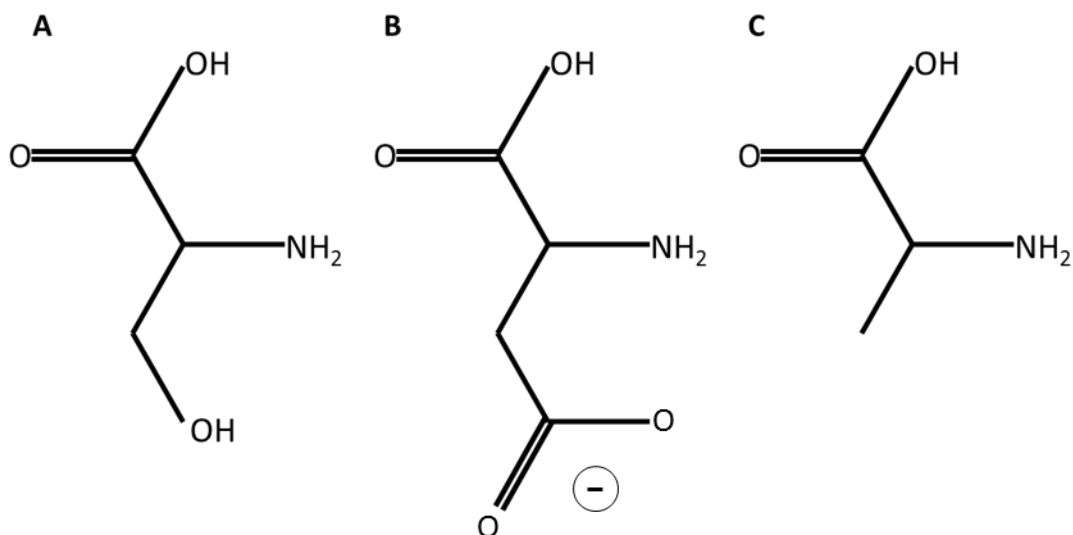
homologous to regions in Net4A outside of the NAB domain, suggesting that these regions may be important structurally or for regulation. These three domains were the region immediately C-terminal to the NAB domain, the absolute C-terminus, and a region close to, but separate from, the absolute C-terminus. The latter of these regions correlates to the area of Net4B which makes up a hinge or turn position in the predicted structure. Three sites were selected, one from each region; S144, S357 and S509. S144 and S357 were selected as sites from the prediction study (table 1), as they were aligned with serine residues in Net4A that could be phosphorylated by the same type of kinase, and were both predicted by the *A. thaliana* specific prediction software PhosPhAt. S509 has been determined as a phosphorylation site experimentally (table 2), but it is not aligned with a C-terminal serine in Net4A. It seemed prudent to test this site, however, because it was found directly in an existing database and it was also proximal to a region of Net4B which is present in Net4A and other proteins not from the Net superfamily, called the IRQ domain. This domain is associated with Rab binding, but the manner in which this binding occurred had not been investigated.

Although the only protein for which proteomics results were generated was Net4B, this protein is highly advantageous to investigate for this project. Net4B is 517 amino acids in length, which is comparable to ERM proteins, which are 500-600 amino acids in length (Pearson et al., 2001). It is also, along with Net4A, most similar to the Net protein ancestor (Hawkins et al., 2014), both in terms of its NAB domain and C-terminal sequence, which means that instances of regulation may have implications for the regulation of other family members. This includes those that may not immediately be apparent from the alignment studies. Finally as previously stated, it has a known C-terminal phosphorylation site.

The *in silico* experiment was performed using the PHYRE2 server, which was also used for the tertiary structure predictions. The effect of a phosphorylation event was predicted by altering the serine (S) to an aspartic acid (D), which had a large negatively charged R group, and is well established experimentally as a phosphomimic. Serine to aspartic acid mutations were henceforth be termed SXD, with X representing the position of the amino acid. Similarly, alanine (A) is a well-established mimic for a non-phosphorylatable

serine residue, and mutations of this nature were termed SXA. A comparison of the chemical structures is shown in figure 21.

Figure 21: Comparison of amino acids used for mutagenesis. **A** Serine **B** Aspartic Acid; the pair of oxygens give a negatively charged, hydrophilic side chain, mimicking a phosphate group **C** Alanine; the lack of hydroxide group in the R group in comparison to serine makes it unavailable for modification by a kinase.



The results of this experiment must be treated with caution as they are generated by aligning the sequence of Net4B with other known models, so the structures generated may not be a true representation of the actual tertiary structure of Net4B. Any changes in structure based on the mutations must also be treated with caution for this reason, but since the experiment is looking for an appreciable change in the relative locations of two domains, not a defined change leading to a predetermined structure, it is possible to glean some information pertaining to whether or not a phosphorylation event may have an effect of some kind. Similarly, if no change is observed, it does not necessarily mean that that site is not phosphorylated *in vivo*. This experiment was designed to inform the selection of sites for site directed mutagenesis.

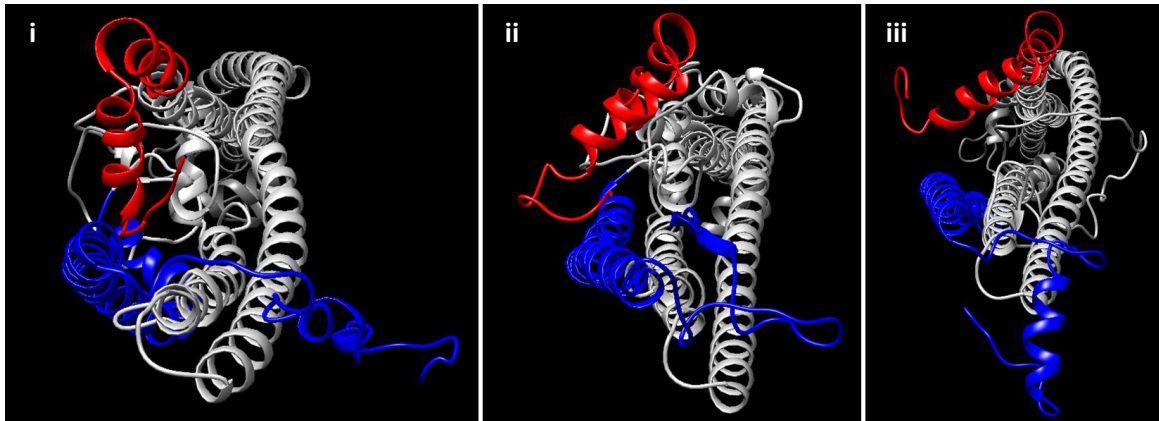
### 3.5.2 *In silico* mutagenesis experiments

All three of the chosen sites were mutated from a serine to either an alanine or aspartic acid residue and input into the PHYRE2 intensive mode prediction software. Two of the sites, S144 (figure 22A) and S357 (figure 22B), made small changes to the relative arrangement of the C- and N-termini, when mutated to

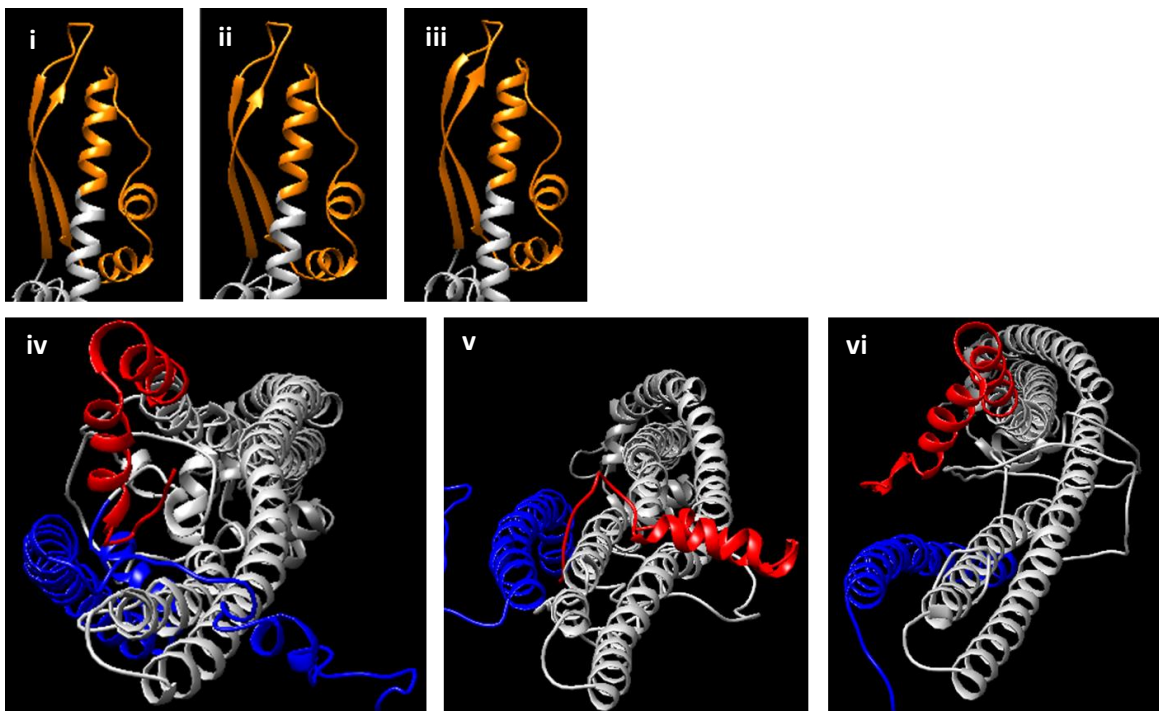
alanine or to aspartic acid. The C terminus would change its orientation to point outwards from the NAB domain, as opposed to pointing into a cleft within it. In all cases, however, the main axis of the C-terminal half of the protein remained aligned to that of the N-terminal half in an overlapping coiled-coil arrangement. This would imply that these changes had a good chance of occurring due to standard error within the model. At a local level the effects of these mutations were small; the S144 mutants did not make a significant alteration to the shape of the N-terminus compared to the wild-type, and the S357 mutants made almost no alterations to the hinge-like region. Comparisons were made using the MatchMaker>Align tool in CHIMERA, which allows alignments based on the reference structure, which was, in this case, the tertiary structure model of the wild-type. The models placed these serine residues on the outside of the structure, meaning the addition of the large hydrophilic group, like that of aspartic acid, would have very limited effects on the structure, but this may not be true for the protein *in vivo*. Phosphorylation may also regulate an interaction with another protein via another mechanism other than changing the structure of Net4B. Both aspartic acid mutations, however, did make alterations to the relative positions of the N- and C-termini. S144D caused the absolute C-terminus to point away from the main axis of the protein. S357D made a more open structure with the C-terminal half of the protein becoming more off-set with the N-terminal half. Without first confirming the phosphorylation state of these residues, however, a site-directed mutagenesis experiment would be highly speculative as these changes could still be a result of the standard error in model generation. Additionally, the S144 site is located in a region of the protein which is predicted with low confidence.

Figure 22: *In silico* mutagenesis in S144 and S357; **A** the S144 mutations (non-mutant (i), S144A (ii) and S144D (iii)) .Small changes were observed in the arrangement the N (blue) and C (red) terminal regions. The S144D mutant displays a slight shift in the most C-terminal alpha helix away from the NAB domain **B** the S357 mutants (non-mutant (i, iv), S357A (ii, v) and S357D (iii, vi) demonstrate almost no change to the hinge region of the protein (i-iii), but demonstrate small changes at the C/N terminus (iv-vi). These changes appear more significant than the S144 mutants. The S357A mutant demonstrates much closer association of the termini and S357D shows a more open tertiary structure.

**A**



**B**



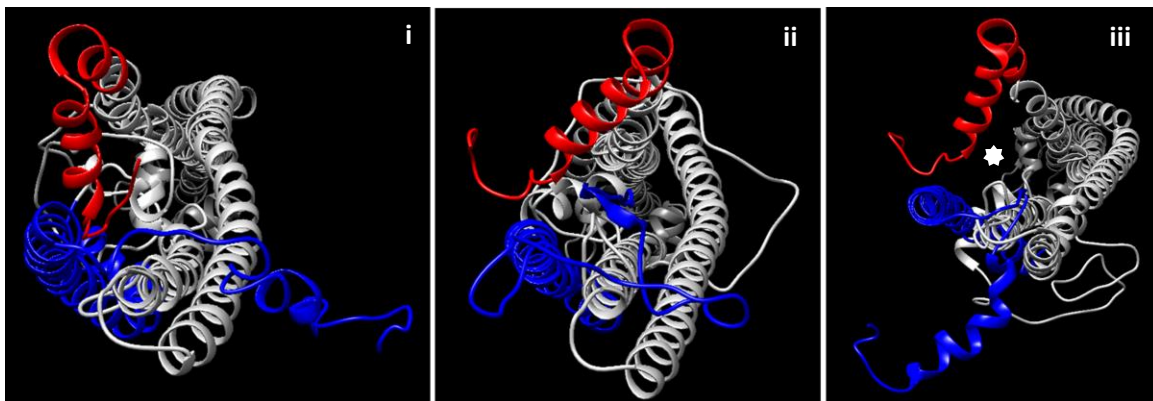
The S509D mutant (figure 23), however, caused a movement of the C-terminus of the protein away from the NAB domain. The axis of the C-terminal half is different from that of the C-terminus of the wild-type, much like S357D, and the absolute C-terminus is not pointing towards the NAB domain, like S144D, making the S509D mutant look like a combination of the two. The S509A mutation also caused the C-terminus to change in its orientation relative to the NAB domain, but the axis of the C-terminal half of the protein relative to the main N-terminal half remained unchanged. The most C-terminal alpha helix still remains close to the N-terminal alpha helices, which includes the NAB domain, however. It was therefore possible to cautiously state that the phosphorylation of S509 may have an effect on any N- and C-terminal interactions in Net4B. The size of this change, relative to the other point mutations, taken with the fact that S509 was taken directly from the PhosPhAt database rather than prediction software, made it very attractive for immediate investigation. This site was therefore targeted for site-directed mutagenesis exclusively, testing both S509D and S509A to determine whether the gain or loss of the phosphate group would cause a change in actin binding when infiltrating Net4B into *N. benthamiana*. The results of all *in silico* mutations are summarised in Table 5.

Table 5: Summary of *in silico* mutagenesis experiments

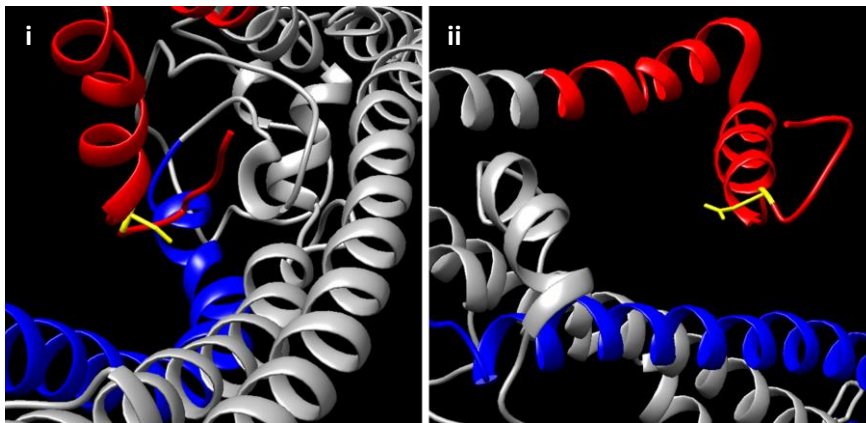
Mutation	Effect
S144A	Slight movement of the C-terminus, N- and C- termini still close together
S144D	Slight movement of the C-terminus, N- and C- termini still close together
S357A	Change to the position of the C-terminus but remains very close to the N-terminus. No effect on the hinge region.
S357D	Movement of the C-terminus away from the N-terminus. No effect on the hinge region.
S509A	Slight movement of the C-terminus, N- and C- termini still close together
S509D	Largest movement of the C-terminus, observable space between N and C termini, C terminus points away from the main axis of the protein
All Double mutant configurations	No additional effect
All Triple mutant configurations	No additional effect

Figure 23: *In silico* mutagenesis of S509; **A** Small changes in the arrangement of the N- (blue) and C-termini (red) were observed when comparing the non-mutant (i) to S509A (ii), but a very cohesive tertiary structure is maintained. In contrast, the tertiary structure of S509D (iii) is much more open, with a visible space (white asterisk) seen between the C-terminus and the main axis (grey) of the structure. **B** Here the residues of the non-mutant (i) and S509D (ii) are marked (yellow). In the non-mutant, the residue is shown pointing into the N-terminal cleft, whereas in S509D, it is shown pointing along the main axis of the structure. In the case of S509A the residue is also shown pointing towards the N-terminal cleft (not shown). **C** Another angle of the interaction, showing that in the normal protein (i) the C-terminus is pointing towards the NAB domain, whereas in the the S509D (ii) mutant the C-terminus is pointing out of the page, and away from the NAB domain.

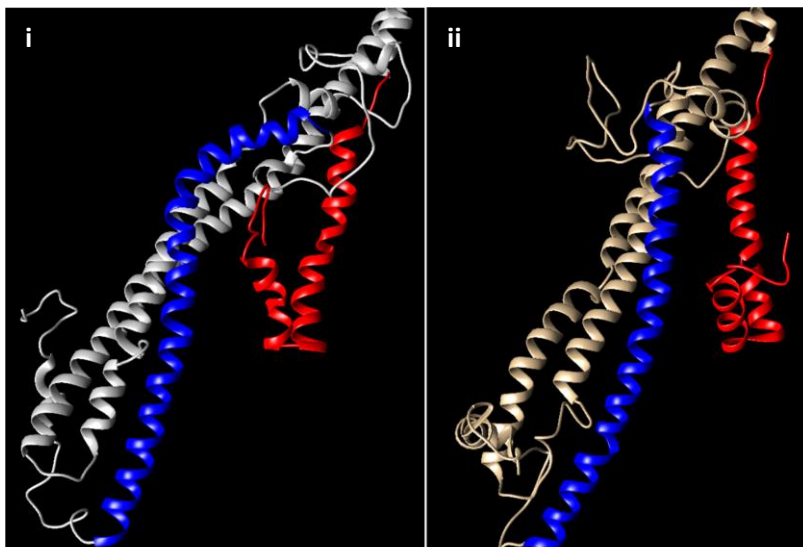
**A**



**B**



**C**



### **3.6 Site-directed mutagenesis of S509 in Net4B**

#### 3.6.1 Summary of rational selection of S509 for mutation

The use of extensive bioinformatics made S509 the obvious target for mutagenesis, as it is an experimentally determined phosphorylation site that is placed at a predicted interface between the C terminus and the NAB domain. The latter is rationalisation for the prediction that a mutation so distant from the actin binding domain of Net4B may have an effect of its actual actin binding activity. An investigation (Dixon, 2013) into phosphorylation sites within the NAB domain failing to yield results indicating a regulatory phosphorylation event. The targeted sites were thought to have a structural rather than regulatory role. Combined, this evidence suggested that S509 was an excellent candidate for an ERM protein-like model of activation for Net4B. Given mutations in other conserved areas within the Net4 family had been predicted to make insignificant changes to the tertiary structure of Net4B, it was prudent to focus efforts on S509, given the limited timescale of the project. These sites were also not confirmed sites of phosphorylation. Multiple mutagenesis kits were tested for this experiment, leading to the utilisation of the QuikChange Lightning Kit (Aligent) as this was the most reliable. Similarly, numerous rounds of diagnostic PCR were necessary to determine that the vectors being mutagenized were effective.

#### 3.6.2 Mutagenesis Reactions

The vectors used had been previously created by David Mentlak (pDONR207-Net4B, PMDC83-Net4B-GFP) and Martin Dixon (PMD43-GFP) during their respective PhDs. These were used for mutagenesis and cell transformation reactions, after having been confirmed to contain the appropriate genes by diagnostic PCR using Net4B internal and vector specific primers. The QuikChange Lightning Kit was used to introduce the mutations S509A and S509D into Net4B in the pDONR207 vector. This was then transferred to PMDC83 by LR reaction to conjugate the mutant to GFP, allowing it to be visualised. It was unknown whether S509 was predominantly phosphorylated or not prior to this work; S509A was used to determine the actin binding efficiency of the non-phosphorylated form, and S509D of the phosphorylated form. In the ERM protein model, the phosphorylated form of the protein is the one which can bind

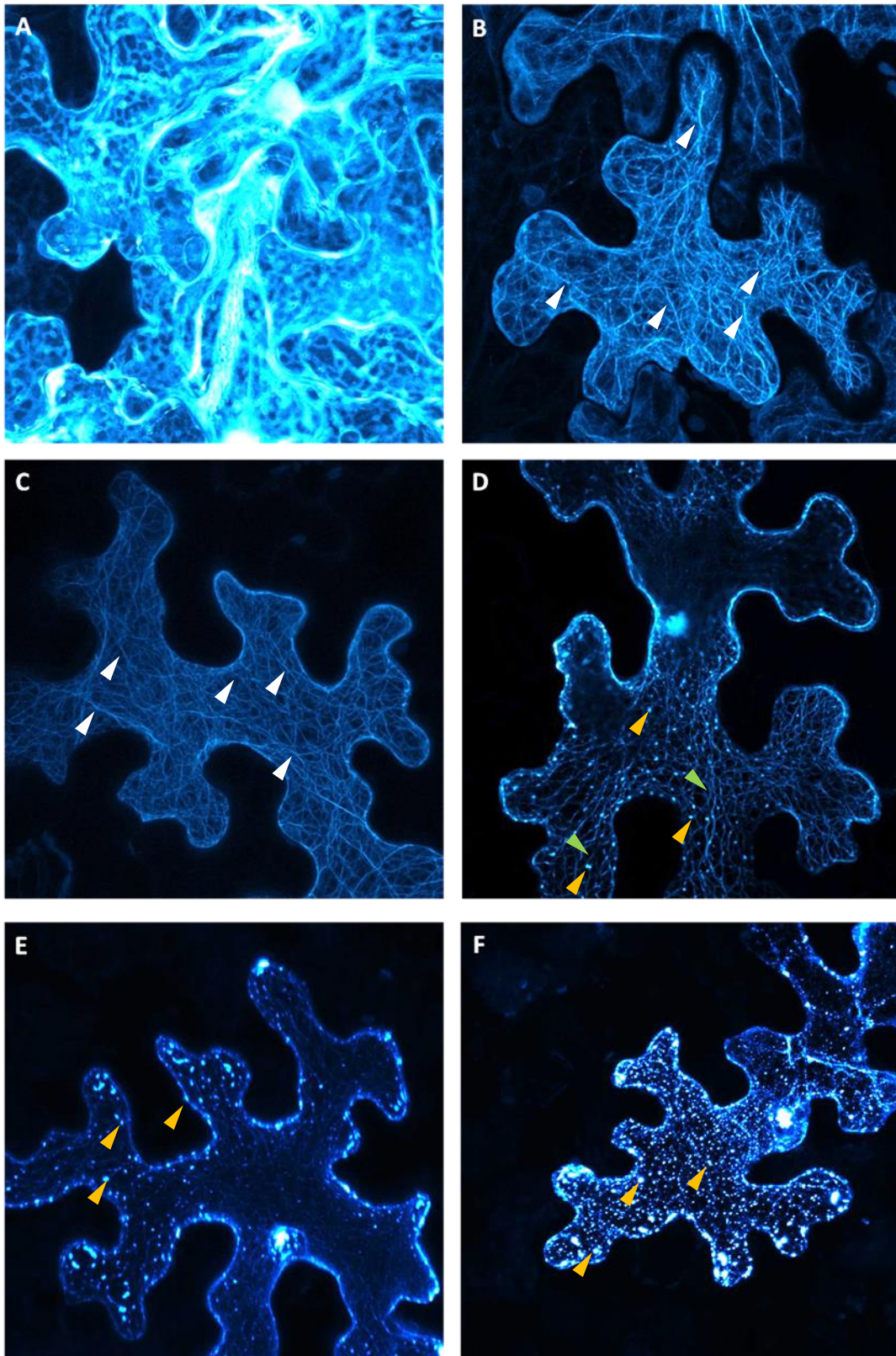
actin, so the expected result was to observe S509D lining actin filaments evenly, like full length non-mutated Net4B as previously observed (Mentlak, unpublished), and the S509A mutant would appear to be cytosolic, much like the GFP-only vector, as the C-terminus was rendering the NAB domain unavailable for binding.

### 3.6.3 Relative Actin Binding efficiency of the Net4B mutants

*A. tumefaciens* GV3101 strain bacteria were transformed with the PMDC83-Net4B-GFP or PMDC43-GFP plasmids and used for transient expression of Net4B in *N. benthamiana* leaves. Full length Net4B gave the expected result, evenly covering an extensive filament network (figure 24B), which had been confirmed previously by David Mentlak to be the actin cytoskeleton, in the epidermal cells of the underside of the leaf. As was expected, the S509D mutation exhibited a similar appearance (figure 24C), lining the actin filaments with no evidence of punctae or aggregation. Creating a phosphomimic residue at S509 therefore had no discernible effect.

S509A had an unexpected appearance (figure 24D-F) relative to the actin filaments however; as opposed to appearing like free GFP (figure 24A) - entirely cytosolic with no evidence of filaments - the mutant had a punctate appearance across all cells. This is in contrast to the clearly labelled filaments of the wildtype and S509D. There was also some variability appearance in different cells, even those from the same leaf. Filaments could be seen in some, but in others they were barely visible or absent altogether, meaning the mutation did not abolish actin binding completely. In cells where the actin filaments were visible, these punctae were aligned along them, in a 'beads on a string' appearance not previously seen in Net4B, but observed in many other Net proteins from across the superfamily. Punctae or aggregates have only been observed in the case of Net4B when it has been overexpressed (Mentlak, unpublished), at which point the nucleus also becomes visible, which is not observed here. All infiltrations were performed using the same concentration of cells. The S509A is therefore still capable of binding to actin, probably by virtue of simply having the NAB domain, but also causes aggregation of Net4B along actin filaments and favours this more punctate localisation over actin binding in some

Figure 24: Zeiss 880 confocal microscope images of Net4B mutants transiently expressed in *N. benthamiana*; **A** Free GFP is largely cytoplasmic **B** Non-mutant Net4B shows even distribution of fluorescence along filaments (white arrows). **C** S509A Net4B shows a similar distribution to the non-mutant (white arrows). S509A however, shows a range of appearances; **D** small aggregates (yellow arrows) aligning with marked filaments (green arrows), **E** aggregates (yellow arrows) with poor marking of filaments, **F** aggregates (yellow with no marking of filaments).



cells. This result also suggests that Net4B exists primarily in the phosphorylated form. The question remains as to why Net4B must be phosphorylated at its C-terminus to ensure regular actin binding by its N-terminus in terms of the mechanism the protein undergoes *in vivo*. What is clear is that the S509A mutant causes Net4B to have an appearance much like that of other families of Net proteins – ‘beads on a string’ – when transiently expressed in *N. benthamiana* leaves. The formation of these punctae may be associated with the ER-associating activity of IRQ domain (Mentlak, unpublished).

## **Chapter 4: Discussion**

### **4.1 Introduction**

The Networked (Net) superfamily represents a group of ABPs which may offer new understanding of the way actin is coordinated at a diverse range of membranes in plant cells. An N-terminal fragment, a portion of which subsequently became known as the Net Actin Binding (NAB) domain, of Net1A was observed by transient expression in *Nicotiana benthamiana* to localise to the actin cytoskeleton (Deeks et al., 2012). The superfamily is defined by the NAB domain and consists of 13 members, which may be subdivided into four families based on their length and homology (Deeks et al., 2012) (Hawkins et al., 2014). Expression of GFP fusions of Net proteins in BY-2 cells or pollen tubes has demonstrated that Net proteins localise to distinct membranes and structures (Deeks et al., 2012) (Wang et al., 2014). The mechanisms by which the Net proteins are regulated in their association with actin and membranes was unknown, and thus the aim of this project was to determine through bioinformatics analysis and experimentally what types of post-translational modifications occur on the Net proteins and to identify mechanisms pertaining to their coordination.

The project began by looking generally at the entire Net family, and by comparative alignments of the Net proteins it was possible to predict conserved post-translational modifications of various types – phosphorylation, acylation and SUMO-interaction. Phosphorylation was selected as the main focus of the project due to the high number of predicted conserved phosphorylation sites and the discovery of multiple known phosphorylation sites on 8 of the 13 Net proteins in the PhosPhAt database (Zulawski et al., 2013) (Durek et al., 2010) (Heazlewood et al., 2008). The use of tertiary structure modelling software, PHYRE2 (Kelley et al., 2015), demonstrated that Net4B may have a folded structure where the NAB domain and the C-terminus may interact, much like FERM-domain proteins in animals (Pearson et al., 2001). This bioinformatics work, combined with independent 2-dimensional gel electrophoresis showing that Net4B was highly likely to be phosphorylated, lead to site-directed mutagenesis of S509, a phosphorylation site in the C-terminal region of Net4B found in the PhosPhAt database. The mutation of this serine residue to an alanine, which mimics a non-

phosphorylated serine, resulted in weakened labelling of actin filaments. The punctate appearance of this mutant may indicate localisation to specific vesicles. These results have previously not been observed in the case of Net4B and are important for two reasons; the phosphorylation of Net4B at a residue distant from the NAB domain alters actin binding activity, and the desphosphorylation of this residue causes Net4B to demonstrate a 'beads on a string'-like appearance which is seen in other Net proteins. Further to this these results imply that Net4B interacts with another protein or complex in its non-phosphorylated form. It is now possible to propose two potential models for the regulation of Net4B.

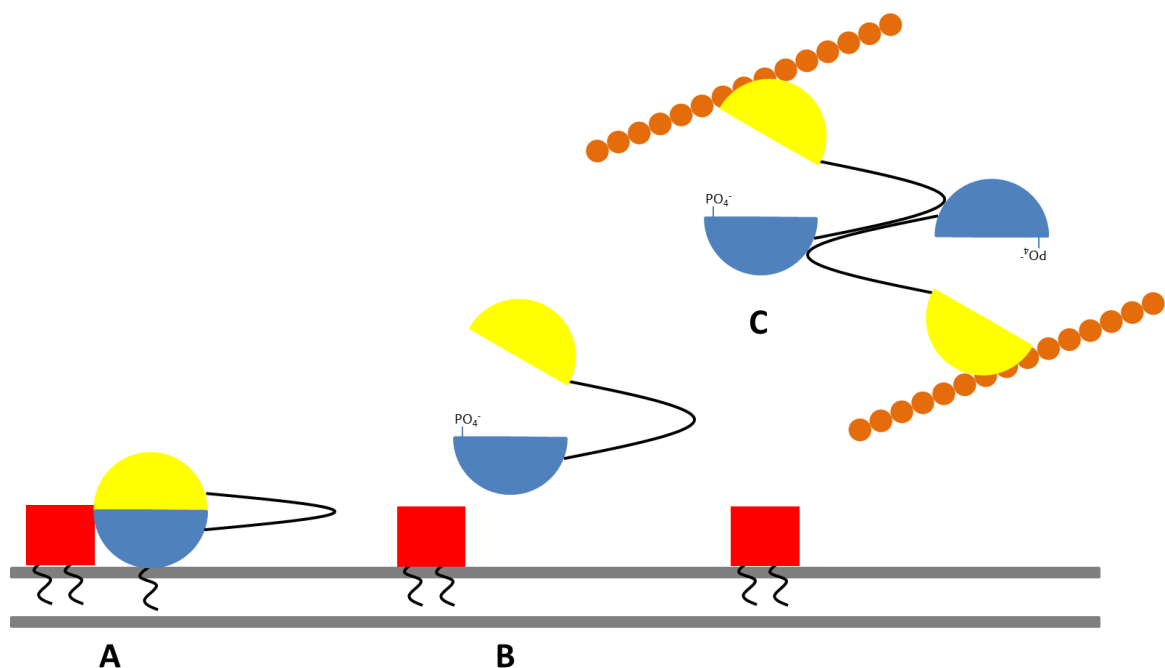
#### 4.1.1 Net4B may operate in an ERM-protein-like mechanism with a key difference

Certain members of the FERM-domain family operate by a self-masking mechanism, whereby their FERM domain, a terminal domain that binds to membranes via an adaptor protein, is covered and rendered inactive by the opposite terminus, which has actin binding capabilities (Pearson et al., 2001) (Fievet et al., 2004). The activation of these proteins, known as ERM proteins (Ezrin/Radixin/Moesin), relies on the phosphorylation of a threonine residue in this actin binding region, the resulting hydrophobicity of which causes the protein to open up (Pearson et al. 2001) (Fievet et al., 2004), allowing the activity of both the actin binding and FERM domains. It is thought that initial targeting to the plasma membrane is required for this process (Fievet et al., 2004).

Tertiary structure predictions performed as part of this project have shown that the N- and C-termini of Net4B could be closely associated with one another, with the protein folded along much of its length (figure 12). The mutation of S509 to an alanine residue, preventing a phosphorylation from occurring at this point, resulted in the localisation of transiently expressed Net4B to be altered drastically. The mutant demonstrated a punctate appearance which aligned variably with filaments (previously identified as actin by Hawkins and Mentlak, unpublished). In many cases the filamentous network apparent from the wild-type protein was absent or partial, showing that the interaction between Net4B and actin was weakened or focussed at particular points. Given the mutation of S509 to aspartic acid, a phosphomimic residue, had no effect on the localisation of Net4B, it appears that actin binding is influenced by phosphorylation at S509 (figure 23). It seems likely that, especially when transiently expressed in *N.*

*benthamiana*, Net4B exists primarily in its phosphorylated form. In this model (figure 25), NET4B in its non-phosphorylated form is associated at a membrane in small aggregates, and is only able to bind actin weakly. Its membrane association would be derived from the S-acylation of C487 (Hussey and Helmsley, personal correspondence), and the interaction of the C-terminal IRQ domain of Net4B with a membrane bound constitutively active RabG3 protein (Hawkins and Mentlak, unpublished). Both Net4A and Net4B exhibit this activity and therefore defined as classic Rab effectors. Following phosphorylation, the protein would unfold, releasing the NAB domain for its full actin bundling functionality whilst abolishing the association of Net4B with the membrane. In this respect the unfolding mechanism is similar to ERM proteins, but this model for Net4B differs from it because it does not link actin to the membrane in its phosphorylated state.

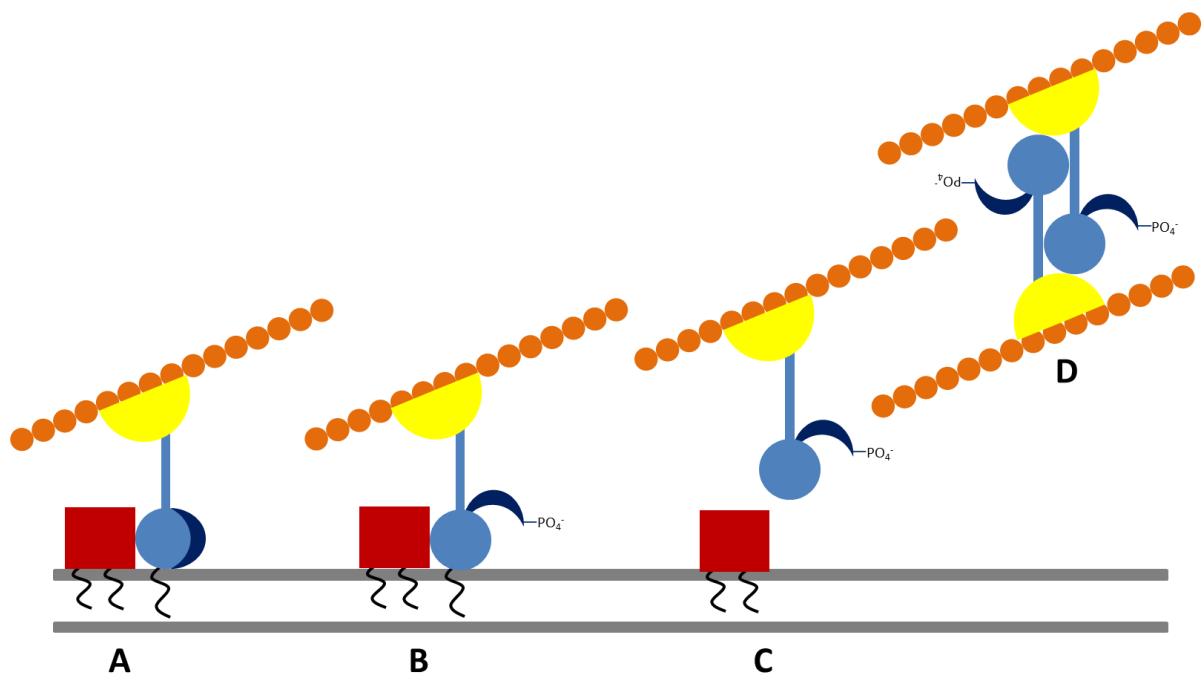
Figure 25: Proposed model for ERM-protein-like regulation of NET4B, which results in the activation of strong actin bundling activity. **A** In its non-phosphorylated state, the NAB domain (yellow) interacts with the C-terminus (blue), resulting in no or weak actin binding. Interaction with the vacuolar membrane is facilitated by the interaction of the IRQ domain with a RabG3 GTPase (red) and a lipid modification (black) **B** Phosphorylation of S509 (indicated by  $\text{PO}_4^-$ ), dissociates the NAB domain and C-terminus. This change in tertiary structure results in loss of association with the membrane. **C** The open structure of Net4B allows for strong actin (orange) binding. Subsequent dimerization of Net4B proteins results in actin filament bundling.



#### 4.1.2 Non-phosphorylated Net4B may act as a linker between actin filaments and Rab-labelled vesicles

An exciting prospect raised by the punctate appearance of the S509A mutant is that it resembles the appearance of transient expression of a Net4A or Net4B IRQ domain-GFP construct in *N. benthamiana* leaves, connected by the C-

Figure 26: Proposed model for phosphorylation of S509 resulting in removal of Net4B from the vacuolar membrane; **A** Net4B is linked to the vacuolar membrane via the association of its IRQ domain (light blue circle) with the GTP-bound RabG3 GTPase (red square) and by a lipid modification (black line) at C487, and is bound to actin (orange) by the NAB domain (yellow semi-circle). The C-terminal linker domain (dark blue crescent) protects against the cleavage of the lipid modification. **B** The phosphorylation of S509 (indicated by  $\text{PO}_4^-$ ) then causes the C-terminal linker to move away from the IRQ domain, exposing the lipid modification. **C** Thioesterase cleavage of the lipid modification results in a much weaker interaction with the vacuolar membrane. **D** Net4B is lost from the membrane and acts as an actin bundling protein by dimerization with other Net4B proteins. **E** IRQ domain (red), showing the location of C487 (blue) where it would be acylated, and the linker region (black) with S509 (green).

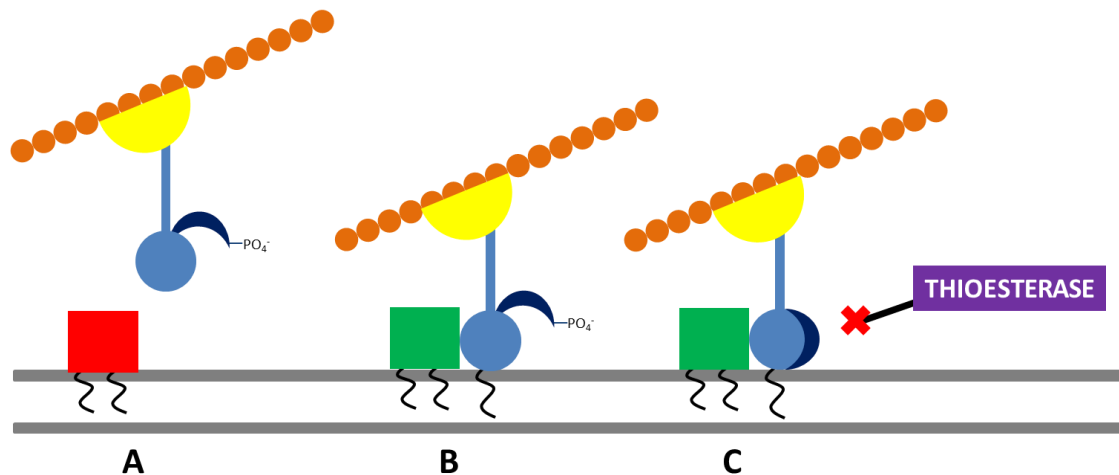


**E**

EVERTRVSASEMAEQKREAIRQLCMSLDHYRDGYDRLWRVVAGHKSKRVVVLST  
 ↑  
 C-TERMINUS

terminal linker region, which consists of the remaining amino acids C-terminal to the IRQ domain. These punctae were highly mobile and thought to be associated with moving vesicles, which may resemble Rab GTPase labelled vesicles (Mentlak, unpublished). The IRQ domain, a C-terminal domain in both Net4 species, has been shown by yeast two-hybrid screening to interact with activated GTP-bound members of the RabG3 family, (Hawkins and Mentlak, unpublished). The C-terminal linker region, however, is also essential for Rab binding, as the punctate appearance is lost upon transient expression of only the IRQ domain in *N. benthamiana*. A signalling cascade ending in kinase or phosphatase activity at S509 could attenuate the localisation of Net4B to the vacuole under certain developmental or stress circumstances. S509 resides just outside the IRQ domain in the C-terminal linker region. Net4B may be constitutively phosphorylated at this residue when transiently expressed in *N. benthamiana*, as implied by the similarity in appearance of the wildtype and the S509D mutant. Dephosphorylation, as mimicked by S509A, shows the Rab-labelled-vesicle-like punctae and therefore the non-phosphorylation of S509 may be required for the localisation of Net4B at membranes via their interaction with RabG3 proteins. Important avenues to explore would be to determine whether these punctae moved, whether the motility observed here is comparable to those observed previously, and whether Net4B and RabG3 proteins are colocalised in these punctae. This model may explain the requirement for the C-terminal linker for the punctate appearance in the aforementioned IRQ-GFP experiments, with the specific conformation conferred by the dephosphorylation of S509 crucial to membrane binding. Furthermore, a conformational change caused by a phosphorylation event may allow thioesterase activity to remove the lipid group from C487, reducing Net4Bs association to the membrane, which *in vivo* would be the vacuole. The C-terminal linker may physically protect this group (figure 26). Evidence for this is discussed in section 4.3. Net4B may then go on to have another role in actin dynamics, such as becoming a filament cross-linking protein. The proposed model *in vivo* for the regulation of the interaction of Net4B with RabG3 at the vacuole is shown in figure 27.

Figure 27: Proposed model for the recruitment of Net4B to the vacuole by RabG3. **A** Net4B is bound to actin (orange) via its NAB domain (yellow hemisphere), whilst RabG3 is inactive (red square). Net4B is phosphorylated in the linker region (dark blue crescent), adjacent to the IRQ domain (light blue circle). **B** RabG3 is activated (green square), allowing the recruitment of Net4B to the vacuolar membrane, where it is lipid modified (black line). **C** Phosphatase activity removes the phosphate group from the linker region, allowing it to close over the IRQ domain, protecting the new lipid modification from cleavage by thioesterases, which in turn allows its retention at the vacuole.



#### 4.2 Phosphorylation of Net4B may facilitate the cleavage of another post-translational modification

The single phosphorylation event at S509 is, in either model, extremely important for the regulation of Net4B. The 2-dimensional gel analysis (2-DGE) of Net4B suggests that there may be as many as eight phosphorylation sites, given that in the horizontal axis there are eight different isoelectric points detected, each 0.3 pI units apart, which is characteristic of a pI change induced by a phosphorylation event (figure 20). Using the 3-10 IPG strip, it was demonstrated that Net4B was also present at two different molecular weights. Upon performing a western blot at higher resolution, it can be seen that after five phosphorylation events, there is a diagonal shift, demonstrating a decrease in the molecular weight upon that fifth phosphorylation. This suggests that these two modifications are performed simultaneously. The molecular weight change may be due to the already identified S-acylation of C487, which could be confirmed by western blotting, using Net4B antibodies, of a protein extract from wildtype *A. thaliana* seedlings treated with thioesterase. In this case all of the spots would have the same

apparent molecular weight. The exact nature of the lipid group added is unknown, but the change in apparent molecular weight appears to be very small, and may be indicative of a palmitate group (Gao et al., 2011). Given the proposed changes in membrane localisation (sections 4.1.1 and 4.1.2) as an explanation of the observations in the S509A mutant, the phosphorylation of S509 may represent this fifth phosphorylation event.

Importantly, S509 is not conserved in Net4A as the C-terminal linker regions of the two Net4 proteins are very different, and Net4A demonstrates thicker 'actin staples' when transiently expressed in *N. benthamiana* (Hawkins and Hussey, unpublished), similar to the stationary 'beads on a string' appearance of other Net proteins. The S-acylation site at C487 is predicted to be conserved with Net4A; if phosphorylation of S509 is required for cleavage of the lipid modification, this could explain why Net4A is able to make stationary aggregates. Sequential post-translational modifications dependent on one another are not unprecedented (Lin et al., 2009) (Vogt et al., 2005). A 2-DGE western blot experiment would be extremely useful to determine whether Net4A underwent an apparently phosphorylation-mediated decrease in molecular weight or not. If it did not, this would provide further evidence that the presence of the phosphorylation site at S509 in Net4B could be the reason for the dynamic models presented.

This project has also identified many other predicted phosphorylation sites in Net4B that would be prime targets for investigation by site directed mutagenesis, as it may be a sequence of phosphorylation events that facilitate this loss in molecular weight. In particular S357 presents an exciting prospect, as it is conserved with Net4A. It was not pursued in this project only because phosphorylation at the absolute C-terminus was a major focus of the work, as it was important to both the ERM protein model and the implications of a phosphorylation event close to IRQ domain.

### **4.3 Phosphorylation is a widespread post-translational modification of Net proteins**

Despite the lack of 2-DGE evidence for the other Net families, it can be stated that seven of the eight proteins constituting the Net1 and 2 families are

phosphorylated given the data drawn from the PhosPhAt database (Zulawski et al., 2013) (Durek et al., 2010) (Heazlewood et al., 2008). Subsequent analysis in this project has shown that some of these phosphorylation sites are predicted to be conserved (table 3). These sites are all found outside of the NAB domain, and some are found at the C-terminus. These sites would therefore make prudent targets for site-directed mutagenesis. Furthermore, the 2-DGE analysis of Net4B suggests that the phosphorylation sites found in the PhosPhAt database only scratch the surface, as Net4B may have as many as eight phosphorylation sites. The collection of conserved predicted phosphorylation sites presented in this thesis could therefore act as a solid base for the identification of phosphorylation sites. Only the Net3 family have expressed no evidence of phosphorylation.

#### **4.4 S-acylation may be a conserved post-translational regulatory mechanism in Net1, Net2 and Net4 protein families**

The bioinformatics analysis presented in section 3.2.2 demonstrates the potential three of the Net families have for being S-acylated. In particular the Net1 proteins exhibited many conserved predicted S-acylation sites along much of their respective lengths. These sites are often conserved between the most similar proteins, Net1A with Net1B and Net1C with Net1D respectively, however there were three instances of conserved sites between all four members, one just after the NAB domain (around amino acid position 350) and two others separated by a single residue at the absolute C-terminus. The extensiveness of the predicted S-acylation combined with the fact that no S-acylation sites within the NAB domain may indicate that the Net1 family are strongly associated with membranes, or interact with multiple proteins through hydrophobic interactions facilitated by lipid modifications. In the case of Net1A, strong association with multiple membranes may be important for a potential role in regulating plasmodesmatal function (Deeks et al., 2012).

The Net2 family exhibited limited predicted S-acylation conservation between the most closely related pairs, Net2A with Net2B and Net2C with Net2D respectively, but two conserved sites were predicted across the whole family. Interestingly, one of these sites was just after the NAB domain (around amino acid position 260), and the other was at the C-terminus. This is very similar to the

positions of the conserved residues in the Net1 family. The Net4 family only possessed a single conserved S-acylation site between the two members; the C487 residue in Net4B and C527 in Net4A. Net4B is known to be S-acylated (Hussey and Helmsley, personal communication). These residues fall within the IRQ domain. This may indicate that three of the Net protein families rely on a C-terminal S-acylation site as part of their regulation. The evolution of the Net1 and Net2 families involved an initial divergence from the Net4 family (Hawkins et al., 2014). It could be proposed that the Net1/2 family ancestor gained a second S-acylation site during this divergence.

The conserved S-acylation site predicted the Net4 family resides in the IRQ domain, which itself is conserved between both Net4 proteins. Given the bioinformatics data, this may suggest that the S-acylation of this residue is important to interaction of the IRQ domain and RabG3 GTPases. Site-directed mutagenesis experiments could be used to confirm this, and test other non-conserved sites as they cannot be ruled out at this stage. This informed the decision to make the lipid modification a separate membrane attachment in the models of the regulation of Net4B in section 4.2.

#### **4.5 Prenylation may be a conserved post-translational modification of the Net1 family**

The pair of conserved S-acylation sites predicted by CSS-PALM (section 3.3.2) at the C-termini of the Net1 family proteins were both also predicted to be prenylation sites by GPS-Lipid (section 3.3.3). The Net1 proteins have a CGC motif at their C-termini which is the consensus sequence for geranylgeranylation of Rab proteins (Khosravi-Far et al., 1992). Net1 family proteins are not identified as Rab proteins, but Rab proteins function as regulators of membrane trafficking pathways. Given the proposed importance of Net1A at plasmodesmata, investigation of the prenylation state of this C-terminal pair of residues would make for an exciting experimental avenue. Prenylation of these residues may act as a membrane targeting signal (Helmsley & Grierson, 2008) for the Net1 family of proteins.

#### **4.6 SUMO-interaction may be a conserved regulatory mechanism in the NAB domain**

The final type of post-translational modification investigated in this project was sumoylation. Whilst conserved sumoylation sites in Net proteins were not forthcoming, two sumo-interacting motifs (SIMs) were found to be conserved within the NAB domain (see section 3.3.6), meaning that they may be present in all of the members of the Net superfamily. SIMs allow proteins containing them to interact with sumoylated proteins. More importantly, both of these SIMs were proximal to a group of conserved hydrophilic residues (aspartic and glutamic acid). In many of the Net proteins this group took the form of an EDXD motif. Groups of hydrophilic residues are important for the orientation of SUMO when it binds non-covalently to the SIM (Kerscher, 2007). The site-directed mutagenesis of residues within both of these SIMs and in the EDXD motif is an important avenue for the investigation of this regulatory mechanism. Actin in the nucleus is sumoylated, which allows for a tenuous connection to be drawn with Net3A, which is localised to the nuclear membrane (Deeks et al., 2012). Net3A could come into contact with actin as it is exported from the nucleus (Vartiainen, 2008). A pull-down experiment using the NAB domain as bait, followed by a western blot of the interacting proteins brought down probed using anti-SUMO antibodies, would allow determination of a population of sumoylated Net protein interactors.

Previously, a hydrophilic residue predicted to be important for actin binding, E66 in Net1A, was mutated to a glycine residue (Cartwright, 2011). The result of this mutation resulted in the obvious separation of the Net1A mutant from actin microfilaments. Interestingly, the Net1A punctae were still aligned with actin, but were not as strongly as the non-mutant, suggesting that these punctae were slightly offset from the actin cytoskeleton. A potential explanation of this is that the mutation of the hydrophilic residue was causing Net1A to misorientate itself relative to a sumoylated binding partner. There is also a possibility that the short hydrophobic regions may represent the point of contact with actin itself, using a slotting mechanism similar to that of a SIM, but without requiring actin to be sumoylated.

#### 4.7 Concluding remarks

This project aimed to form the foundation for future work concerning the post-translational modification of the Net superfamily and identify potential mechanisms by which this family of proteins was regulated. Extensive bioinformatics analysis has allowed the identification of multiple phosphorylation and acylation sites for future investigations. Work became focused on the phosphorylation of Net4B following the determination that a possible eight phosphorylation events could be occurring using 2-DGE. Site-directed mutagenesis of a selected site, S509, caused drastic changes to the localisation of Net4B transiently expressed in *N. benthamiana*. This demonstrates the success of the method used to identify sites that are likely to be important for regulation from a collection of predicted sites from pieces of online software.

The results of the site-directed mutagenesis show that a phosphorylation event at the C-terminus of Net4B may have the potential to affect the actin-binding affinity of the N-terminal NAB domain. Despite being evolutionarily distinct, a model similar to that of the ERM proteins from animals is one of two proposed mechanisms for the regulation of Net4B. The other mechanism may explain the lack of the 'beads on a string' appearance demonstrated by many other Net proteins. It would be interesting in future work in this area of study on the Net proteins to investigate the importance of the C-terminal acylation sites predicted during this project in their location. Furthermore, the second model for the regulation of Net4B has important implications for the membrane-binding activity of Net4A. Net4B could be a more dynamically regulated protein that is often associated with or detached from the vacuolar membrane in order to facilitate changes in its shape or function, whereas Net4A represents a more static protein, important for maintaining particular vacuolar morphologies.

## Appendix 1

### Net4B constructs cloned

Vector	Insert	Purpose
pDONR207	Net4B S509D	For LR reaction into PMDC83
pDONR207	Net4B S509A	For LR reaction into PMDC83
PMDC83	Net4B S509D	Transient expression of GFP-tagged construct
PMDC83	Net4B S509A	Transient expression of GFP-tagged construct

### Primers used for site-directed mutagenesis

Mutation	Forward	Reverse
S509D	GAGTTGTTGCAGGACATAAGGA TAAGAGAGTAGTGGTCTTATC	GATAAGACCACTACTCTCTTATC CTTATGTCCTGCAACAACCTC
S509A	GAGTTGTTGCAGGACATAAGGC TAAGAGAGTAGTGGTCTTATC	GATAAGACCACTACTCTCTTAGC CTTATGTCCTGCAACAACCTC

### Primers used for sequencing confirmation

Primer	Sequence
pDONR207 Fw	TCGCGTTAACGCTAGCATGGATCT
pDONR207 Rv	GTAACATCAGAGATTTTGAGACAC
NET4B -NAB Fw	GGGGACAAGTTTGTACAAAAAAGCAGGCTTC- ACATCTGAGATCCAGTCACAGAGCTCTCTTGAG
NET4B -IRQ Stop Rv	GGGGACCACTTTGTACAAGAAAGCTGGGTC- TCATTCCGTAAGCTCACTTGACCGTCTTC
NET4B IRQ Fw	GGGGACAAGTTTGTACAAAAAAGCAGGCTTC- GAAGTGGAAAGGACGAGAGTGTCTGC
NET4B IRQ Stop Rv	GGGGACCACTTTGTACAAGAAAGCTGGGTC- TCATCTCCAAAGTCTGTCGTACCCATCTCTG
NET4BFw	GGGGACAAGTTTGTACAAAAAAGCAGGCTTC- ATGGCTTCGTCTACGGCTCAGAG

## Bibliography

- Allwood, E.G., Anthony, R.G., Smertenko, A.P., Reichelt, S., Drobak, B.K., Doonan, J.H., Weeds, A.G., Hussey, P.J., 2002. Regulation of the pollen-specific actin-depolymerizing factor LIADF1. *Plant Cell* 14, 2915–2927. doi:10.1105/tpc.005363
- Allwood, E.G., Smertenko, A.P., Hussey, P.J., 2001. Phosphorylation of plant actin-depolymerising factor by calmodulin-like domain protein kinase. *FEBS Lett.* 499, 97–100. doi:10.1016/S0014-5793(01)02528-5
- Alonso, A., Greenlee, M., Matts, J., Kline, J., Davis, K.J., Miller, R.K., 2015. Emerging roles of sumoylation in the regulation of actin, microtubules, intermediate filaments, and septins. *Cytoskeleton* 72, 305–339. doi:10.1002/cm.21226
- Augustine, R.C., Vidali, L., Kleinman, K.P., Bezanilla, M., 2008. Actin depolymerizing factor is essential for viability in plants, and its phosphoregulation is important for tip growth. *Plant J.* 54, 863–875. doi:10.1111/j.1365-313X.2008.03451.x
- Avisar, D., Abu-Abied, M., Belausov, E., Sadot, E., Hawes, C., Sparkes, I.A., 2009. A comparative study of the involvement of 17 *Arabidopsis* myosin family members on the motility of golgi and other organelles. *Plant Physiol.* 150, 700–709. doi:10.1104/pp.109.136853
- Calcutt, J. R., 2009. ABP195, a novel Actin Binding Protein. PhD thesis
- Camacho, C., Coulouris, G., Avagyan, V., Ma, N., Papadopoulos, J., Bealer, K., Madden, T.L., 2009. BLAST+: architecture and applications. *BMC Bioinformatics* 10, 421. doi:10.1186/1471-2105-10-421
- Carlier, M.-F., Laurent, V., Santolini, J., Melki, R., Didry, D., Xia, G.-X., Hong, Y., Chua, N.-H., Pantaloni, D., 1997. Actin depolymerizing factor (ADF/Cofilin) enhances the rate of filament turnover: implication in actin-based motility. *J. Cell Biol.* 136, 1307–1322.
- Cartwright, E. F., 2011. Investigating Functional Motifs within the N-terminal Domain of Novel Actin Binding Proteins NET1A and NET2A. Master's Thesis
- Castillo-Lluva, S., Tatham, M.H., Jones, R.C., Jaffray, E.G., Edmondson, R.D., Hay, R.T., Malliri, A., 2010. SUMOylation of the GTPase Rac1 is required for optimal cell migration. *Nat. Cell Biol.* 12, 1078–1085. doi:10.1038/ncb2112
- Catala, R., Ouyang, J., Abreu, I.A., Hu, Y., Seo, H., Zhang, X., Chua, N.-H., 2007. The *Arabidopsis* E3 SUMO ligase SIZ1 regulates plant growth and drought responses. *Plant Cell* 19, 2952–2966. doi:10.1105/tpc.106.049981
- Chen, C., Zhang, Y., Zhu, L., Yuan, M., 2010. The actin cytoskeleton is involved in the regulation of the plasmodesmal size exclusion limit. *Plant Signal. Behav.* 5, 1663–1665. doi:10.4161/psb.5.12.14018
- Cheung, A.Y., Wu, H., 2004. Overexpression of an *Arabidopsis* Formin Stimulates Supernumerary Actin Cable Formation from Pollen Tube Cell Membrane. *Plant Cell* 16, 257–269. doi:10.1105/tpc.016550
- Conti, L., Nelis, S., Zhang, C., Woodcock, A., Swarup, R., Galbiati, M., Tonelli, C., Napier, R., Hedden, P., Bennett, M., Sadanandom, A., 2014. Small Ubiquitin-like modifier protein SUMO enables plants to control growth independently of the phytohormone gibberellin. *Dev. Cell* 28, 102–110. doi:10.1016/j.devcel.2013.12.004
- Corbin, C., Decourtil, C., Marosevic, D., Bailly, M., Lopez, T., Renouard, S., Doussot, J., Dutilleul, C., Auguin, D., Giglioli-Guivarc'h, N., Lainé, E., Lamblin, F., Hano, C., 2013. Role of protein farnesylation events in the ABA-mediated regulation of the Pinoresinol–Lariciresinol Reductase 1 (LuPLR1) gene expression and lignan biosynthesis in flax (*Linum usitatissimum* L.). *Plant Physiol. Biochem., Plant Phenolics: biosynthesis, genetics, and ecophysiology* 72, 96–111. doi:10.1016/j.plaphy.2013.06.001
- Davidson, A.J., Insall, R.H., 2011. Actin-Based Motility: WAVE Regulatory Complex Structure Reopens Old SCARs. *Curr. Biol.* 21, R66–R68. doi:10.1016/j.cub.2010.12.001

- Deeks, M.J., Cvrcková, F., Machesky, L.M., Mikitová, V., Ketelaar, T., Zársky, V., Davies, B., Hussey, P.J., 2005. Arabidopsis group Ie formins localize to specific cell membrane domains, interact with actin-binding proteins and cause defects in cell expansion upon aberrant expression. *New Phytol.* 168, 529–540. doi:10.1111/j.1469-8137.2005.01582.x
- Deeks, M.J., Hussey, P.J., 2005. Arp2/3 and SCAR: plants move to the fore. *Nat. Rev. Mol. Cell Biol.* 6, 954–964. doi:10.1038/nrm1765
- Deeks, M.J., Hussey, P.J., Davies, B., 2002. Formins: intermediates in signal-transduction cascades that affect cytoskeletal reorganization. *Trends Plant Sci.* 7, 492–498. doi:10.1016/S1360-1385(02)02341-5
- de la Fuente van Bentem, S., Hirt, H., 2009. Protein tyrosine phosphorylation in plants: more abundant than expected? *Trends Plant Sci.* 14, 71–76. doi:10.1016/j.tplants.2008.11.003
- Didry, D., Carlier, M.-F., Pantaloni, D., 1998. Synergy between actin depolymerizing factor/cofilin and profilin in increasing actin filament turnover. *J. Biol. Chem.* 273, 25602–25611. doi:10.1074/jbc.273.40.25602
- Dixon, M. R., 2013. Net2A: bridging the gap in plant specific actin-membrane interactions. PhD thesis
- Dominguez, R., Holmes, K. C., 2011. Actin structure and function. *Annu Rev Biophys.* 40, 169–186. doi: 10.1146/annurev-biophys-042910-155359
- Durek, P., Schmidt, R., Heazlewood, J.L., Jones, A., MacLean, D., Nagel, A., Kersten, B., Schulze, W.X., 2010. PhosPhAt: the *Arabidopsis thaliana* phosphorylation site database. An update. *Nucleic Acids Res.* 38, D828–D834. doi:10.1093/nar/gkp810
- Eisenhaber, B., Wildpaner, M., Schultz, C.J., Borner, G.H.H., Dupree, P., Eisenhaber, F., 2003. Glycosylphosphatidylinositol lipid anchoring of plant proteins. Sensitive prediction from sequence- and genome-wide studies for *Arabidopsis* and rice. *Plant Physiol.* 133, 1691–1701. doi:10.1104/pp.103.023580
- Elrouby, N., Bonequi, M.V., Porri, A., Coupland, G., 2013. Identification of Arabidopsis SUMO-interacting proteins that regulate chromatin activity and developmental transitions. *Proc. Natl. Acad. Sci. U. S. A.* 110, 19956–19961. doi:10.1073/pnas.1319985110
- Evans, D.E., Pawar, V., Smith, S.J., Graumann, K., 2014. Protein interactions at the higher plant nuclear envelope: evidence for a linker of nucleoskeleton and cytoskeleton complex. *Front. Plant Sci.* 5. doi:10.3389/fpls.2014.00183
- Feng, Y., Walsh, C.A., 2004. The many faces of filamin: A versatile molecular scaffold for cell motility and signalling. *Nat. Cell Biol.* 6, 1034–1038. doi:10.1038/ncb1104-1034
- Fletcher, D.A., Mullins, R.D., 2010. Cell mechanics and the cytoskeleton. *Nature.* 463, 485–492. doi: 10.1038/nature08908
- Fodor-Dunai, C., Fricke, I., Potocký, M., Dorjgotov, D., Domoki, M., Jurca, M.E., Ötvös, K., Žárský, V., Berken, A., Fehér, A., 2011. The phosphomimetic mutation of an evolutionarily conserved serine residue affects the signaling properties of Rho of plants (ROPs). *Plant J.* 66, 669–679. doi:10.1111/j.1365-313X.2011.04528.x
- Gao, J., Liao, J., Yang, G.-Y., 2009. CAAX-box protein, prenylation process and carcinogenesis. *Am. J. Transl. Res.* 1, 312–325.
- George, S.P., Wang, Y., Mathew, S., Srinivasan, K., Khurana, S., 2007. Dimerization and actin-bundling properties of villin and its role in the assembly of epithelial cell brush borders. *J. Biol. Chem.* 282, 26528–26541. doi:10.1074/jbc.M703617200
- Gillmor, C.S., Lukowitz, W., Brininstool, G., Sedbrook, J.C., Hamann, T., Poindexter, P., Somerville, C., 2005. Glycosylphosphatidylinositol-anchored proteins are required for cell wall synthesis and morphogenesis in *Arabidopsis*. *Plant Cell* 17, 1128–1140. doi:10.1105/tpc.105.031815
- Gisbergen, P.A.C. van, Li, M., Wu, S.-Z., Bezanilla, M., 2012. Class II formin targeting to the cell cortex by binding PI(3,5)P2 is essential for polarized growth. *J. Cell Biol.* 198, 235–250. doi:10.1083/jcb.201112085

- Gu, Y., Fu, Y., Dowd, P., Li, S., Vernoud, V., Gilroy, S., Yang, Z., 2005. A Rho family GTPase controls actin dynamics and tip growth via two counteracting downstream pathways in pollen tubes. *J. Cell Biol.* 169, 127–138. doi:10.1083/jcb.200409140
- Halligan, B.D., Ruotti, V., Jin, W., Laffoon, S., Twigger, S.N., Dratz, E.A., 2004. ProMoST (Protein Modification Screening Tool): a web-based tool for mapping protein modifications on two-dimensional gels. *Nucleic Acids Res.* 32, W638–W644. doi:10.1093/nar/gkh356
- Harashima, H., Shinmyo, A., Sekine, M., 2007. Phosphorylation of threonine 161 in plant cyclin-dependent kinase A is required for cell division by activation of its associated kinase. *Plant J.* 52, 435–448. doi:10.1111/j.1365-313X.2007.03247.x
- Hawkins, T.J., Deeks, M.J., Wang, P., Hussey, P.J., 2014. The evolution of the actin binding NET superfamily. *Plant Traffic Transp.* 5, 254. doi:10.3389/fpls.2014.00254
- Hawkins, T. J., and Mentlak, D. A., 2012-2015. Net4/Rab interaction study. Unpublished raw data
- Heazlewood, J.L., Durek, P., Hummel, J., Selbig, J., Weckwerth, W., Walther, D., Schulze, W.X., 2008. PhosPhAt: a database of phosphorylation sites in *Arabidopsis thaliana* and a plant-specific phosphorylation site predictor. *Nucleic Acids Res.* 36, D1015–D1021. doi:10.1093/nar/gkm812
- Hecker, C.-M., Rabiller, M., Haglund, K., Bayer, P., Dikic, I., 2006. Specification of SUMO1- and SUMO2-interacting Motifs. *J. Biol. Chem.* 281, 16117–16127. doi:10.1074/jbc.M512757200
- Hemsley, P.A., Grierson, C.S., 2008. Multiple roles for protein palmitoylation in plants. *Trends Plant Sci.* 13, 295–302. doi:10.1016/j.tplants.2008.04.006
- Higaki, T., Kutsuna, N., Okubo, E., Sano, T., Hasezawa, S., 2006. Actin microfilaments regulate vacuolar structures and dynamics: Dual observation of actin microfilaments and vacuolar membrane in living tobacco BY-2 cells. *Plant Cell Physiol.* 47, 839–852. doi:10.1093/pcp/pcj056
- Higaki, T., Kutsuna, N., Sano, T., Kondo, N., Hasezawa, S., 2010. Quantification and cluster analysis of actin cytoskeletal structures in plant cells: role of actin bundling in stomatal movement during diurnal cycles in *Arabidopsis* guard cells. *Plant J.* 61, 156–165. doi:10.1111/j.1365-313X.2009.04032.x
- Hofmann, W.A., Arduini, A., Nicol, S.M., Camacho, C.J., Lessard, J.L., Fuller-Pace, F.V., de Lanerolle, P., 2009. SUMOylation of nuclear actin. *J. Cell Biol.* 186, 193–200. doi:10.1083/jcb.200905016
- Honing, H.S. van der, Kieft, H., Emons, A.M.C., Ketelaar, T., 2012. *Arabidopsis* VILLIN2 and VILLIN3 are required for the generation of thick actin filament bundles and for directional organ growth. *Plant Physiol.* 158, 1426–1438. doi:10.1104/pp.111.192385
- Huang, S., Blanchoin, L., Chaudhry, F., Franklin-Tong, V.E., Staiger, C.J., 2004. A gelsolin-like protein from papaver rhoeas pollen (PrABP80) stimulates calcium-regulated severing and depolymerization of actin filaments. *J. Biol. Chem.* 279, 23364–23375. doi:10.1074/jbc.M312973200
- Huang, S., Gao, L., Blanchoin, L., Staiger, C.J., 2006. Heterodimeric capping protein from arabidopsis is regulated by phosphatidic acid. *Mol. Biol. Cell* 17, 1946–1958. doi:10.1091/mbc.E05-09-0840
- Huang, S., Robinson, R.C., Gao, L.Y., Matsumoto, T., Brunet, A., Blanchoin, L., Staiger, C.J., 2005. *Arabidopsis* VILLIN1 generates actin filament cables that are resistant to depolymerization. *Plant Cell* 17, 486–501. doi:10.1105/tpc.104.028555
- Hussey, P.J., Ketelaar, T., Deeks, M.J., 2006. Control of the actin cytoskeleton in plant cell growth. *Annu. Rev. Plant Biol.* 57, 109–125. doi:10.1146/annurev.arplant.57.032905.105206
- Ikezawa, H., 2002. Glycosylphosphatidylinositol (GPI)-anchored proteins. *Biol. Pharm. Bull.* 25, 409–417. doi:10.1248/bpb.25.409
- Ingle, E. K. S., 2011. An analysis of the NET1 proteins. PhD thesis

- Jia, H., Li, J., Zhu, J., Fan, T., Qian, D., Zhou, Y., Wang, J., Ren, H., Xiang, Y., An, L., 2013. Arabidopsis CROLIN1, a novel plant actin-binding protein, functions in cross-linking and stabilizing actin filaments. *J. Biol. Chem.* 288, 32277–32288. doi:10.1074/jbc.M113.483594
- Jockusch, B.M., Schoenenberger, C.-A., Stetefeld, J., Aebi, U., 2006. Tracking down the different forms of nuclear actin. *Trends Cell Biol.* 16, 391–396. doi:10.1016/j.tcb.2006.06.006
- Johnson, C.D., Chary, S.N., Chernoff, E.A., Zeng, Q., Running, M.P., Crowell, D.N., 2005. Protein Geranylgeranyltransferase I is involved in specific aspects of abscisic acid and auxin signaling in *Arabidopsis*. *Plant Physiol.* 139, 722–733. doi:10.1104/pp.105.065045
- Kameyama, K., Kishi, Y., Yoshimura, M., Kanzawa, N., Sameshima, M., Tsuchiya, T., 2000. Tyrosine phosphorylation in plant bending. *Nature* 407, 37–37. doi:10.1038/35024149
- Kaothien, P., Ok, S.H., Shuai, B., Wengier, D., Cotter, R., Kelley, D., Kiriakopolos, S., Muschietti, J., McCormick, S., 2005. Kinase partner protein interacts with the LePRK1 and LePRK2 receptor kinases and plays a role in polarized pollen tube growth. *Plant J.* 42, 492–503. doi:10.1111/j.1365-313X.2005.02388.x
- Kelley, L.A., Mezulis, S., Yates, C.M., Wass, M.N., Sternberg, M.J.E., 2015. The Phyre2 web portal for protein modeling, prediction and analysis. *Nat. Protoc.* 10, 845–858. doi:10.1038/nprot.2015.053
- Kerscher, O., 2007. SUMO junction—what’s your function? *EMBO Rep.* 8, 550–555. doi:10.1038/sj.embor.7400980
- Khosravi-Far, R., Clark, G.J., Abe, K., Cox, A.D., McLain, T., Lutz, R.J., Sinensky, M., Der, C.J., 1992. Ras (CXXX) and Rab (CC/CXC) prenylation signal sequences are unique and functionally distinct. *J. Biol. Chem.* 267, 24363–24368.
- Khurana, P., Henty, J.L., Huang, S., Staiger, A.M., Blanchoin, L., Staiger, C.J., 2010. Arabidopsis VILLIN1 and VILLIN3 Have Overlapping and Distinct Activities in Actin Bundle Formation and Turnover[W]. *Plant Cell* 22, 2727–2748. doi:10.1105/tpc.110.076240
- Klein, M.G., Shi, W., Ramagopal, U., Tseng, Y., Wirtz, D., Kovar, D.R., Staiger, C.J., Almo, S.C., 2004. Structure of the actin crosslinking core of fimbrin. *Structure* 12, 999–1013. doi:10.1016/j.str.2004.04.010
- Lalanne, E., Honys, D., Johnson, A., Borner, G.H.H., Lilley, K.S., Dupree, P., Grossniklaus, U., Twell, D., 2004. SETH1 and SETH2, two components of the glycosylphosphatidylinositol anchor biosynthetic pathway, are required for pollen germination and tube growth in *Arabidopsis*. *Plant Cell* 16, 229–240. doi:10.1105/tpc.014407
- Larkin, M.A., Blackshields, G., Brown, N.P., Chenna, R., McGettigan, P.A., McWilliam, H., Valentin, F., Wallace, I.M., Wilm, A., Lopez, R., Thompson, J.D., Gibson, T.J., Higgins, D.G., 2007. Clustal W and Clustal X version 2.0. *Bioinformatics* 23, 2947–2948. doi:10.1093/bioinformatics/btm404
- Lin, D.-T., Makino, Y., Sharma, K., Hayashi, T., Neve, R., Takamiya, K., Huganir, R.L., 2009. Regulation of AMPA receptor extrasynaptic insertion by 4.1N, phosphorylation and palmitoylation. *Nat. Neurosci.* 12, 879–887. doi:10.1038/nn.2351
- Maule, A.J., 2008. Plasmodesmata: structure, function and biogenesis. *Curr. Opin. Plant Biol., Cell Biology* Edited by David Ehrhardt and Federica Brandizzi 11, 680–686. doi:10.1016/j.pbi.2008.08.002
- Mendoza, M.C., 2013. Phosphoregulation of the WAVE Regulatory Complex and Signal Integration. *Semin. Cell Dev. Biol.* 24, 272–279. doi:10.1016/j.semcdb.2013.01.007
- Mentlak, D. A., unpublished Net4B: a novel actin binding protein. PhD thesis
- Meulmeester, E., Melchior, F., 2008. Cell biology: SUMO. *Nature* 452, 709–711. doi:10.1038/452709a
- Miura, K., Jin, J.B., Hasegawa, P.M., 2007. Sumoylation, a post-translational regulatory process in plants. *Curr. Opin. Plant Biol., Cell Signalling and Gene Regulation* Edited by Jian-Kang Zhu and Ko Shimamoto 10, 495–502. doi:10.1016/j.pbi.2007.07.002

- Miura, K., Rus, A., Sharkhuu, A., Yokoi, S., Karthikeyan, A.S., Raghothama, K.G., Baek, D., Koo, Y.D., Jin, J.B., Bressan, R.A., Yun, D.-J., Hasegawa, P.M., 2005. The Arabidopsis SUMO E3 ligase SIZ1 controls phosphate deficiency responses. *Proc. Natl. Acad. Sci. U. S. A.* 102, 7760–7765. doi:10.1073/pnas.0500778102
- Molendijk, A.J., Bischoff, F., Rajendrakumar, C.S.V., Friml, J., Braun, M., Gilroy, S., Palme, K., 2001. *Arabidopsis thaliana* Rop GTPases are localized to tips of root hairs and control polar growth. *EMBO J.* 20, 2779–2788. doi:10.1093/emboj/20.11.2779
- Obenauer, J.C., Cantley, L.C., Yaffe, M.B., 2003. Scansite 2.0: proteome-wide prediction of cell signaling interactions using short sequence motifs. *Nucleic Acids Res.* 31, 3635–3641.
- Otterbein, L.R., Graceffa, P., Dominguez, R., 2001. The crystal structure of uncomplexed actin in the ADP state. *Science* 293, 708–711. doi:10.1126/science.1059700
- Pearson, M.A., Reczek, D., Bretscher, A., Karplus, P.A., 2000. Structure of the ERM Protein Moesin reveals the FERM domain fold masked by an extended actin binding tail domain. *Cell* 101, 259–270. doi:10.1016/S0092-8674(00)80836-3
- Pérez-Munive, C., de la Espina, S.M.D., 2011. Nuclear spectrin-like proteins are structural actin-binding proteins in plants. *Biol. Cell* 103, 145–157. doi:10.1042/BC20100083
- Pierre, M., Traverso, J.A., Boisson, B., Domenichini, S., Bouchez, D., Giglione, C., Meinel, T., 2007. N-Myristoylation Regulates the SnRK1 Pathway in *Arabidopsis*. *Plant Cell* 19, 2804–2821. doi:10.1105/tpc.107.051870
- Ren, J., Gao, X., Jin, C., Zhu, M., Wang, X., Shaw, A., Wen, L., Yao, X., Xue, Y., 2009. Systematic study of protein sumoylation: Development of a site-specific predictor of SUMOsp 2.0. *PROTEOMICS* 9, 3409–3412. doi:10.1002/pmic.200800646
- Ren, J., Wen, L., Gao, X., Jin, C., Xue, Y., Yao, X., 2008. CSS-Palm 2.0: an updated software for palmitoylation sites prediction. *Protein Eng. Des. Sel.* 21, 639–644. doi:10.1093/protein/gzn039
- Resh, M.D., 1999. Fatty acylation of proteins: new insights into membrane targeting of myristoylated and palmitoylated proteins. *Biochim. Biophys. Acta BBA - Mol. Cell Res.* 1451, 1–16. doi:10.1016/S0167-4889(99)00075-0
- Running, M.P., Lavy, M., Sternberg, H., Galichet, A., Gruissem, W., Hake, S., Ori, N., Yalovsky, S., 2004. Enlarged meristems and delayed growth in *plp* mutants result from lack of CaaX prenyltransferases. *Proc. Natl. Acad. Sci. U. S. A.* 101, 7815–7820. doi:10.1073/pnas.0402385101
- Sager, R., Lee, J.-Y., 2014. Plasmodesmata in integrated cell signalling: Insights from development and environmental signals and stresses. *J. Exp. Bot.* eru365. doi:10.1093/jxb/eru365
- Sakurai, N., Utsumi, T., 2006. Post-translational N-Myristoylation is required for the anti-apoptotic activity of human gelsolin, the c-terminal caspase cleavage product of human gelsolin. *J. Biol. Chem.* 281, 14288–14295. doi:10.1074/jbc.M510338200
- Salem, T., Mazzella, A., Barberini, M.L., Wengier, D., Motillo, V., Parisi, G., Muschietti, J., 2011. Mutations in two putative phosphorylation motifs in the tomato pollen receptor kinase LePRK2 show antagonistic effects on pollen tube length. *J. Biol. Chem.* 286, 4882–4891. doi:10.1074/jbc.M110.147512
- Sano, T., Higaki, T., Oda, Y., Hayashi, T., Hasezawa, S., 2005. Appearance of actin microfilament “twin peaks” in mitosis and their function in cell plate formation, as visualized in tobacco BY-2 cells expressing GFP-fimbrin. *Plant J.* 44, 595–605. doi:10.1111/j.1365-313X.2005.02558.x
- Saracco, S.A., Miller, M.J., Kurepa, J., Vierstra, R.D., 2007. Genetic analysis of SUMOylation in *Arabidopsis*: conjugation of SUMO1 and SUMO2 to nuclear proteins is essential. *Plant Physiol.* 145, 119–134. doi:10.1104/pp.107.102285

- Simpson, C., Thomas, C., Findlay, K., Bayer, E., Maule, A.J., 2009. An *Arabidopsis* GPI-Anchor plasmodesmal neck protein with callose binding activity and potential to regulate cell-to-cell trafficking. *Plant Cell* 21, 581–594. doi:10.1105/tpc.108.060145
- Song, J., Zhang, Z., Hu, W., Chen, Y., 2005. Small ubiquitin-like modifier (SUMO) recognition of a SUMO binding motif a reversal of the bound orientation. *J. Biol. Chem.* 280, 40122–40129. doi:10.1074/jbc.M507059200
- Sorek, N., Poraty, L., Sternberg, H., Bar, E., Lewinsohn, E., Yalovsky, S., 2007. Activation status-coupled transient s acylation determines membrane partitioning of a plant Rho-related GTPase. *Mol. Cell. Biol.* 27, 2144–2154. doi:10.1128/MCB.02347-06
- Sugiyama, N., Nakagami, H., Mochida, K., Daudi, A., Tomita, M., Shirasu, K., Ishihama, Y., 2008. Large-scale phosphorylation mapping reveals the extent of tyrosine phosphorylation in *Arabidopsis*. *Mol. Syst. Biol.* 4, 193. doi:10.1038/msb.2008.32
- Su, S., Liu, Z., Chen, C., Zhang, Y., Wang, X., Zhu, L., Miao, L., Wang, X.-C., Yuan, M., 2010. Cucumber mosaic virus movement protein severs actin filaments to increase the plasmodesmal size exclusion limit in tobacco. *Plant Cell Online* 22, 1373–1387. doi:10.1105/tpc.108.064212
- Tamura, K., Iwabuchi, K., Fukao, Y., Kondo, M., Okamoto, K., Ueda, H., Nishimura, M., Hara-Nishimura, I., 2013. Myosin XI-i Links the nuclear membrane to the cytoskeleton to control nuclear movement and shape in *arabidopsis*. *Curr. Biol.* 23, 1776–1781. doi:10.1016/j.cub.2013.07.035
- Thole, J.M., Perroud, P.-F., Quatrano, R.S., Running, M.P., 2014. Prenylation is required for polar cell elongation, cell adhesion, and differentiation in *Physcomitrella patens*. *Plant J.* 78, 441–451. doi:10.1111/tpj.12484
- Vartiainen, M.K., 2008. Nuclear actin dynamics – From form to function. *FEBS Lett., Nuclear Dynamics and Cytoskeleton Signaling* 582, 2033–2040. doi:10.1016/j.febslet.2008.04.010
- Vogt, P.K., Jiang, H., Aoki, M., 2005. Triple layer control: phosphorylation, acetylation and ubiquitination of FOXO Proteins. *Cell Cycle* 4, 908–913. doi:10.4161/cc.4.7.1796
- Wang, P., Hawkins, T.J., Richardson, C., Cummins, I., Deeks, M.J., Sparkes, I., Hawes, C., Hussey, P.J., 2014. The Plant Cytoskeleton, NET3C, and VAP27 Mediate the Link between the Plasma Membrane and Endoplasmic Reticulum. *Curr. Biol.* 24, 1397–1405. doi:10.1016/j.cub.2014.05.003
- Wightman, R., Turner, S.R., 2008. The roles of the cytoskeleton during cellulose deposition at the secondary cell wall. *Plant J.* 54, 794–805. doi:10.1111/j.1365-313X.2008.03444.x
- Wu, S.-Z., Bezanilla, M., 2014. Myosin VIII associates with microtubule ends and together with actin plays a role in guiding plant cell division. *eLife* 3, e03498. doi:10.7554/eLife.03498
- Yokota, E., Tominaga, M., Mabuchi, I., Tsuji, Y., Staiger, C.J., Oiwa, K., Shimmen, T., 2005. Plant villin, Lily P-135-ABP, possesses g-actin binding activity and accelerates the polymerization and depolymerization of actin in a Ca<sup>2+</sup>-sensitive manner. *Plant Cell Physiol.* 46, 1690–1703. doi:10.1093/pcp/pci185
- Yoo, C.Y., Miura, K., Jin, J.B., Lee, J., Park, H.C., Salt, D.E., Yun, D.-J., Bressan, R.A., Hasegawa, P.M., 2006. SIZ1 small ubiquitin-like modifier e3 ligase facilitates basal thermotolerance in *Arabidopsis* independent of salicylic acid. *Plant Physiol.* 142, 1548–1558. doi:10.1104/pp.106.088831
- Yu, J., Zhang, D., Liu, J., Li, J., Yu, Y., Wu, X.-R., Huang, C., 2012. RhoGDI SUMOylation at Lys-138 increases its binding activity to rho gtpase and its inhibiting cancer cell motility. *J. Biol. Chem.* 287, 13752–13760. doi:10.1074/jbc.M111.337469
- Zhang, H., Qu, X., Bao, C., Khurana, P., Wang, Q., Xie, Y., Zheng, Y., Chen, N., Blanchoin, L., Staiger, C.J., Huang, S., 2010. *Arabidopsis* VILLIN5, an actin filament bundling and severing protein, is necessary for normal pollen tube growth. *Plant Cell* 22, 2749–2767. doi:10.1105/tpc.110.076257

- Zhang, Y.-L., Li, E., Feng, Q.-N., Zhao, X.-Y., Ge, F.-R., Zhang, Y., Li, S., 2015. Protein palmitoylation is critical for the polar growth of root hairs in *Arabidopsis*. *BMC Plant Biol.* 15, 50. doi:10.1186/s12870-015-0441-5
- Zhao, Q., Xie, Y., Zheng, Y., Jiang, S., Liu, W., Mu, W., Liu, Z., Zhao, Y., Xue, Y., Ren, J., 2014. GPS-SUMO: a tool for the prediction of sumoylation sites and SUMO-interaction motifs. *Nucleic Acids Res.* 42, W325–W330. doi:10.1093/nar/gku383
- Zhou, X., Graumann, K., Evans, D.E., Meier, I., 2012. Novel plant SUN–KASH bridges are involved in RanGAP anchoring and nuclear shape determination. *J. Cell Biol.* 196, 203–211. doi:10.1083/jcb.201108098
- Zulawski, M., Braginets, R., Schulze, W.X., 2013. PhosPhAt goes kinases--searchable protein kinase target information in the plant phosphorylation site database PhosPhAt. *Nucleic Acids Res.* 41, D1176–D1184. doi:10.1093/nar/gks1081